

University of Southampton Research Repository

Copyright © and Moral Rights for this thesis and, where applicable, any accompanying data are retained by the author and/or other copyright owners. A copy can be downloaded for personal non-commercial research or study, without prior permission or charge. This thesis and the accompanying data cannot be reproduced or quoted extensively from without first obtaining permission in writing from the copyright holder/s. The content of the thesis and accompanying research data (where applicable) must not be changed in any way or sold commercially in any format or medium without the formal permission of the copyright holder/s.

When referring to this thesis and any accompanying data, full bibliographic details must be given, e.g.

Thesis: Jack Lewis Mitchell (2023) “Domain Wall Fermions in Holography”, University of Southampton, Faculty of Engineering and Physical Sciences, PhD Thesis.

Data: Jack Lewis Mitchell (2023) “Domain Wall Fermions in Holography”. URI [dataset]

University of Southampton

Faculty of Engineering and Physical Sciences

School of Physics and Astronomy

**Domain Wall Fermions in
Holography**

by

Jack Lewis Mitchell

M.Phys

ORCID: 0000-0001-7884-7146

*A thesis for the degree of
Doctor of Philosophy*

December 2023

University of Southampton

Abstract

Faculty of Engineering and Physical Sciences
School of Physics and Astronomy

Doctor of Philosophy

Domain Wall Fermions in Holography

by Jack Lewis Mitchell

This thesis will cover the development of *holographic domain wall* models, inspired by implementations of chiral fermions on the lattice. Starting in the D3/D7 holographic system, and solving the Dirac-Born-Infeld (DBI) action for the sinusoidal embedding of the probe sevenbranes, a spatially dependant, step-like mass term for quarks in the dual theory can be included. Where this mass profile sharply passes through zero, massless quarks are isolated on co-dimension one *domain wall* defects in the dual gauge theory. Development of the *large mass limit*, allows us to examine fluctuations in the dimensionally reduced theory living on the domain walls. We show that the domain wall theory is capable of dynamically generating mass for the dimensionally reduced quarks, complete with a *Gell-Mann-Oakes-Renner relation* between the masses of quarks, and pseudoscalar mesons, indicating the spontaneous breaking of “chiral” symmetry. With the construction of the *holographic domain walls* understood, we implement them on the field theory limit of the D5/D7 intersection. This system is holographically dual to a 4+1 dimensional theory of quarks in a 5+1 dimensional confining gauge background. The resulting domain wall theory consists of 3+1 dimensional quarks in a confining geometry, and possesses neither conformal symmetry, nor supersymmetry. We dub this model *Domain Wall AdS/QCD*, and present a numerical calculation of its spectrum of mesonic observables. By including a black hole in the geometry, we can examine the phase transitions of the model at finite temperature, and find that there is a second order meson-melting transition.

Contents

List of Figures	vii
List of Tables	xi
Declaration of Authorship	xiii
Acknowledgements	xv
Definitions and Abbreviations	xvii
1 Introduction	1
2 Non-Abelian Gauge Theories and QCD	5
2.1 QCD across the scales	8
2.2 Large N	14
2.3 Confinement	15
2.4 Summary	18
3 Strings, Branes and Supergravity	19
3.1 Early History and the Bosonic String	20
3.1.1 Classical Bosonic Strings	22
3.1.2 Quantum Bosonic Strings	27
3.1.3 String Mass Formula, Level Matching, and Spectrum	27
3.2 Superstring Theory	31
3.2.1 Spinning Strings, and the GSO Projection	32
3.2.2 Differential Forms, Branes and Supergravity	36
3.3 Holography and the AdS/CFT Correspondence	42
3.3.1 Probe Branes and Fundamental Matter	47
3.3.2 Holographic QCD	52
3.3.2.1 From the bottom up...	52
3.3.2.2 ...and the top down	53
3.4 Summary	54
4 Domain Wall Fermions	57
4.1 Domain Wall Fermions on the lattice, and in the continuum	57
4.2 Domain Walls in the D3/D7 system.	60

4.3	The Large Mass Limit: a tale of U shaped loci	68
4.3.1	One Large Step for Brane-kind	68
4.3.2	Minimal Surface	71
4.3.3	A Non-Supersymmetric D3/D7 Intersection	72
4.4	Fluctuations about the Wall	74
4.4.1	A system of two levels	76
4.5	Dynamical “Chiral” Symmetry Breaking	77
4.5.1	Magnetic Fields on the Probe Brane	77
4.5.1.1	q=10 “effective dilaton flow”	79
4.5.2	Constable-Myers Deformation	83
4.6	Summary	89
5	Domain Wall AdS/QCD	91
5.1	D5 Background	92
5.2	D7 Probes	95
5.2.1	Fluctuations on the Walls	97
5.2.2	Mesons in Domain Wall AdS/QCD	98
5.3	Worldvolume Gauge Fields, Vector Mesons, and Matching to QCD .	101
5.3.1	Worldvolume Gauge Fields	101
5.3.2	Higher Dimension Operators via Witten Prescription	104
5.4	Summary	105
6	Thermal Transitions in Domain Wall AdS/QCD	107
6.1	Black Branes and Finite Temperature	108
6.1.1	Temperature of near extremal p-branes	109
6.1.2	Thermal geometry	111
6.2	Domain Walls and Loci at Finite Temperature	112
6.3	The Width Transition - A Naïve Approach	113
6.4	The Domain Wall Theory at Finite Temperature.	115
6.4.1	Fixed Quark Mass	117
6.4.2	NJL Coupling	118
6.5	Summary	121
7	Conclusion and Outlook	123
	References	127

List of Figures

2.1	Schematic forms of the interaction vertices in QCD: The quark-gluon, three gluon, four gluon, and ghost-gluon vertices are depicted.	8
2.2	A schematic drawing of the Feynman graphs that contribute to the quark-gluon interaction vertex at one loop.	9
2.3	Vertices in QCD (Left), and their analogue at large N (Right) . . .	16
3.1	A cartoon depicting a string (Blue) with endpoints on the boundary of AdS in a confining theory. The string is excluded from the red region, so for sufficiently large Δx the area of the string worldsheet is dominated by the contribution from the part of the string lying across the obstruction.	53
4.1	A plot of the fourier series (4.25) truncated at $n = 10,000$. Here the values $K = 3$, $z_0 = 1$ were used to produce the plot.	64
4.2	Some solutions $f_k(\rho)$ in $AdS_5 \times S^5$ with a hardwall at $\rho = 1$ for: $k = \frac{2\pi}{K}$ (blue), $k = \frac{20\pi}{K}$ (orange), and $k = \frac{60\pi}{K}$ (green).	65
4.3	An example domain wall solution from two perspectives. top: a perspective showing the overall shape, bottom: a perspective “from the boundary” showing the boundary profile of the D7 brane realising (4.20). For these plots $K = 3$, $z_0 = 1.25$, was used and the series was truncated at $n = 350$	66
4.4	The 3+1 d quark condensate at the boundary of AdS plotted against z for 150 Fourier modes (top), 100 Fourier modes (middle), and 50 Fourier modes (bottom). The positions of the domain walls are indicated with red dots on the z axes.	67
4.5	A plot of the solutions to (4.41) (Black, Red), matched to the $L = 0$ contour of their linearised counterparts (Orange, Blue). The solutions are matched by their separation at the boundary.	71
4.6	The domain wall loci in the toy model showing pile up behaviour. The four loci depicted are $\rho_{min} = 1.5$ (Purple), $\rho_{min} = 1$ (Magenta), $\rho_{min} = 0.89$ (Orange), $\rho_{min} = 0.87056$ (Red), the pile up scale $\bar{\rho}$ is also included (Black, Dashed).	80
4.7	Numerical solutions to (4.73) (Blue), on loci that join near the pile up scale $\bar{\rho}$ (Red, Dotted) are plotted. The range of ρ_{min} on the loci plotted is $\bar{\rho} < \rho_{min} \leq \bar{\rho} + 0.0003$	82

4.8	The meson mass squared against the quark mass, corresponding to the vacuum functions in Figure 4.7. A linear guide function has been added to emphasise the behaviour at small m_q (Top). A magnified view of the small quark mass region clearly showing the linear GMOR behaviour (Bottom).	83
4.9	The domain wall loci in the Constable-Myers deformation of $AdS_5 \times S^5$ displaying pile up behaviour. The configurations plotted are: $\rho_{min} \sim 1.6033$ (Purple), $\rho_{min} \sim 1.4033$ (Magenta), $\rho_{min} \sim 1.3043$ (Orange), $\rho_{min} = \bar{\rho} + 0.00001 \sim 1.30327$ (Red).	86
4.10	Plot of the numerical solutions to (4.89) for the vacuum function $L(\rho)$ (Blue) on loci that join near the pile up scale $\bar{\rho}$ (Red,Dotted). The range of ρ_{min} on the loci plotted is $\bar{\rho} < \rho_{min} < \bar{\rho} + 0.00015$	87
4.11	Meson mass squared M_ϕ^2 plotted against quark mass m_q for domain walls in the Constable-Myers deformation of $AdS_5 \times S^5$, a linear plot has been added to emphasise the GMOR behaviour (Top). A zoomed in section about small quark mass (Bottom)	88
5.1	The domain wall loci (Blue/Red, Solid) in the capped AdS/QCD geometry. The loci display pile up behaviour, widening as they approach the cap in the geometry (Black, Dashed).	97
5.2	Solutions to (5.26) for the vacuum functions L (Blue). The cap at $\rho = 1$ is also plotted (Black, Dashed), alongside the line $L(\rho_{min}) = \rho_{min}$ (Red) representing the boundary condition on the vacuum functions in the IR.	98
5.3	The meson mass squared against the quark mass, corresponding to the vacuum functions in Figure 5.2. A linear guide function has been added to emphasise the behaviour at small m_q (Top). A magnified view of the small quark mass region clearly showing the linear GMOR behaviour (Bottom).	100
5.4	Mesonic observables in the Domain Wall AdS/QCD model. QCD data is displayed in the lefthand column, with the three chosen vacua displayed alongside. The starred numbers indicate quantities that were used to set scales and are not predictions. The two doubly starred values in the rightmost column are found from minimising (5.37). The percentages in brackets indicate the deviation from the QCD value.	104
5.5	Mesonic observables in the base Model, and the numerical results of the improvement to the model to more accurately describe the excited states. The starred numbers are fixed to set scales and normalisations. The percentages in brackets are the deviations from the QCD values	105
6.1	The asymptotic separation of a domain wall pair, against ρ_{min} for system at a temperature of $U_0(T) \sim 0.066\Lambda_{UV}$	114
6.2	A cartoon depicting the set of three loci for a chosen width and temperature, in the dimensionful ‘‘U’’ co-ordinate system.	114

6.3	A plot of the regulated free energy against temperature U_0/Λ , for an asymptotic width of $W \sim 0.964$. The two U shaped loci are depicted (Blue, Red), alongside the zero line representing the flat disconnected loci (Black).	115
6.4	A cartoon showing the evolution of a domain wall system, with fixed quark mass m/Λ , as the temperature is increased from $U_0(T_1)$ (Dashed configuration), to $U_0(T_2) > U_0(T_1)$ (solid configuration), finally to $U_0(T_c)$ where the tip of the U-shape has fallen into the horizon, becoming two disconnected flat pieces (dotted configuration). The position of the horizon is drawn in red (dashed, solid, and dotted respectively).	118
6.5	Numerical results tracking the asymptotic width of configurations with fixed quark mass $m/\Lambda \sim 0.2$ as the temperature is varied. At a critical temperature of $U_0(T_c)/\Lambda \sim 0.2$ the loci dip into the horizon and disconnect.	118
6.6	The chiral condensate (in units of Λ) plotted for the configurations in Figure 6.5. We see explicitly that at the critical temperature $U_0(T_c) \sim 0.2$, the condensate drops to zero, indicating the transition to a chirally restored phase.	119
6.7	A plot of the numerical results of the critical temperature $U_0(T_c)$ varying with quark mass m/Λ	119
6.8	The free energy of the three configurations with fixed $g^2 \sim 0.57$, at varying temperature. The two U-shaped solutions are displayed (Red, Blue), the disconnected solutions are also drawn on (Black)	120
6.9	A plot of the numerical results of the critical temperature $U_0(T_c)$ varying with the NJL coupling g^2 . Again there are numerical difficulties at very low temperatures.	121

List of Tables

3.1	The D-brane content of type IIB string theory	38
3.2	The D-brane content of type IIA string theory	39
3.3	The $\frac{1}{2}BPS$ supergravity solution, in string frame, corresponding to a stack of N co-incident Dp -branes.	41

Declaration of Authorship

I declare that this thesis and the work presented in it is my own and has been generated by me as the result of my own original research.

I confirm that:

1. This work was done wholly or mainly while in candidature for a research degree at this University;
2. Where any part of this thesis has previously been submitted for a degree or any other qualification at this University or any other institution, this has been clearly stated;
3. Where I have consulted the published work of others, this is always clearly attributed;
4. Where I have quoted from the work of others, the source is always given. With the exception of such quotations, this thesis is entirely my own work;
5. I have acknowledged all main sources of help;
6. Where the thesis is based on work done by myself jointly with others, I have made clear exactly what was done by others and what I have contributed myself;
7. Parts of this work have been published as: [1, 2, 3]

Signed:..... Date:.....

Acknowledgements

Although unusual, I think it is fitting to recognise *when* this work took place. When I first moved down to Southampton in September 2019, I had no idea what to expect. I certainly did not expect that five short months later the world would stop. The coronavirus pandemic has spanned a large portion of my time in Southampton. In honesty, it has been a hard time to be a PhD student. Between cost of living crises, global pandemics, and a painfully slow return to office life for theorists, it is a small miracle that anything has been done in the past few years at all. I am incredibly thankful for the people around who lifted me up throughout the past four years. Without you all, this would not have been possible.

Firstly, I owe a great deal of thanks to Nick Evans, who supervised this body of work. I have learned an awful lot about branes, QCD, holography, and research itself from our discussions. I am grateful for his patience, and his good humor. He knew how best to push me, even when I doubted myself.

I have been lucky to share an office with some amazing people over the past four years, most notably: Alessandro, Vlad, Shubhani, and Matt, who started this journey with me; Nakorn; and Callum.

There were a number of students with mutual interest in holography and string theory whom I benefitted greatly from conversations with. In particular I'd like to thank: Matt, Michele, Ben, Pietro, Wan-Xiang, James, and Jonas, for interesting discussions over the years.

I'd be remiss not to mention Aaron, Dalius, Raj, and Ben; for all the dice rolled, monsters slain, and laughs along the way.

I was very fortunate to have been friends with Nikolai. I will miss our weekly coffee break/several hour long physics argument, that often spilled over several days.

Whilst in Southampton, I had the pleasure of living with: Geraint, Sebastian, Dawid, Rajnandini, Christopher, Ryan, and Jesse. I am thankful in particular to G, for hundreds of rounds of smash, and his vicious King K.Rool play.

Outside of the University, I am incredibly thankful for the friendship of Kit, Dan Pad, Jacob, Raj, and Roden, who were always there to talk, no matter the reason; and to Dan, whose occasional distraction from thesis writing was greatly appreciated.

I would not be in the position I am today were it not for my parents, James, and Joanne. They are without a doubt the greatest teachers I have ever had, and have shaped me into the person I am today. I am very lucky to have had their love and

support throughout this process, and the love and kindness their partners Elaine, and Andrea.

I am forever thankful for the love and support of my partner Lucy, who celebrated every success with me; read every paper we wrote, even if the physics was “made up”; who helped me to proof read this thesis; but most importantly, who stood by me on the difficult days, and held me up on the days where I just wanted to quit. I could not have done it without you.

Definitions and Abbreviations

This thesis aims to be as consistent as humanly possible, and keeps to the following conventions:

metric	mostly plus
$L(\rho, z)$	The D7 embedding field, used also for fluctuations on the locus dual to the quark mass/ chiral condensate pair
$\phi(\rho, z, x^i)$	The field dual to the pseudoscalar meson (pion)
Domain Wall(s)	A brane configuration with a pair of step like quark mass defects on the asymptotic boundary
Domain wall locus (loci)	The co-dimension one defect where $L = 0$ in higher dimensional theory
DBI	Dirac-Born-Infeld (D-brane action)
S_{D7}	D7 brane action functional
S_{locus}	Locus action functional
S_{DW}	Action functional for fluctuations on locus
ρ	The radial direction on the probe brane(s)
z	The direction the domain wall “lives” in

$z(\rho)$	The embedding of the locus
$\Phi(r)$	The (radial) dilaton profile of the theory
UV	Ultraviolet
IR	Infrared
QCD	Quantum chromodynamics

Chapter 1

Introduction

Quantum Chromodynamics, or QCD, is a quantum field theory that describes the interactions of elementary quarks and gluons. It is asymptotically free [4]; which is to say that at high energy scales, it approaches a free field theory of quarks and gluons. However at low energy scales non-perturbative dynamics dominate. The QCD vacuum, a far cry from the peace of the electromagnetic vacuum, froths violently with quarks and gluons. The theory *confines* the *colour* degrees of freedom, and the quarks and gluons join together to form the spectrum of *colour singlet* bound states which are observed in experiment. This has been verified in computational studies of QCD done on discrete euclidean space-time lattices, where confinement is characterised by area-law behaviour of gauge invariant operators, called Wilson loops [5]. Outside of lattice studies, there are few approaches that are capable of characterising the non-perturbative behaviour of QCD. It is here at the low energies where we are presented with an issue. We lack the proper tools to calculate in the non-perturbative regime of quantum field theories (outside of a few special cases with greatly enhanced symmetry, such as [6]). We will circumvent this by turning to *gravity*.

Gravity is an altogether different beast. It is most successfully described by a classical theory, *General Relativity* [7], which tells us that gravity arises from the geometry of spacetime itself. Attempts to quantize gravity, and put it on a similar footing to the rest of the standard model, have been numerous. However, field theory approaches seem plagued by divergences and non-renormalisability [8]. String theory stands as a leading candidate for a quantum theory of gravity and contains in its spectrum spin 1, 1/2 and 0 excitations. This would allow it to describe matter, the gauge fields that carry the fundamental forces, and gravity, which make it a candidate theory of everything. Perhaps the most striking feature of string

theory are its dualities, which map between the various string theories suggesting that they are all limits of some unknown parent theory. It is with one particular duality that this thesis will be concerned. The AdS/CFT correspondence, conjectured by Maldacena in 1997 [9], sets out the duality between type IIB string theory on five dimensional Anti-de-Sitter space (times a five sphere) and maximally supersymmetric Yang-Mills theory in 4 dimensions. This duality is striking for a number of reasons: firstly, it is a duality between a theory containing gravity and a non-gravitating theory (in this case a gauge theory); and secondly it is a duality which links the strong coupling regime of one theory, with the weak coupling limit of the other. This opens the window to many possibilities and has, in the 25 years since its inception, revolutionised high-energy physics. There have been an incredible number of checks across either side of this duality, matching elements of the *holographic dictionary*. One early example of this was the work by Witten [10], matching of spectrum of *Kaluza-Klein modes* in IIB supergravity on $AdS_5 \times S^5$ to the chiral operators of $\mathcal{N} = 4$ Super-Yang-Mills (SYM). Here it was identified that the field theory could be thought of as “living” on the asymptotic conformal boundary of the space.

Whilst one may use such dualities, to attempt to understand the nature of quantum gravity; our goal going forward will be to examine the non-perturbative regime of quantum field theories. In particular, we will exploit the dual nature of non-perturbative objects in string theory, called *D-branes*, to construct a *top-down* holographic model of low energy QCD. There are rich non-perturbative phenomena associated with strongly coupled QCD, such as the dynamical breaking of chiral symmetry and confinement, that are difficult to describe in perturbative field theory. Through holography, we will come to understand these features in terms of simple geometry.

This thesis will be structured as follows: Chapter 2 will discuss the relevant theoretical background on the gauge theory side of the duality. Namely, it will be a discussion of Non-Abelian Gauge theories and QCD. The chapter will review some of the aspects of these theories which are most puzzling from the perspective of field theory. Chapter 3 will be devoted to the relevant background in string theory and supergravity, it will discuss some of the historic origins of string theory, as a theory of Hadrons, and will cover some of the essential non-perturbative ingredients, such as D-branes which are the real main characters of this story. Chapter 4 will discuss domain walls, and some of the context (and inspiration) from lattice field theory. This chapter will then go on to discuss our domain wall construction in the D3/D7 brane intersection. The D3/D7 domain wall system, first detailed in [1], which is dual to a theory of “chiral” fermions in 2+1 dimensions. Chapter

5 will go on to discuss the construction (and spectrum) of the D5/D7 domain wall model, dual to a 3+1 dimensional confined model of quarks and gluons, which we dub *Domain Wall AdS/QCD* [2]. Chapter 6, will then examine the D5/D7 model in a black brane background, dual to a 3+1 dimensional model of gluons and quarks at finite temperature [3].

Chapter 2

Non-Abelian Gauge Theories and QCD

This chapter will cover some of the requisite theoretical background pertaining to Quantum Chromodynamics. It is by no means intended to be a historical record of the strong force, indeed the history of QCD is both long and fascinating, with the close interplay of experiment and theory throughout the mid 20th century. Instead this chapter will aim to be a relatively concise introduction to Non-Abelian gauge theories, and some of the properties and behaviour that makes them interesting! We will start by writing down the QCD Lagrangian, and discussing some of the behaviour at high energies, where the theory is weakly coupled. Here we can do trustworthy perturbative calculations in quantum field theory. The calculation of the running of the Yang-Mills coupling, due to Gross and Wilczek [4], reveals two interesting facets of QCD: Firstly, that the coupling constant runs to zero in the far UV, and the theory is *asymptotically free*; secondly that in the IR, the theory becomes very strongly coupled and we lack the ability to do perturbative computations in quantum field theory. The strong coupling regime of QCD is somewhat of a mystery from a theoretical standpoint, and understanding: the confinement of colour, the masses of hadrons, and their emergence from the QCD Lagrangian as degrees of freedom is still out of reach. Still theorists persevere and a phenomenological model exists, that describe the dynamics of mesons based on the approximate chiral symmetry of QCD, called *chiral perturbation theory* (or χ PT). Methods do exist to tackle QCD non-perturbatively. The most prominent of these is *lattice QCD*, wherein the background spacetime is treated as a discrete Euclidean lattice of finite size¹ on which QCD can be tackled using Monte-Carlo methods. It

¹a T^4 lattice to be precise

should be said here that appropriately discretising the QCD lagrangian seemingly recovers the wealth of emergent long range phenomena when moving to the strong coupling regime. It is also possible in principle to solve the renormalisation group flow equations exactly, which would provide the ability to calculate at strong coupling. This approach, known as the functional renormalisation group, or fRG, in the context of QCD is reviewed here [11] (though with emphasis on QCD at finite density and temperature). A great deal of progress was made in the late 90's on the supersymmetric relatives of QCD [6, 12]. Here the greatly enhanced symmetry of the theory, and subsequent applicability of the tools of complex analysis, allowed a first analytic example of confinement in gauge theories. It is not yet known whether the mechanisms discussed in these theories extend to their less supersymmetric cousins. Another notable avenue of approach is through *String Theory*, which will be discussed in much more detail in Chapter 3². String-like behaviour is common in non-abelian gauge theories, and indeed QCD contains a kind of string! It is not a “fundamental string” but a tube of colour flux that stretches between spatially separated quarks and anti-quarks. This string-like behaviour will be discussed towards the end of the chapter, and will culminate in a discussion of Yang-Mills theory at “large N ”. It is here that stringiness comes to the foreground. The Feynman diagrams are best organised by their topology, and alongside the *t'Hooft double line formalism*, there is a striking resemblance to string perturbation theory (where instead of Feynman diagrams, we have string world-sheets organised by their Euler characteristic). Lastly we will discuss the confinement of colour charged degrees of freedom, and the characterisation of the confined phase of QCD by Wilson loops.

We will start by examining the Lagrangian density that describes QCD, which can be written neatly as³

$$\mathcal{L}_{QCD} = -\frac{1}{4}G_{\mu\nu,a}G^{\mu\nu}_a + \sum_f \bar{\psi}_f (i\not{D} - m_f) \psi_f, \quad (2.1)$$

but the simplicity of this closed form masks a great deal of complexity underneath the surface. We will start by discussing the matter content of the Lagrangian. There are six Dirac fermions, ψ_f , that can roughly be grouped⁴ into the “light” quarks: the up u , the down d , and the strange s quarks; and the “heavy” quarks: the charm c , bottom b , and top t quarks. These quarks are interesting objects in

²and indeed, the rest of this thesis.

³There could also be a term proportional to $G \wedge G$ and a “gauge fixing” term, but these will not be discussed here.

⁴based on their relative masses

their own right. For one they are never seen as asymptotic states in scattering experiments, and for a long time were considered merely a mathematical device to describe the observed groupings of the mesons and baryons. After the results from the Deep Inelastic Scattering (DIS) experiments at the Stanford Linear Accelerator Centre (SLAC) in 1968, it became clear that the hadrons had substructure [13, 14]. Whilst the quarks were not observable, they are physical and must carry internal degrees of freedom to describe the proton. This internal degree of freedom is known as ‘colour’. In more mathematical terms, the quarks are fermions that transform in the fundamental representation of the gauge group $SU(3)$. In order to make the symmetry under $SU(3)$ transformations local, there must be a vector field that “carries the colour force”. These are the eight gluons, who form an adjoint representation of $SU(3)$, $(A_\mu)_{ij} = (t_{ij}^a) A_\mu^a$, where the matrices t_{ij}^a are the generators of the adjoint representation of $SU(3)$, commonly parameterised as the Gell-Mann matrices, $t_a = \lambda_a/2$. These fields allow us to write down a gauge covariant derivative,

$$D_\mu = \partial_\mu - igA_\mu^a t^a, \quad (2.2)$$

such that under a transformation

$$\psi(x) \rightarrow V(x)\psi(x), \quad V(x) \in SU(3) \quad (2.3)$$

the covariant derivative of ψ transforms in the same way⁵

$$D_\mu\psi(x) \rightarrow V(x) (D_\mu\psi(x)). \quad (2.4)$$

A more mathematical way to talk about this is to realise that the gauge field A_μ is in fact a connection!⁶ Equivalently we can then define a curvature from the covariant derivatives,

$$G_{\mu\nu,a} = \frac{i}{g} [D_\mu, D_\nu]_a = \partial_\mu A_{\nu,a} - \partial_\nu A_{\mu,a} + gf_{abc} A_{\mu,b} A_{\nu,c} \quad (2.5)$$

where the structure constants f_{abc} comes from the commutator of the matrices t_a , which satisfy

$$[t_a, t_b] = if_{abc} t_c. \quad (2.6)$$

A clear difference between QCD and Quantum Electrodynamics, is the presence of the last term in Equation 2.5, which arises because the gluon fields A_μ are matrix

⁵thus the kinetic term $i\bar{\psi}\gamma^\mu D_\mu\psi$ is both a lorentz scalar, and gauge invariant.

⁶The pullback of the connection on the principle bundle $\mathcal{M} \times \mathcal{G}$, to the base space \mathcal{M} .

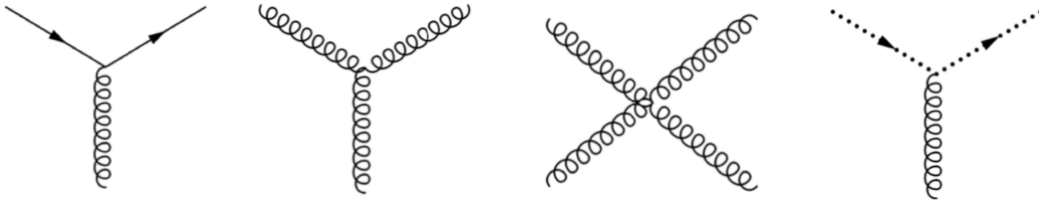


FIGURE 2.1: Schematic forms of the interaction vertices in QCD: The quark-gluon, three gluon, four gluon, and ghost-gluon vertices are depicted.

valued, and as such their commutator does not vanish. As a result the QCD Lagrangian contains a self interaction term for the gluons, including both three and four gluon interactions, stemming from the $Tr G^2$ term; and an interaction between the quarks and gluons, from the $\bar{\psi} i \not{D} \psi$ term. To calculate physical observables, one must also “fix the gauge”. This involves removing, one way or another, unphysical degrees of freedom baked into the theory. Using the Faddeev-Popov procedure as an example⁷, one introduces unphysical states that only appear at loop level, Faddeev-Popov ghosts, which are Grassman valued scalar fields [15]. When properly accounted for these extra fields remove the extra unphysical degrees of freedom. As a result, there is another interaction term, though one that should only formally show up at loop level, because the ghost fields cannot lead to asymptotic particle states. This interaction vertex is a ghost-ghost-gluon vertex. All the interaction vertices of the theory are displayed schematically in Feynman diagram form in Figure 2.1.

2.1 QCD across the scales

Any discussion of QCD would be remiss without at least a mention of the renormalisation of the QCD coupling. The basic interaction vertex between quarks and gluons at one loop order, receives contributions from eight diagrams, which are displayed in Figure 2.2. These contributions can roughly be grouped into: the tree level contribution, external leg corrections, one particle irreducible vertex corrections, and counter terms which absorb the ultraviolet divergence from the diagrams. They must also be defined with respect to a reference scale, M_1 , such that the higher order contributions vanish at this scale, and the interaction is well described by the tree level diagram. Interactions at a different scale, $M_2 \neq M_1$ are then described by the full set of diagrams in the perturbative expansion. Equally

⁷other gauge-fixing methods are available

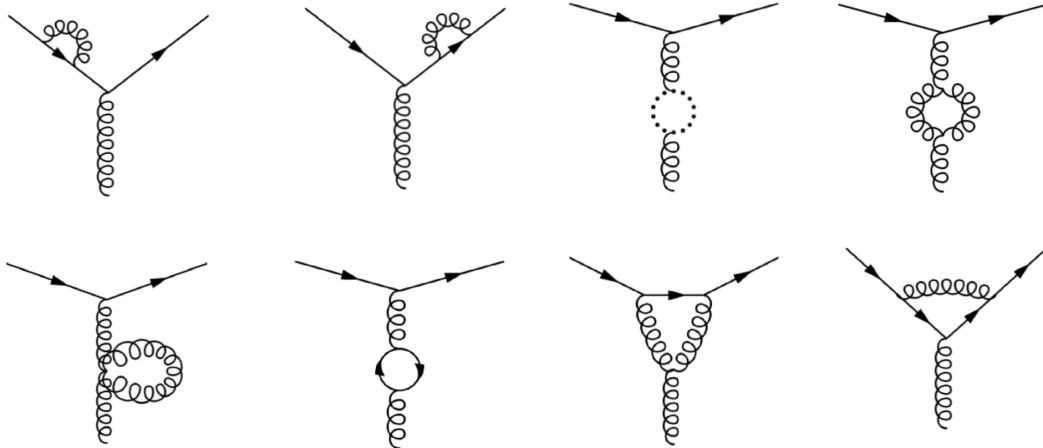


FIGURE 2.2: A schematic drawing of the Feynman graphs that contribute to the quark-gluon interaction vertex at one loop.

one could have initially decided that M_2 was a good reference scale, and then one would define their renormalisation scheme at this scale, setting the corrections to vanish at M_2 . However this potentially presents a contradiction, the way out of which is to realise that the coupling constant is not a constant at all. It must be dependant on the scale at which it is measured⁸. One can then calculate, at one loop from the diagrams in Figure 2.2, the (logarithmic) variation in the coupling at an arbitrary scale μ . This result is known as the “beta function” and was calculated at one loop in QCD by Gross and Wilczek in 1973, for which they would win the Nobel prize in 2004. The one loop result is

$$\beta_{QCD}(g) = \frac{\partial g(\mu)}{\partial \log(\mu)} = - \left(\frac{11}{3} C_2(G) - \frac{4}{3} n_f T(R) \right) \frac{g^3}{(4\pi)^2} \quad (2.7)$$

where $C_2(G)$ is the quadratic Casimir invariant of the gauge group G , n_f is the number of Dirac fermions, and $T(R)$ is a Casimir of the representation of the gauge group that the fermions transform under. For n_f fermions in the fundamental representation of $SU(3)$, this evaluates to

$$\beta_{QCD}(g) = - \left(11 - \frac{2}{3} n_f \right) \frac{g^3}{(4\pi)^2} \quad (2.8)$$

which for fewer than $33/2$ Dirac fermions, has an overall negative sign. The negativity of β_{QCD} has vast physical significance, and implies that the physical

⁸outside of a special class of theories with enhanced symmetry.

coupling at a scale μ , which can be solved from (2.7)

$$g^2(\mu) = \frac{g_0^2}{1 + \frac{g_0^2}{(4\pi)^2} \left[\frac{11}{3} C_2(G) - \frac{4}{3} n_f T(R) \right] \log\left(\frac{\mu}{M}\right)}. \quad (2.9)$$

with reference to the coupling at scale M , $g_0 = g(M)$, vanishes asymptotically. Conversely there is a scale at which the coupling begins to diverge, even from the naïve one loop calculation. This is not obvious from (2.9) and the scale at which the theory becomes very strongly coupled is not determinable from first principles, being generated by the dynamics of the theory itself! We can however estimate it from experiments, which give a typical determination of $\Lambda_{QCD} \sim 200 - 300$ MeV. It is at energy scales μ below Λ_{QCD} that the theory is its most mysterious!

Perhaps a sensible avenue of approach to QCD at long distances is to discuss the symmetries of the theory. As mentioned previously there is a local, or *gauge*, symmetry under $SU(3)$ transformations that forms the backbone of QCD. This is not the only symmetry that the theory possesses! It is invariant under Lorentz transformations, and under the combined actions of charge conjugation (C), parity (P), and time reversal (T), known collectively as CPT. There is also an approximate $SU(3)$ *flavour symmetry*. The interactions in QCD are “flavour blind” in that they treat the six quark flavours identically, the real difference comes down to the quark masses. The three lightest quarks: the up, down and strange; all have masses that are small compared to typical nuclear binding energies, and thus there is an approximate $SU(3)$ global symmetry that rotates between them. This is a different symmetry from the local $SU(3)$ colour gauge symmetry that the quarks are charged under. A consequence of this is that the mesonic bound states of quarks and anti-quarks arrange themselves into a representation of this symmetry, the so-called *eightfold way* [16, 17, 18]. Within this $SU(3)$ symmetry is an $SU(2)$ subgroup of rotations between the up and down quarks dubbed *isospin*⁹. This is due to the difference in masses between the up and down quarks, around ~ 2 MeV and ~ 5 MeV respectively, compared to the strange quark which weighs in at ~ 95 MeV. Whilst these are only approximate symmetries, they proved to be effective organising principles for the slew of QCD bound states discovered at collider experiments in the mid 20th century. In the limit that we take the quarks to be massless, the QCD Lagrangian has an enhanced $U(N_f)_R \times U(N_f)_L$ *flavour-chiral* symmetry, which will play a large role in the discussion to come. This particular symmetry is interesting because it is *dynamically broken*; meaning that while it is

⁹Historically, isospin was a symmetry between nucleons, though this later turned out to be a reflection of the approximate symmetry of their constituent quarks.

a symmetry of the Lagrangian, it is not a symmetry respected by the QCD vacuum. Still for the discussion of the low energy properties of QCD this symmetry is a good starting point. The $U(N_F)_L \times U(N_F)_R$ symmetry can be decomposed into $SU(N_F)_L \times SU(N_F)_R \times U(1)_B \times U(1)_A$, of the two $U(1)$ symmetries, only the $U(1)_B$ associated with the conservation of baryon number survives. The $U(1)_A$ symmetry, associated with axial transformations is broken by anomalies. Including a quark mass term, even one proportional to the identity, explicitly breaks the $SU(N_F)_L \times SU(N_F)_R$ to the diagonal subgroup $SU(N_F)_V$. This can be seen by the following, imagine a quark mass term in three flavour QCD

$$\bar{q}_{L,i} M_{ij} q_{R,j} + h.c. \quad (2.10)$$

where M_{ij} is a 3×3 matrix, and the i, j run over three quark flavours. Under an $SU(3)_L \times SU(3)_R$ transformation this term becomes

$$\bar{q}_L L^\dagger M_{ij} R q_R + h.c. \quad (2.11)$$

Taking a case where you have $M_{ij} \sim m\delta_{ij}$, then it becomes clear that the subgroup of these transformations that leaves this mass term invariant must also obey $L^\dagger R = \mathbf{I}_{3 \times 3}$, and thus we have the breaking of $SU(3)_L \times SU(3)_R$ to the ‘‘vector’’ subgroup $SU(3)_V$, though this is an explicit breaking of the symmetry. If this symmetry is spontaneously broken it will come along with a set of *Goldstone bosons*, one for each generator of the broken symmetry. The Goldstone bosons in this case are the light pseudoscalar mesons, which form an $SU(3)$ octet. So to examine this symmetry further, we should write down a Lagrangian consistent with the symmetries that describes the Goldstone bosons. This is commonly done in the form of a non-linear sigma model, known as *chiral perturbation theory* (for an introduction see [19]). We will start from a non-linear realisation of the chiral symmetry¹⁰, starting from an exponential of the eight Goldstone boson fields, noted π_a ,

$$U = \exp\left(2i\tilde{\Pi}/f\right), \quad (2.12)$$

with¹¹

$$\tilde{\Pi} = \pi_a T_a, \quad (2.13)$$

where U is both a unitary, and unimodular, 3×3 matrix; f is a constant with dimensions of mass; and the T_a are the generators of $SU(3)$. Requiring that U

¹⁰much of the following was taken from Howard Georgi’s book [20], which has a nice section on chiral Lagrangians

¹¹the overhead tilde will denote this contraction on $SU(3)$ indices in this section

transforms linearly under $SU(3) \times SU(3)$ we have

$$U \rightarrow U' = L U R^\dagger = \exp(2i\pi'_a T_a / f) \quad (2.14)$$

we may then parameterise the matrices L , and R as

$$L = e^{i\tilde{c}} e^{i\tilde{\epsilon}}, \quad R = e^{-i\tilde{c}} e^{i\tilde{\epsilon}}, \quad (2.15)$$

where the c_a and ϵ_a 's are real parameters. If $c_a = 0$, then the transformation

$$U \rightarrow L U R^\dagger = e^{i\tilde{\epsilon}} U e^{-i\tilde{\epsilon}} \quad (2.16)$$

is an ordinary $SU(3)$ transformation, and the ϵ_a 's parameterise the $SU(3)_V$ subgroup that is left unbroken. Conversely if the ϵ_a 's are set to zero then the transformation must be a purely chiral transformation, under which U transforms as

$$U \rightarrow U' = e^{2i\pi'_a T_a / f} = e^{i\tilde{c}} U e^{i\tilde{c}} \quad (2.17)$$

expanding the exponential functions in term of the matrices $\tilde{\Pi}$ and \tilde{c} , we see that

$$\tilde{\Pi}' = \tilde{\Pi} + f\tilde{c} \quad (2.18)$$

and the inhomogeneous term is a sign of the spontaneous breaking of the flavour-chiral symmetry to the vector subgroup. Writing the simplest Lagrangian that nonlinearly realises the $SU(3) \times SU(3)$ symmetry¹², to lowest order we have the two-derivative term

$$\frac{f^2}{4} \text{tr} (\partial_\mu U^\dagger \partial^\mu U) \sim \frac{1}{2} \partial_\mu \pi_a \partial^\mu \pi_a + \dots \quad (2.19)$$

where the prefactor $f^2/4$ is chosen to canonically normalise the kinetic term for the Goldstone modes, and the higher order terms include the self-interactions of the Pions. Including classical sources in the Lagrangian for massless QCD we have

$$\mathcal{L} = \mathcal{L}_0^{QCD} + \bar{q} \gamma^\mu (v_\mu + a_\mu \gamma_5) q - \bar{q} (s + ip \gamma_5) q \quad (2.20)$$

or written in terms of the chiral quark variables

$$\mathcal{L} = \mathcal{L}_0^{QCD} + \bar{q}_L \gamma^\mu l_\mu q_L + \bar{q}_R \gamma^\mu r_\mu q_R - \bar{q}_R (s + ip) q_L - \bar{q}_L (s - ip) q_R \quad (2.21)$$

¹²to avoid introducing extra fields that do not describe the Goldstone modes

where the $l_\mu = v_\mu + a_\mu$, and $r_\mu = v_\mu - a_\mu$ act as classical gauge fields for the $SU(3)_L$ and $SU(3)_R$ symmetries respectively, transforming as

$$\begin{aligned} r_\mu &\rightarrow Rr_\mu R^\dagger + iR\partial_\mu R^\dagger \\ l_\mu &\rightarrow Ll_\mu L^\dagger + iL\partial_\mu L^\dagger \\ s + ip &\rightarrow R(s + ip)L^\dagger \end{aligned} \quad (2.22)$$

we must also include these in the low energy effective theory, if we are to properly discuss symmetry breaking, and the *pseudo-Goldstone* nature of the light mesons. Generically we will have some Lagrangian that is $\mathcal{L} = \mathcal{L}(U, r, l, s, p)$, naturally the derivatives in (2.19) should be promoted to covariant derivatives to reflect the introduction of the gauge fields l_μ, r_μ . The unique lowest order term that includes the s, p and U is

$$v^3 \text{tr}(U(s + ip)) + h.c. \quad (2.23)$$

With the constant v added in on dimensional grounds. We can see from (2.21) that the combination $s + ip$ mixes the left and right handed quarks, and so acts like a mass term. Setting $s = \text{diag}(m, m, M)^{13}$ and $p = 0$, and expanding U in powers of $\tilde{\Pi}$ yields at lowest order a term quadratic in Π

$$\mathcal{L} \supset -4\frac{v^3}{f} \text{tr}(s\tilde{\Pi}^2) \quad (2.24)$$

which is the mass term of a scalar field theory $-\frac{1}{2}m^2\phi^2$. Writing explicitly the matrix $\tilde{\Pi}$ in terms of the pseudoscalar meson octet, we have

$$\tilde{\Pi} \sim \begin{pmatrix} \pi^0 + \eta/\sqrt{6} & \pi^+ & K^+ \\ \pi^- & -\pi^0 + \eta/\sqrt{6} & K^0 \\ K^- & \bar{K}^0 & -2\eta/\sqrt{6} \end{pmatrix} \quad (2.25)$$

expanding this in terms of the fields π_a , particularly for the pion, reveals that

$$m_\pi^2 = 4\frac{v^3}{f^2}m. \quad (2.26)$$

This is the Gell-Mann-Oakes-Renner relation, and tells us that for small quark masses, the square of the pion mass is linear in the quark mass. This will appear frequently later when we discuss the holographic models of Chapters 4 and 5, and is characteristic pseudo-Goldstone bosons.

There is much more that could be discussed within the remit of chiral perturbation

¹³this is the limit of isospin invariance, with small $m_u = m_d \neq m_s$

theory, inclusion of higher orders in the momenta presents a phenomenologically viable model of low energy QCD in terms of the psuedo-scalar mesons. Interestingly, this model presents the possibility of studying single baryon systems which appear as soliton (this is discussed in some detail in the context of QCD here [21]). A non-trivial field configuration, that whilst satisfying the equations of motion, does not have zero action. Solitons, and instantons, in gauge theories present their own subfield of theoretical physics that is well developed and will not be discussed here¹⁴. Indeed there are a few more relevant areas that should be mentioned in this chapter before moving on, the next of which will be the large N limit of Yang-Mills theories [22].

2.2 Large N

The idea behind the large N limit, is to imagine that one has a Yang-Mills theory, gauged under $SU(N)$, where both the number of colours N and the gauge coupling g are arbitrary parameters that one can choose at will, and quark multiplets transforming in the fundamental representation of $SU(N)$. The Lagrangian associated with such a theory is, with the colour indices, i, j written explicitly,

$$\mathcal{L} = -\frac{1}{4}(F_{\mu\nu})_i{}^j (F^{\mu\nu})_j{}^i + \sum_f \bar{\psi}_i^f (i\not{D} - m)\psi^{i,f}. \quad (2.27)$$

Where there is a gauge covariant derivative, defined similarly to 2.2 but with $N^2 - 1$ “gluon” fields and the $N^2 - 1$ generators t_a of $SU(N)$, and $F_{\mu\nu}$ is a field strength tensor defined as the commutator of gauge covariant derivatives (as in (2.5)). The Feynman rules for this theory can then be written in terms of oriented sets of lines (and famously double lines), which show the contraction of colour indices. A diagrammatic representation of the vertices in large N QCD is displayed in Figure 2.3. Including c-number sources on the external legs, which functionally ties up external lines, the Feynman diagrams become sets of polygons stuck on a two dimensional surface. Gluon lines, noted by the double solid lines then act like rules for gluing the polgyons together, into a solid surface. Wherever a colour line is closed, the diagram picks up a combinatoric factor of N . This closed line can be counted by the number of faces of the various polygons on the two dimensional surface. Each vertex in the theory carries a similar combinatoric factor of N , and the edges carry a factor of $1/N$. Naïvely counting the powers of N in a diagram

¹⁴this thesis needs to be a reasonable length after all.

with V vertices, E edges, and F faces, one arrives at

$$\text{power of } N \text{ multiplying the diagram} = N^{F+V-E} \quad (2.28)$$

This combination $F + V - E$ is the famous Euler characteristic, χ , of a surface and is a topological invariant. It can alternatively be written as $\chi = 2 - 2g$, where g is the genus of a surface, and so

$$N^{F+V-E} = N^{2-2g}, \quad (2.29)$$

and we see that the diagrams arrange themselves not by powers of gauge couplings, or number of loops, but by the topology of the diagrams themselves! In this limit, the leading diagrams are not the tree level, but the planar diagrams. That is, diagrams with genus zero. This is a striking feature of the large N limit of gauge theories, and is a first hint of the emergence of stringy behaviour. In string theories, the perturbation series for calculating the scattering of string states comes with powers of the string coupling g_s that increase with the genus of the string worldsheet, though this will be discussed more in the next chapter. Indeed it is still anticipated that true dual of large N Yang-Mills theory, or QCD, at strong coupling is likely a non-critical string theory living in some five dimensional space [23]. This is not the only sign of string-like physics in QCD. Studies of QCD on the lattice reveal that tubes of chromoelectric flux stretch between spatially separated quarks and anti-quarks. This picture originates from the “dual superconductor” picture of the QCD vacuum, where confinement is the product of the condensation of chromomagnetic charges which cause the confinement of electric flux akin to the confinement of magnetic flux in the BCS theory of superconductors [24, 25].

2.3 Confinement

The final aspect of QCD that we will discuss in this chapter, having been mentioned off-handedly before, is confinement. At collider experiments, only colour singlet states such as mesons and baryons have been detected as asymptotic states. This is a property of QCD for which the evidence is almost purely experimental, and experimental searches have produced no evidence of free quarks [26]. Lattice QCD provides numerical results which support the claim that quarks are confined. A paper written by Wilson [5] discusses confining behaviour in terms of non-local gauge invariant operators, called Wilson loops. The Wilson loops are defined as

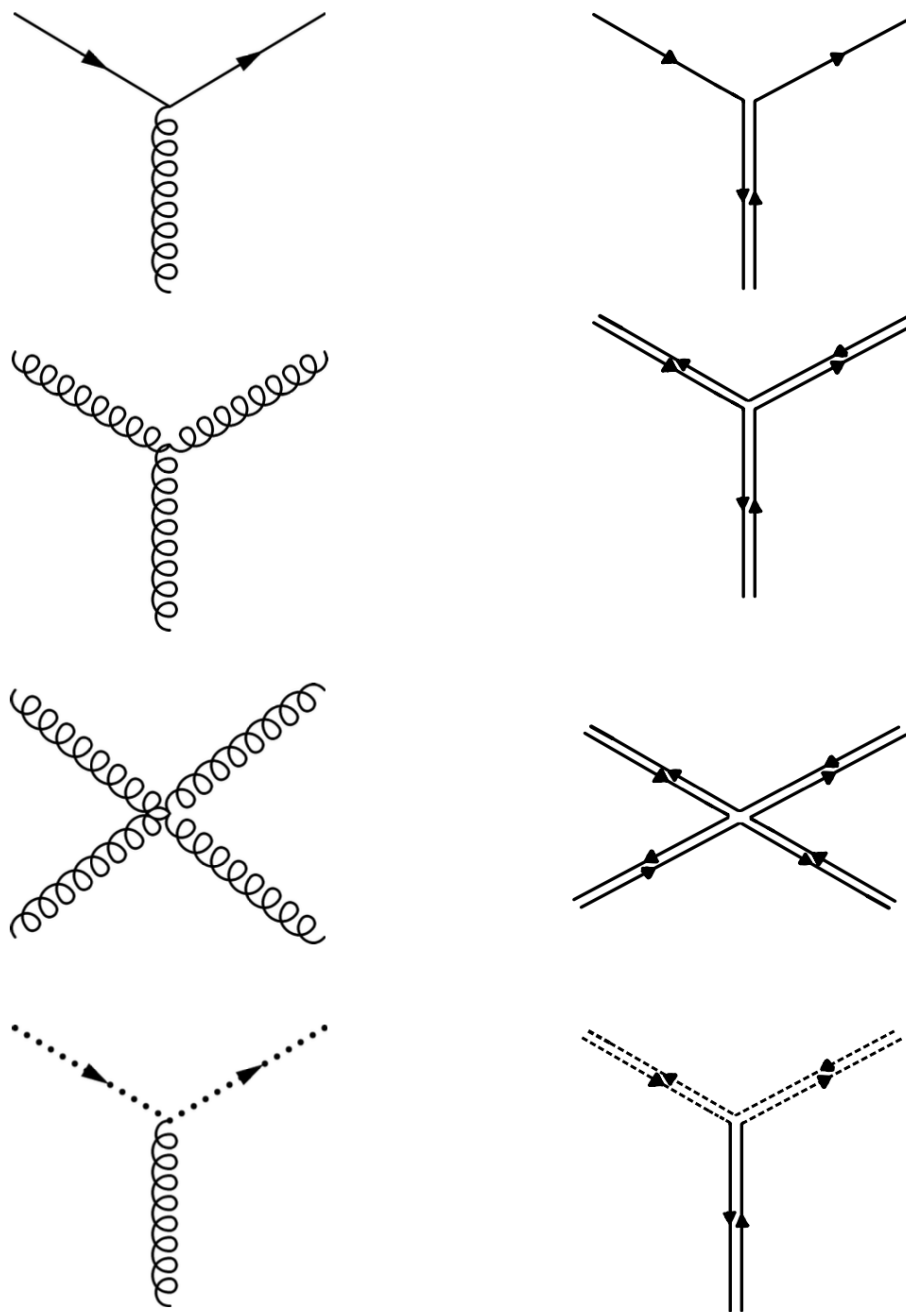


FIGURE 2.3: Vertices in QCD (Left), and their analogue at large N (Right)

the trace of path ordered integrals of gauge fields around a closed loop¹⁵, or

$$W[\gamma] = \text{tr} \left(\mathcal{P} \exp \left[i \oint_{\gamma} A_{\mu} dx^{\mu} \right] \right), \quad (2.30)$$

where γ is a closed path in the background space. This operator acts as an order parameter of theory, where its expectation value characterises the phase of the

¹⁵or as the trace of the holonomy of the gauge connection

theory¹⁶. In this case, we are interested in whether the theory is in a confined, or deconfined phase. For example in pure Yang-Mills theory the expectation value for the Wilson loop gives an *area law* in the confined phase,

$$\langle W[\gamma] \rangle \propto e^{-A[\gamma]} \quad (2.31)$$

where $A[\gamma]$ is the area enclosed by the loop γ ; and a *perimeter law* in the deconfined (or Higgs) phase

$$\langle W[\gamma] \rangle \propto e^{-L[\gamma]} \quad (2.32)$$

where similarly $L[\gamma]$ is the length of the loop γ . To motivate the first of these results consider a rectangular Wilson loop, in the (t, x) plane, with sides R, T and $T \gg R$. In axial gauge¹⁷ we have $A_0 = 0$ and only the component in the x axis contributes to the Wilson loop,

$$\langle W[\gamma] \rangle = \left\langle \mathcal{P}exp \left[i \int_0^R A_1(t=0) dx^1 - i \int_R^0 A_1(t=T) dx^1 \right] \right\rangle. \quad (2.33)$$

Writing this in a slightly different notation, with

$$\Psi_{ij}(t) = \mathcal{P}exp \left[i \int_0^R A_1(t) dx^1 \right]_{ij} \quad (2.34)$$

where i, j are $SU(3)$ indices, we have

$$\langle W[\gamma] \rangle = \langle \Psi_{ij}(t=0) | \Psi_{ij}^\dagger(t=T) \rangle. \quad (2.35)$$

By inserting a complete set of states we have

$$\langle W[\gamma] \rangle = \sum_n \langle \Psi_{ij}(0) | n \rangle \langle n | \Psi_{ij}^\dagger(T) \rangle = \sum_n |\langle \Psi_{ij}(0) | n \rangle|^2 e^{-E_n T} \quad (2.36)$$

and at very long times, the dominant contribution is the ground state so

$$\langle W[\gamma] \rangle \propto e^{-E_0 T}. \quad (2.37)$$

A characteristic of the confining phase is that the potential between two spatially separated quark anti-quark pairs grows linearly, $V(r) \sim \sigma r$, with thier separation

¹⁶This is true in pure Yang-Mills theory, however light quarks can break extended Wilson lines/loops. So *formally* there is no order parameter in a theory with light quarks.

¹⁷This argument comes from a nice review of Wilson loops and large N written by Yuri Makeeno [27]

r . Thus if we attribute the rectangular Wilson loop to the interaction of a separated quark anti-quark pair we have $E_0 = V(R) \sim \sigma R$, and

$$\langle W[\gamma] \rangle \sim e^{-\sigma RT} = e^{-\sigma A}. \quad (2.38)$$

The variable σ has dimensions of energy per unit length, and is called the QCD string tension. We will see a *holographic* representation of this area law in the next chapter.

2.4 Summary

This chapter has been a lightning review of some of the salient features of quantum chromodynamics. It is by no means comprehensive, but has touched upon some of the aspects that make QCD particularly fascinating. Starting by writing the QCD Lagrangian, and showing the interaction vertices, and going from there to sketch the famous β function calculation which reveals the asymptotic freedom of the theory. We then discuss the symmetry structure of the theory, stopping for a while to examine the *flavour-chiral* symmetry that the Lagrangian enjoys in the chiral limit, and talk about how it is broken by the QCD vacuum, with an aside on chiral Lagrangians to uncover the Gell-Mann-Oakes-Renner relation that we will later come across in a holographic setting. The next significant thing to talk about, particularly for later discussion, is the large N limit of Yang-Mills theories and QCD. In this limit the leading contributions in the perturbation series come from planar diagrams (which can be drawn on a two dimensional surface of genus zero). Lastly we discuss perhaps the most mysterious feature of QCD from a theoretical perspective, colour confinement. Whilst the mechanism behind confinement remains a mystery from a theoretical perspective, we know how to characterise the confined phase in terms of Wilson loops, which act as order parameters for the confined phase.

The next chapter will go on to cover some of the necessary ingredients of string theory, and the AdS/CFT correspondence¹⁸. We will see direct holographic interpretations of the phenomena mentioned in this chapter, such as confinement and chiral symmetry breaking, which manifest geometrically in the dual gravity theory.

¹⁸or gauge/gravity correspondence, or holography, as the reader prefers.

Chapter 3

Strings, Branes and Supergravity

This chapter will be devoted to the discussion of the aspects of string theory that are required for understanding holographic approaches to QCD. We will begin with a short reflection on the history of string theory, before going on to discuss the spectrum of the bosonic string; showing that the lowest lying modes on the open string describe spin one gauge fields, and that the low energy modes on the closed string include a massless spin two field that can describe the graviton. In requiring that these modes are massless it is revealed that string does not live in the familiar four dimensions that are expected at low energies, but in 26 dimensions. From here we will go on to discuss the addition of fermionic degrees of freedom to the theory in the form of the superstring. Introducing fermions, reduces the number of dimensions required for the theory to be consistent from 26 to 10. Some time will be spent on the introduction of D-branes, which are non-perturbative states in string theory first identified by Polchinski in 1995 [28] (though p -branes had been identified as solitonic objects allowed in supersymmetric theories of gravity earlier). These objects brought with them the second superstring revolution and lead to the construction of more realistic low energy effective theories from the various string theories. They break half the supersymmetries of the parent theory, and host string states that are restricted to live on a hypersurface within the 10 dimensional bulk space. These are key ingredients necessary to come to the most significant topic in this section, holographic duality¹. We will present the results in [9] leading to the famous AdS/CFT conjecture, that type IIB string theory on $AdS_5 \times S^5$ is dynamically equivalent to maximally supersymmetric Yang-Mills theory in four dimensions. We will then highlight some of the key results that have built on top of this conjecture in the nearly 26 years since its advent. One

¹at least so far as this thesis is concerned

such key result is the addition of probe branes in the supergravity theory, which represent the inclusion of fundamental matter supermultiplets in the dual gauge theory. This already pushes the AdS/CFT correspondence closer to being able to describe the gauge theories that are testable in terrestrial collider experiments (that is we can reduce the amount of supersymmetry, and can include dynamical quarks). Lastly we will discuss some of the features that a gravity dual must possess if it is to describe QCD at low energies, namely that there is a holographic representation of confinement, and chiral symmetry breaking.

3.1 Early History and the Bosonic String

String theory emerged from the S-matrix program of the mid twentieth century. Attempts were underway to *bootstrap* the underlying scattering amplitudes, or elements of the S-matrix, from simple consistency conditions without relying on some microscopic Lagrangian that describes the elementary degrees of freedom. In a 1968 paper by Veneziano [29] an amplitude for meson scattering was presented, which had the properties that it was symmetric under interchange of the s , t and u channels, where s , t , and u refer to the Mandelstam variables of four-particle scattering. The s channel can be interpreted as two particles, coming together to form an intermediate state which decays into the two final states. The energy of the two initial particles in the centre of mass frame is \sqrt{s} . Similarly, the t and u channels can be thought of as two initial particles interacting by exchange of an intermediate state, and in these cases the four-momentum transfer by the intermediate particle is \sqrt{t} , and \sqrt{u} respectively. The amplitude also displays the expected *Regge* behaviour, that the masses of particles lie on *Regge trajectories*, increasing linearly with their angular momentum. This was the first of the *dual resonance models*, which were early attempts at an S-matrix theory of strong interactions. Ultimately these models were dropped in favour of Quantum Chromodynamics for a myriad of reasons, but among them is that the amplitudes were far too soft in the ultraviolet regime to describe the scattering of ordinary particles. This is however because they were not describing the scattering of ordinary particles but of open string states. This identification can be attributed to Nambu (the papers are reprinted in [30]), Susskind [31], and Nielsen [32]. The present view of string theory is vastly different from its original conception as a theory of hadrodynamics. It was realised that the formula of Virasoro [33], written shortly after the Veneziano amplitude and constructed with similar properties, described the scattering of closed string states. Among the closed string states is a massless spin two particle which is

not a desirable feature of a theory of the strong interaction. Alongside this it was realised that the model comes with a *critical dimension* [34]², a natural number of physical spacetime dimensions that the model lives in, where dynamics simplify. In this case it was noted that unless the model lived in 26 spacetime dimensions, the theory would not have space-time Lorentz symmetry. These features, and the aforementioned rise of QCD, meant that string theory fell from grace as a model of hadrons. However, it is precisely these properties that make it a candidate theory of *quantum gravity*. In a 1974 paper by Scherk and Schwarz [35] it was realised that fluctuations on the closed string had the right properties to be a candidate *graviton*, and that in a low energy limit general relativity emerged from the theory³. Moreover, with the inclusion of massless vector degrees of freedom, it was suggested that string theory might be a candidate unified theory of gravity with electroweak interactions. In the six short years between the advent of dual resonance models, there was an abundance of papers, that took us from a model of Hadrodynamics, to a potential theory of unified interactions. It would be another ten years before the landmark paper of Green and Schwarz [36] which, by examining anomaly cancellation in the type I superstring, recognised that the gauge anomalies only cancel if the gauge group is either $SO(32)$ or $E_8 \times E_8$. Both of these groups are large enough to contain the standard model gauge group as a subgroup, and thus the superstring may be a theory that unifies all the fundamental forces of nature, and the matter contents. This began a period in time known as *the first superstring revolution*, and by 1985 there were five, seemingly distinct, superstring theories: Type I, Type IIA, Type IIB, Heterotic $SO(32)$, and Heterotic $E_8 \times E_8$. In 1989, two critical pieces of the puzzle were uncovered by Polchinski, Dai, and Leigh in the paper [37]; which posited that the IIA, and IIB theories *T-dualise* on tori to one another, and discovered the *D-brane*⁴. Another ten years later, in 1995, these D-branes would be identified with the solitonic *p-brane* solutions in type II supergravity [28]. Around this time it was realised by Witten that the five superstring theories, could be considered different limits of another theory, which he dubbed *M-theory* [39]. To this day, a suitable description of M-theory in terms of its microscopic degrees of freedom remains unfound, however its low energy limit is thought to be *eleven dimensional supergravity*⁵. Strikingly, eleven dimensional supergravity has no strings at all. It does contain a

²I would like to note that due to writing this out of sequence, there was a point where this was reference number 26, and it made me smile

³with an extra scalar

⁴D-branes were also discovered independently by Hořava [38] at the same time

⁵An interesting note here is that eleven dimensions is the largest number of dimensions it is possible to formulate a supersymmetric theory.

two, and five, dimensional membrane; which when properly compactified on torii, give the D-branes of the type II string theories. Not only that, but the approach from eleven dimensional supergravity seemingly predicts the RR charge/tension of the type II D-branes. This sparked the *second superstring revolution*. The last milestone that will be mentioned in this brief retrospective, is the 1997 paper by Maldacena [9], which sets out the AdS/CFT correspondence. This paper would go on to become the most cited paper in the history of high-energy physics, and would carve out a new discipline examining the dualities between gauge theories and gravity.

The quick historical tangent also sets out somewhat the path we will take through the introductory material. We will start by looking at the Nambu-Goto and Polyakov actions for the classical relativistic string, before examining its first quantisation⁶.

3.1.1 Classical Bosonic Strings

Since the strings are extended objects, we will need a method by which to discuss their motion. In the case of a classical point particle, we can consider the trajectory that they trace out via their time evolution, $x^\mu(\tau)$. This is the particle's *worldline*, and is a map from some internal variable τ to the d -dimensional spacetime the particle propagates in. We can consider the equivalent for strings, which is the *worldsheet*. Given that the path traced out by the string is a two-dimensional surface, we will need to parameterise it by a pair of variables σ^i , with $i = 0, 1$. Generally we will consider these to be the worldsheet time σ^0 , and position along the length of the string σ^1 . The analogous embedding functional is then $x^\mu(\sigma^0, \sigma^1)$, which is a map from a point on the worldsheet to a position in the bulk spacetime. Strings are tensionful objects, and as such will aim to reduce the area of their worldsheet. The action functional that implements this most obviously is the *Nambu-Goto* action,

$$S_{NG} = -T \int \sqrt{-\det \tilde{g}} d^2\sigma = -T \int d^2\sigma \sqrt{-\det \left(g_{\mu\nu} \frac{\partial x^\mu}{\partial \sigma^a} \frac{\partial x^\nu}{\partial \sigma^b} \right)}. \quad (3.1)$$

In this equation, $g_{\mu\nu}$ is the metric of the spacetime in which the strings propagate, and \tilde{g} is the *pullback* of the bulk metric to the string worldsheet. This action functional is just the proper volume integral on a two dimensional surface, the worldsheet, living in a higher dimensional curved space. We can make note of

⁶the following section largely follows the analysis in chapter 2 of Becker, Becker, Schwarz [40]

an interesting property of the string without further calculation, it is reparameterisation invariant! Meaning that upon a change of worldvolume co-ordinates $\sigma^i \rightarrow \tilde{\sigma}^i(\sigma)$ the action remains unchanged, making this a symmetry of the theory⁷. However, this action is incredibly difficult to quantise due to the presence of the square root. Fortunately, there is another action that is classically equivalent the *Polyakov action*, or *string sigma-model action*,

$$S = -\frac{T}{2} \int d^2\sigma \sqrt{-\det h} h^{ab} g_{\mu\nu} \partial_a x^\mu \partial_b x^\nu. \quad (3.2)$$

This action includes an auxiliary field h_{ab} which, is identified with the *worldsheet metric*. This field has no kinetic term, and as such is non-dynamical. This automatically implies that the worldsheet energy momentum tensor T_{ab} vanishes. Concretely,

$$T_{ab} = -\frac{2}{T} \frac{\delta S}{\delta h^{ab}} = 0, \quad (3.3)$$

where the $\frac{\delta S}{\delta h^{ab}}$ denotes the functional differential of the action with respect to the worldsheet metric. Performing the functional differential, this evaluates to

$$T_{ab} = \partial_a x \cdot \partial_b x - \frac{1}{2} h_{ab} h^{cd} \partial_c x \cdot \partial_d x = 0, \quad (3.4)$$

or more usefully,

$$\partial_a x \cdot \partial_b x = \frac{1}{2} h_{ab} h^{cd} \partial_c x \cdot \partial_d x. \quad (3.5)$$

In these two formulae, the \cdot represents the contraction on the bulk spacetime indices on the embedding fields x^μ . Taking the (-ve) determinant of both sides we have

$$-\det \tilde{g} = \frac{1}{2} (-\det h) (h^{cd} g_{\mu\nu} \partial_c x^\mu \partial_d x^\nu)^2. \quad (3.6)$$

Taking the square root of both sides reveals that the integrand of (3.1) and (3.2) are equal when h_{ab} is set on its equation of motion. Therefore (3.1) and (3.2) are equivalent descriptions of the classical relativistic string. The real bonus here is that the string sigma model action is much simpler to work with! It is easier to quantise due to the lack of square roots, and reveals an interesting facet of the classical string. If we take the worldsheet metric to be a two dimensional Minkowski

⁷this is just a property of proper volume elements. They are defined such that any Jacobian factor induced by the integral measure is counteracted by the one induced by the determinant of the metric, which is a tensor density.

metric, which is equivalent to a choice of gauge using the reparameterisation symmetry of the string worldsheet^{8,9}, and we examine the string in a d-dimensional Minkowski background spacetime then we have

$$S = -T \int d^2\sigma \frac{1}{2} \eta^{ab} \partial_a x \cdot \partial_b x. \quad (3.7)$$

This is the Lagrangian for a collection of massless scalar fields in two dimensions. The classical equations of motion are then

$$\partial_a \partial^a x^\mu = 0. \quad (3.8)$$

The fields x^μ are also subject to the constraint that the worldsheet energy momentum tensor vanishes,

$$T_{10} = T_{01} = \partial_0 x^\mu \partial_1 x_\mu = 0, \quad (3.9)$$

and

$$T_{00} = T_{11} = \frac{1}{2} (\partial_1 x^\mu \partial_1 x_\mu + \partial_0 x^\mu \partial_0 x_\mu) = 0. \quad (3.10)$$

The last ingredient to add before being able to solve the classical equations of motion, is that since strings have a finite spatial extent, one must carefully consider the allowed boundary conditions at the edges of the worldsheet. Usually when solving classical field equations, it is sufficient to require that the fields fall off at spatial infinity (or at an asymptotic boundary). In this case, the string endpoints are not infinitely far away, and we must carefully consider what happens at the edges of the string. Taking the worldsheet spatial parameter to be $\sigma \in \{0, \pi\}$. There are three cases to consider. The first is the closed string. Taking the embeddings to be periodic with respect to the worldsheet spatial co-ordinate $x^\mu(\sigma, \tau) = x^\mu(\sigma + \pi, \tau)$ one does away with the necessity for boundary conditions, because there are no spatial boundaries. Secondly, there are open strings with two types of allowed boundary conditions: Neumann and Dirichlet. At the spatial boundary the Neumann condition is $\partial_\sigma x^\mu = 0$ at $\sigma = 0, \pi$, and the Dirichlet condition is $x^\mu = a^\mu$ at $\sigma = 0$, and $x^\mu = b^\mu$ at $\sigma = \pi$ with a, b being arbitrary constant vectors. The Dirichlet condition implies that the string endpoints are stuck in

⁸The caveat here is that we are considering worldsheets that have vanishing Euler characteristic, though we'll get to this a bit later

⁹Also in 1 + 1 dimensions, Einstein gravity is purely topological. The Einstein-Hilbert action is total derivative and evaluates to the Euler character of the surface. So even the choice of metric is not particularly consequential.

place, interestingly this was initially considered unphysical, and the Dirichlet condition would initially be neglected in favour of solely working with closed strings or a Neumann boundary condition. In part this is because the Dirichlet condition seemingly allows momentum to flow off the end of the string. Clearly this is unphysical, unless there is another object there that the momentum is transferred to, which is where D-branes come into the picture [37]. One way to think about these objects is as a hypersurface on which strings may end, satisfying a Dirichlet condition (having their endpoints on the brane). In this vein, it is also possible to have *mixed* boundary conditions, with a Neumann condition at one end of the string, and a Dirichlet condition at the other. These mixed boundary conditions are important when discussing intersections of D-branes. The discussion of branes will be largely relegated to the penultimate section of this chapter. The resulting equations of motion, from solving (3.8), subject to constraints from the vanishing of the worldsheet energy momentum tensor (3.9), (3.10) and the appropriate boundary conditions follow straight-forwardly. We will first discuss the closed string, which has classical solutions,

$$x^\mu = x_c^\mu + \alpha' p_c^\mu \tau + \frac{i}{2} \alpha'^{1/2} \sum_{n \neq 0} \frac{1}{n} (\alpha_n^\mu e^{-2in(\tau-\sigma)} + \tilde{\alpha}_n^\mu e^{-2in(\tau+\sigma)}). \quad (3.11)$$

Where an important parameter α' has been introduced, the *string Regge slope parameter*, which is related to the length scale of fundamental strings $l_s = \sqrt{\alpha'}$. At a first glance this looks complicated, but the terms are x_c , an initial reference position, $\alpha' p_c^\mu \tau$ the displacement of the string “centre of mass” from the initial position, and the last term encodes the oscillations of the string. The requirement that x^μ is real, that it represents a position, forces the following property of the oscillator modes

$$(\alpha_n^\mu)^* = \alpha_{-n}^\mu \quad \text{and} \quad (\tilde{\alpha}_n^\mu)^* = \tilde{\alpha}_{-n}^\mu. \quad (3.12)$$

It is convenient to decompose this into a left-moving and right-moving sector

$$x_R^\mu = \frac{1}{2} x_c^\mu + \frac{1}{2} \alpha' p_c^\mu (\tau - \sigma) + \frac{i}{2} \alpha'^{1/2} \sum_{n \neq 0} \frac{1}{n} \alpha_n^\mu e^{-2in(\tau-\sigma)}, \quad (3.13)$$

and

$$x_L^\mu = \frac{1}{2} x_c^\mu + \frac{1}{2} \alpha' p_c^\mu (\tau + \sigma) + \frac{i}{2} \alpha'^{1/2} \sum_{n \neq 0} \frac{1}{n} \tilde{\alpha}_n^\mu e^{-2in(\tau+\sigma)}. \quad (3.14)$$

Functionally, this is also a move to light-cone gauge on the string, with $\sigma^\pm = \tau \pm \sigma$. This allows us to package the solutions nicely in the form

$$\partial_+ x_R^\mu = 0, \quad \partial_- x_R^\mu = \alpha'^{1/2} \sum_{n=-\infty}^{\infty} \alpha_n^\mu e^{-2in\sigma^-}, \quad (3.15)$$

and

$$\partial_- x_L^\mu = 0, \quad \partial_+ x_L^\mu = \alpha'^{1/2} \sum_{n=-\infty}^{\infty} \tilde{\alpha}_n^\mu e^{-2in\sigma^+}, \quad (3.16)$$

if we identify a common oscillator zero mode for the left and right movers,

$$\alpha_0^\mu = \tilde{\alpha}_0^\mu = \frac{1}{2} \alpha'^{1/2} p_c^\mu. \quad (3.17)$$

In order to quantise the theory, we must identify the symplectic structure that defines the classical theory. To do so the canonical momentum conjugate to x^μ is introduced,

$$p^\mu = \frac{\delta S}{\delta(\partial_\tau x_\mu)} = \frac{1}{2\pi\alpha'} \partial_\tau x^\mu, \quad (3.18)$$

and the Poisson brackets, $\{\cdot, \cdot\}_{PB}$, of the theory can be defined. They are, at equal time,

$$\{p^\mu, p^\nu\}_{PB} = \{x^\mu, x^\nu\}_{PB} = 0, \quad (3.19)$$

$$\{p^\mu(\sigma, \tau), x^\nu(\sigma', \tau)\}_{PB} = \eta^{\mu\nu} \delta(\sigma - \sigma'). \quad (3.20)$$

By inserting the solutions for x^μ we can write the above Poisson bracket in terms of the oscillator modes $\alpha, \tilde{\alpha}$. This is

$$\{\alpha_m^\mu, \tilde{\alpha}_n^\nu\}_{PB} = 0, \quad (3.21)$$

and

$$\{\alpha_m^\mu, \alpha_n^\nu\}_{PB} = \{\tilde{\alpha}_m^\mu, \tilde{\alpha}_n^\nu\}_{PB} = im\eta^{\mu\nu} \delta_{m,-n}, \quad (3.22)$$

respectively. The theory can be quantised by promoting the oscillators to operators, and replacing the Poisson brackets with commutators of operators. It should be noted here that the open string with Neumann boundary conditions at both ends is very similar, with the caveat that there is only one set of oscillators, because the boundary condition at the string end-points functionally reflects the right-movers into the left-movers. The Neumann condition also projects out the sinusoidal component of the exponential functions in (3.11).

3.1.2 Quantum Bosonic Strings

Replacing the Poisson brackets by the commutation relations $-i\{\cdot, \cdot\}_{PB} \rightarrow [\cdot, \cdot]$, we have

$$[\alpha_m^\mu, \tilde{\alpha}_n^\nu] = 0, \quad (3.23)$$

and

$$[\alpha_m^\mu, \alpha_n^\nu] = [\tilde{\alpha}_m^\mu, \tilde{\alpha}_n^\nu] = im\eta^{\mu\nu}\delta_{m,-n}. \quad (3.24)$$

Rescaling the operators, defining¹⁰

$$a_m^\mu = \frac{1}{\sqrt{m}}\alpha_m^\mu, \quad (a_m^\mu)^\dagger = \frac{1}{\sqrt{m}}\alpha_{-m}^\mu \quad (3.25)$$

subject to $m \in \mathbb{Z}^+$, reveals that the commutation relations (3.24) are the commutator algebra of a set of d independent quantum harmonic oscillators, where d is the dimension of the spacetime,

$$[a_m^\mu, a_n^{\nu\dagger}] = \eta^{\mu\nu}\delta_{m,n}. \quad (3.26)$$

Thus the operators $a_m^{\mu\dagger}$, and a_m^μ are creation and annihilation operators, that respectively create and annihilate states on the string worldsheet, by acting on the vacuum state $|0\rangle$. There is however a glaring issue here, that the $\mu = 0$ index leads to negative norm states, which have $\langle 0|\alpha_m^0\alpha_m^{0\dagger}|0\rangle = -1$. This negative norm state must be eliminated from the theory to maintain unitarity! This hits upon some interesting facets of the quantum theory. Firstly, that not all states are created equal! There are consistency conditions that come from the vanishing of the worldsheet energy momentum tensor that must be obeyed by the quantum theory also. Secondly, quantisation promotes the mass of string states to being a mass operator, and we must deal with ambiguities arising from ordering of ladder operators before we can determine the mass of string states.

3.1.3 String Mass Formula, Level Matching, and Spectrum

Turning back to the classical theory for now, and working in light-cone gauge on the string worldsheet, by inserting the oscillator mode expansion (3.11) for the

¹⁰The algebra is the same for the tilde'd variables, but will not be rewritten.

closed string into (3.4) one arrives at the conditions

$$T_{--} = 4\alpha' \sum_{m=-\infty}^{\infty} L_m e^{-2im\sigma^-}, \quad T_{++} = 4\alpha' \sum_{m=-\infty}^{\infty} \tilde{L}_m e^{-2im\sigma^+}, \quad (3.27)$$

with Fourier coefficients

$$L_m = \frac{1}{2} \sum_{n=-\infty}^{\infty} \alpha_{m-n} \cdot \alpha_n, \quad \tilde{L}_m = \frac{1}{2} \sum_{n=-\infty}^{\infty} \tilde{\alpha}_{m-n} \cdot \tilde{\alpha}_n. \quad (3.28)$$

These coefficients are the generators of the *Virasoro algebra*. The vanishing of the energy momentum tensor implies that

$$L_m = \tilde{L}_m = 0, \quad \forall m \in \mathbb{Z}. \quad (3.29)$$

In particular the vanishing of the zero mode can be used to determine the mass of string states,

$$L_0 = \sum_{n=1}^{\infty} \alpha_{-n} \cdot \alpha_n + \frac{1}{2} \alpha_0^2 = \sum_{n=1}^{\infty} \alpha_{-n} \cdot \alpha_n + \alpha' p^2, \quad (3.30)$$

which in conjunction with the mass shell condition, $m^2 = -p_\mu p^\mu$, leaves

$$m^2 = \frac{1}{\alpha'} \sum_{n=1}^{\infty} \alpha_{-n} \cdot \alpha_n. \quad (3.31)$$

Of course there are contributions from both sets of Fourier coefficients, so for the closed string this should be extended to

$$m^2 = \frac{2}{\alpha'} \sum_{n=1}^{\infty} \alpha_{-n} \cdot \alpha_n + \tilde{\alpha}_{-n} \cdot \tilde{\alpha}_n. \quad (3.32)$$

Unfortunately while this holds for the classical string, the quantum string is plagued by *normal ordering ambiguities*. The operators in the quantum theory are defined to be normal ordered, with the annihilation operators to the right of the creation operators. This poses a particular problem for the zero mode L_0 (and \tilde{L}_0). Normal ordering of the zero mode

$$L_0 = \frac{1}{2} \sum_{n=-\infty}^{\infty} : \alpha_{-n} \cdot \alpha_n : := \frac{1}{2} \alpha_0^2 + \sum_{n=1}^{\infty} \alpha_{-n} \cdot \alpha_n, \quad (3.33)$$

is ambiguous. This ambiguity boils down to the question *which* α_0 *acts first*? The other Virasoro generators avoid this problem, and are nicely defined quantum operators which, as a result of the constraint that the worldsheet energy momentum tensor vanishes, must *annihilate the physical states*. Here one comes to the realisation that just because one can generate states with the action of the ladder operators, it does not mean they are physical! The states that obey the constraint equations, or in this case are annihilated by the Virasoro generators¹¹, live in the *physical Hilbert space* of the theory. A similar constraint for the zero mode must also exist, but in the quantum theory it is modified. One must include a *normal ordering constant* a , that makes the constraint well defined. As such we must have

$$(L_0 - a) |phys\rangle = (\tilde{L}_0 - a) |phys\rangle = 0. \quad (3.34)$$

Nicely, for the closed string, the normal ordering constant cancels for the difference of these operators acting on a physical state

$$(L_0 - \tilde{L}_0) |phys\rangle = 0. \quad (3.35)$$

This combination can be rewritten as

$$L_0 - \tilde{L}_0 |phys\rangle = \sum_{n=1}^{\infty} \alpha_{-n} \cdot \alpha_n - \tilde{\alpha}_{-n} \cdot \tilde{\alpha}_n |phys\rangle = 0. \quad (3.36)$$

When written in terms of the annihilation and creation operators, $\sum_{n=1}^{\infty} \alpha_{-n} \cdot \alpha_n$ is the familiar *number operator* of the quantum harmonic oscillator. Equation (3.36) can then be written in terms of the number operators N and \tilde{N} as

$$(N - \tilde{N}) |phys\rangle = 0, \quad (3.37)$$

which implies for the physical states, the number of left moving modes, is equal to the number of right moving modes. This is the *level matching condition* of the closed string, any physical states must have the same number of left movers as right movers. Returning to the string mass formula, it too must be corrected by the normal ordering constant a . The mass operator is therefore

$$m^2 = \frac{1}{\alpha'} \sum_{n=1}^{\infty} \alpha_{-n} \cdot \alpha_n - a = \frac{N - a}{\alpha'}, \quad (3.38)$$

¹¹Half of them in this case.

for the open string, and

$$m^2 = \frac{2}{\alpha'} \left(\sum_{n=1}^{\infty} \alpha_{-n} \cdot \alpha_n + \tilde{\alpha}_{-n} \cdot \tilde{\alpha}_n - 2a \right) = \frac{2N + 2\tilde{N} - 4a}{\alpha'}, \quad (3.39)$$

for the closed string. We can see the issues with the bosonic string now clearly. Imagine we would like the open string to have in its spectrum a massless spin one state. We would create this vector state, by acting on the vacuum by the creation operator

$$a_1^{\mu\dagger} |0\rangle = |A^\mu\rangle. \quad (3.40)$$

For this state to be massless, given that we have excited one mode on the open string $N = 1$ and thus $m^2 = \frac{1-a}{\alpha'}$, we must have $a = 1$. However immediately this can be problematic, this implies that the vacuum state is a tachyon, with mass $m^2 = -1/\alpha'$. Tachyonic states are not unfamiliar from field theories, indeed they arise in cases where you create states from the *wrong vacuum*, this signals an instability of the theory. The second problem¹² is that the first excited state of the closed string, which must have at least one left mover and one right mover is also massless,

$$a_1^{\mu\dagger} \tilde{a}_1^{\nu\dagger} |0\rangle = |T^{\mu\nu}\rangle, \quad (3.41)$$

but it has spin two. From the perspective of string theory as a theory of quantum gravity this is necessary! So for the bosonic string the massless states are a vector field on the open string and a spin two tensor field on the closed string. Generically any rank two tensor can be decomposed into three parts: a symmetric traceless part $g_{\mu\nu}$, *the graviton*; a totally antisymmetric part $B_{\mu\nu}$, *the Kalb-Ramond two-form*; and the trace ϕ , *the dilaton*. The Kalb-Ramond field, is an analogue of a gauge field that couples to the string. As one could write the coupling of a point particle to a gauge field as

$$-q \int A_\mu \frac{\partial x^\mu}{\partial \tau} d\tau, \quad (3.42)$$

equally one can write the coupling of this two form to a string as

$$\propto - \int B_{\mu\nu} \frac{\partial x^\mu}{\partial \sigma^0} \frac{\partial x^\nu}{\partial \sigma^1} d^2\sigma. \quad (3.43)$$

Infact we will later see that the appearance of p -forms in the spectrum is linked to the existence of p dimensional objects that couple to them electrically. Whilst the justification of wanting a massless spin one particle was invoked here to quickly see that such a string theory would have massless propagating spin two degrees

¹²At least from the perspective of theorists in the 60s

of freedom and tachyons, it is not actually a choice. In the quantum theory the Virasoro generators L_m obey the algebra

$$[L_m, L_n] = (m - n)L_{m+n} + \frac{c}{12}m(m^2 - 1)\delta_{m+n,0}, \quad (3.44)$$

which is the *Virasoro algebra* [41]. This is a central extension of the *Witt algebra* with central charge c . In the case of a collection of free bosons, we can relate the central charge with the number of spacetime dimensions. Examining the generators of spacetime Lorentz transformations, and requiring that the strings transform sensibly in the spacetime, leads to relations between the generators L_m and the condition that the normal ordering constant must be $a = 1$, and $d = 26$. In fact, there are several routes to this result, for example this is the number of dimensions that the negative norm states discussed earlier decouple from the theory [42]¹³. This string theory discussed to this point also lacks fermions! Describing nature requires that we have a model that includes fermions¹⁴. So the next step in our discussion of string theories will be the inclusion of fermions on the string worldsheet, introducing the *superstring*.

3.2 Superstring Theory

Interestingly, the superstring also began life as a dual resonance model. Among the issues with the Veneziano model, were that it described bosons but not fermions. A dual model for free fermions was concted in 1970 by Ramond [43]. Around the same time Neveu, and Schwarz were attempting to extend the original dual models by including anti-commutation relations [44]. Neveu and Schwarz would eventually combine their model with Ramonds, in what they would dub a quark model of dual pions [45]. This RNS model was later identified as a model of “spinning strings”¹⁵ [46], which propagates in ten spacetime dimensions [42]. The spinning string has many interesting properties, among them is that it contains the same number of bosonic degrees of freedom as fermionic degrees of freedom on the string worldsheet, which is an incarnation of *supersymmetry*¹⁶. Whilst this model has *manifest* supersymmetry on the worldsheet, it is not obvious that it possesses *spacetime supersymmetry*. The RNS model still has a tachyon, though this state

¹³Technically there are no ghosts in $d \leq 26$, because one can think of the lower dimensional theory as a subspace of the full 26 dimensional theory.

¹⁴and interactions between fermions and bosons for that matter.

¹⁵In the sense of intrinsic spin.

¹⁶In fact the dual model by Ramond includes the first *superalgebra* written down.

can be removed by performing a *GSO projection*, which removes a subset of the allowed states from the theory [47]. Not only does this project the tachyonic state out of the ground state, but it also makes the RNS spinning string, equipped with the GSO projection, *spacetime supersymmetric* [48, 49].

3.2.1 Spinning Strings, and the GSO Projection

The action functional that describes the RNS spinning string from the worldsheet perspective is¹⁷

$$S_{RNS} = -\frac{T}{2} \int d^2\sigma \sqrt{-h} (g_{\mu\nu} h^{ab} \partial_a x^\mu \partial_b x^\nu + 2i\alpha' g_{\mu\nu} \bar{\psi}^\mu \rho^a \partial_a \psi^\nu + F^\mu F_\mu). \quad (3.45)$$

There is a lot to unpack in this action, but the first thing to discuss is spinor representations. Generically on some curved d -dimensional manifold, co-ordinate transformations come packaged as elements of $GL(d, \mathbb{R})$, which does not admit spinor representations. However the manifolds we are most interested in are pseudo-Riemannian; so around each point on the manifold, there is a frame where the metric is locally Minkowski, and infinitesimal co-ordinate transformations belong to the group $SO(1, d-1)$ which does have spinor representations. So to appropriately describe fermions on a curved manifold, one has to transform to some locally flat frame, which we will do by the introduction of the vielbein formalism. The frame fields are defined such that,

$$g_{\mu\nu} = e_\mu^a e_\nu^b \eta_{ab}, \quad (3.46)$$

with μ, ν the *Einstein indices* associated to the full manifold, and a, b the *Lorentz indices* associated with the locally Minkowski patch. In this regard, the vielbein field swaps an Einstein index for a Lorentz index. A useful relation is that follows from the above is,

$$\det g = \det e \times \det e \times \det \eta, \quad (3.47)$$

and thus,

$$\sqrt{-\det g} = \det e \equiv e. \quad (3.48)$$

For this reason the vielbein are sometimes likened to the square roots of the metric. In this case our manifold is the two dimensional string worldsheet, so we will

¹⁷This section follows the conventions from *Blumenhagen, Lüst, and Theisen* [50], the discussion loosely follows their discussion of the classical fermionic string

introduce a *zweibein* such that

$$h_{ab} = e_a^c e_b^d \eta_{cd}. \quad (3.49)$$

Usually the metric on a two dimensional surface can be “gauged away” by using the reparameterisation symmetry of the strings, however this is only up to topological obstructions which become important when discussing interactions! The fields $\bar{\psi}^\mu, \psi^\mu$ are then two dimensional spinors on the string worldsheet, they carry indices of the bulk spacetime, but in this case it simply means that there are d spinors on the worldsheet (as with the d two dimensional scalars of the bosonic string). ρ^a is the analogue of the Dirac matrices for a two dimensional manifold. Generally the Dirac matrices satisfy a Clifford algebra defined on a flat space $\{\gamma^a, \gamma^b\} = \pm 2\eta^{ab}\mathbb{I}_d$, which clearly doesn’t hold for the full curved manifold. As such when we talk about the Dirac matrices on some general manifold, we mean the Dirac matrices supplanted with the appropriate vielbein $\gamma^\mu = e_a^\mu \gamma^a$. In this case on the string worldsheet, this is denoted ρ^a . The fields $\bar{\psi}, \psi$ are Dirac fermions on the worldsheet which can be decomposed into two *Majorana* fermions. When the fermions are on shell the *Majorana condition* implies that there are only d -propagating fermionic degrees of freedom, rather than $2 \times d$. So there are an equal number of bosonic and fermionic degrees of freedom on-shell. Off-shell is another matter, and here we must introduce the auxiliary field F^μ which carries d bosonic degrees of freedom but is non-dynamical, and as such these degrees of freedom vanish on-shell. The result is that both on- and off-shell the action (3.45) has *manifest worldsheet supersymmetry*¹⁸. The remainder of the action for the RNS spinning string is familiar, as it is identical to that of the bosonic string. A direct consequence of this is that the spinning string contains the spectrum of the bosonic string as a subset of its spectrum (though in a different number of dimensions). By considering the variation of (3.45) with respect to the new fermionic fields, we arrive at,

$$\rho^a \partial_a \psi^\mu = 0, \quad (3.50)$$

or in light-cone coordinates on the string worldsheet

$$\partial_- \psi_+^\mu = \partial_+ \psi_-^\mu = 0. \quad (3.51)$$

¹⁸it is not locally supersymmetric however, which requires an addition term in the action, that includes the worldsheet gravitino. This is then typically removed using a mix of reparameterisation on the worldsheet and gauge fixing.

Here the Dirac fermion has been decomposed into the Majorana components,

$$\psi^\mu = \begin{pmatrix} \psi_+^\mu \\ \psi_-^\mu \end{pmatrix}. \quad (3.52)$$

As was the case for the bosonic string, one must also consider boundary conditions on the fermions that live on the worldsheet. We will focus here on closed string, and the allowed boundary conditions are,

$$\psi_+^\mu(\sigma, \tau) = \pm \psi_+^\mu(\sigma + \pi, \tau), \text{ and, } \psi_-^\mu(\sigma, \tau) = \pm \psi_-^\mu(\sigma + \pi, \tau). \quad (3.53)$$

Wrapping once around the string worldsheet, the fermions can be either periodic, or anti-periodic. These conditions are dubbed the Ramond (R), or Neveu-Schwarz (NS) boundary conditions respectively. The two fermions, or to use the terminology from the last section, the left movers and right movers, can be chosen separately which gives rise to four sectors

$$(R,R), (R,NS), (NS,R), (NS,NS). \quad (3.54)$$

From the perspective of the bulk spacetime, string states arising from the (R,R) and (NS,NS) sectors are (spacetime) bosons, where states from the (R, NS) and (NS,R) sectors are (spacetime) fermions. The bosonic sectors however, contain tachyons, which must be projected out. To do this, an operator is defined $(-1)^F$ which has eigenvalues $+1$ on bosonic states, and -1 on fermionic states. To define how $(-1)^F$ acts on any given state, one must first define how it acts on the ground state. In the NS sector the ground state has

$$(-1)^F |\text{NS}\rangle = -|\text{NS}\rangle, \quad (3.55)$$

that is the ground state is fermionic. One can split the sectors into sub-sectors based on whether the states are bosonic or fermionic, which will be denoted with a plus or a minus respectively (such as NS+,NS-). The NS- sector is contains tachyons, so choosing the NS+ sector is the quickest way to a consistent theory. The Ramond sector is more complicated, and has two sets of ground-states, one set has $(-1)^F = 1$, the other has $(-1)^F = -1$, though both carry spinor indices. Ultimately it does not matter which you chose, both have the same number of states so either way half must be projected out. For closed strings this leads to two distinct string theories. Because the closed string has both left and right moving sectors, the choice of projection can be made independently for both the left and right moving sectors. Both will have an NS+ sector and an R± sector,

the key difference comes in whether the sign of the R sector is matching on the left and right sector or not. For example we can have

$$\begin{array}{c|c} \text{Left} & \text{Right} \\ NS+ & NS+ \\ R- & R+ \end{array} \quad (3.56)$$

or

$$\begin{array}{c|c} \text{Left} & \text{Right} \\ NS+ & NS+ \\ R- & R- \end{array} \quad (3.57)$$

which give the type IIA and type IIB string theories respectively. This *consistent truncation* of the four sectors down to the subsectors defined above is known as the *GSO projection*, and is required for the theories to have spacetime supersymmetry [47]¹⁹. These theories have different spectra. In particular they have the following massless fields that come from the Ramond-Ramond sectors:

$$\text{Type IIA: } C^{(1)}, C^{(3)}, \quad (3.58)$$

$$\text{Type IIB: } C^{(0)}, C^{(2)}, C^{(4)}, \quad (3.59)$$

which are intertwined with the stability of objects that couple electrically to them, *D-branes*. Equally, both share an NS–NS sector which gives rise to

$$\text{Both: } g_{\mu\nu}, B_{\mu\nu}, \phi, B^{(6)}. \quad (3.60)$$

The first three of these are familiar from the classical string, however the fourth is not. The NS–NS sector contains a massless six-form field that implies the existence of a stable object that couples to it called the NS-fivebrane.

The main moral of the story so far is that the both types of closed string presented so far contain a graviton, and different p -form fields that imply the existence of objects that couple to them electrically. There are three other ten dimensional supersymmetric string theories: type I, heterotic $SO(32)$, and heterotic $E_8 \times E_8$, which will not be covered in any detail here. At low energies, *all* string theories include gravity. Even if one tries to consider only open strings, closed strings arise as bound states of open strings, leading back to gravity. For the type II

¹⁹This sort of projection might seem unnatural, but when looking at superstring perturbation theory the same condition can be realised as summing over spin structures arising from having non-contractible loops [51]

theories, where one tries to only consider closed strings, they contain hints of non-perturbative states (D-branes) in their spectrum which naturally begin to include open string degrees of freedom back into the theory. In fact, all of the listed theories are limits of another parent theory, *M-theory* [39], and are linked by the *web of dualities* that are a feature of superstring theories. This is a particularly interesting observation that kick-started the *second superstring revolution*. This however is a slight digression, and the main focus of the remainder of this thesis will be on the rich physics of *D-branes*.

3.2.2 Differential Forms, Branes and Supergravity

This following section will discuss D-branes from the perspective of string theory, and supergravity. In the spectrum of the type II superstring theories are a selection of massless p -form gauge fields that arise from the Ramond-Ramond sectors of the closed strings. We will start by examining these p -forms, which are intrinsically linked to the existence of the D-branes, and their stability. In the type IIA theory, there is a one-form and a three-form, and in the type IIB theory, there is an additional massless scalar (or zero-form), a two-form, and a four-form. These fields are *differential forms* and are particularly useful for discussions of higher dimensional analogues of electromagnetism. They can be written in component notation as,

$$A^{(p)} = \frac{1}{p!} A_{\mu_1 \dots \mu_p} dx^{\mu_1} \wedge \dots \wedge dx^{\mu_p}, \quad (3.61)$$

where \wedge is the *wedge product*, which is totally antisymmetric on the indices²⁰ μ_i , for example, for a two form in two dimensions

$$\frac{1}{2} A_{ab} dx^a \wedge dx^b = \frac{1}{2} A_{12} (dx^1 dx^2 - dx^2 dx^1) = A_{12} dx^1 dx^2. \quad (3.62)$$

This is a particularly useful way to write things for two reasons. Firstly, it is co-ordinate invariant, and the above expressions hold without particular reference to a choice of co-ordinates. Secondly, it allows us to very neatly write integrals of the differential forms over p -volumes; which can simply be written as,

$$\int A^{(p)}, \quad (3.63)$$

²⁰As a consequence, in component notation the field $A_{\mu_1 \dots \mu_p}$ is completely antisymmetric on exchange of any of its indices.

with the caveat that we are integrating a p -form over a p -dimensional surface. The wedge product can also be applied to differential forms, and generally the product of a p -form and a q -form is a $(p+q)$ -form, which can naturally be integrated over a $(p+q)$ -dimensional surface (though this integral must be supplemented with a factor of the induced metric on the surface). A notion of a derivative exists for differential forms, called the *exterior derivative*. Acting on a p -form with the exterior derivative gives a $(p+1)$ -form,

$$dA^{(p)} = \frac{1}{p!} \partial_\mu A_{\mu_1 \dots \mu_p} dx^\mu \wedge dx^{\mu_1} \wedge \dots \wedge dx^{\mu_p} = F^{(p+1)}. \quad (3.64)$$

This operation is clearly nilpotent²¹, and the object $d(dA^{(p)}) = dF^{(p+1)} = 0$. This is the analogue of the Maxwell equations in the vacuum for extended objects charged under a p -form. This also implies that $A^{(p)}$ is equivalent to any field configuration that can be written as $A^{(p)} + d\lambda^{(p-1)}$, since they give the same *field strength tensor*, $F^{(p+1)}$, upon taking the exterior derivative. This transformation $A^{(p)} \rightarrow A^{(p)} + d\lambda^{(p-1)}$ is a gauge transformation, and with the above definitions relativistic electrodynamics follows from the case $p = 1$. This approach generalises Stokes theorem, which can be written for some general manifold M as,

$$\int_M dA = \int_{\partial M} A, \quad (3.65)$$

where in this case, A is a p -form and the manifold is of dimension $p+1$. The last operation to define here is the *Hodge dual*. If one has a p -form field A , in a d -dimensional space, the Hodge dual defines a $(d-p)$ -form $*A$ by contraction on the d -dimensional epsilon symbol,

$$*A = \int \sqrt{-g} \epsilon^{\nu_1 \dots \nu_p}{}_{\mu_{p+1} \dots \mu_d} A_{\nu_1 \dots \nu_p} dx^{\mu_{p+1}} \wedge \dots \wedge dx^{\mu_d} \quad (3.66)$$

$$= \int (*A)_{\mu_{p+1} \dots \mu_d} dx^{\mu_{p+1}} \wedge \dots \wedge dx^{\mu_d}. \quad (3.67)$$

Note that the metric has appeared in both the contraction on the epsilon symbol, and as a determinant out at the front to maintain the nice transformation properties of the differential forms. The key take away from this however is that one can define this operation that maps a p -form to a $(d-p)$ -form. This really suggests that the spectrum of the type II theories should be extended further!

Each p -form field implies the existence of a p -dimensional object that is charged under it. These objects are the D-branes. A Dp -brane couples electrically to a

²¹Writing the expression explicitly reveals that there is a symmetric tensor contracted on an antisymmetric one which vanishes automatically.

$(p + 1)$ -form by a term proportional to (3.63)²². Taking as an example the type IIB string theory, which has massless fields $C^{(0)}$, $C^{(2)}$, and $C^{(4)}$. The theory will have stable: $D(-1)$ -, $D1$ - and $D3$ -branes charged under these forms respectively. Corresponding to the above differential forms, one can define the field strength tensors: $F^{(1)}$, $F^{(3)}$, and $F^{(5)}$. One can define the Hodge dual of these *field strength tensors*, so the theory should also have the forms $F^{(9)}$, and $F^{(7)}$. The five-form field strength is self dual in ten dimensions, so we need not include another five-form. These new field strengths could equally be written as the exterior derivative of $p - 1$ forms, and as such there also should be $C^{(8)}$ and $C^{(6)}$ fields in the theory as well, which implies the existence $D7$ -, and $D5$ -branes living in the theory. There also can be a ten-form gauge field under which the $D9$ brane is charged. However it is not possible to write down a differential form with $p > d$, so it is also not possible to write down the field strength, which would be an “eleven-form”. It is also not possible to write down a kinetic term for the gauge field, which is proportional to $\int F \wedge *F$, so the ten form is non-dynamical. They won’t be discussed in the remainder of this thesis, but the $D9$ -branes are an important ingredient in the web of dualities that link the five consistent superstring theories. The brane content of the type IIB string theory is summarised in Table 3.1, which shows the differential forms in the theory, and which branes couple *electrically* and *magnetically* to them²³.

p -form	Electrically coupled brane	Magnetically coupled brane
$C^{(0)}$	$D(-1)$	$D7$
$C^{(2)}$	$D1$	$D5$
$C^{(4)}$	$D3$	$D3$
$C^{(6)}$	$D5$	$D1$
$C^{(8)}$	$D7$	$D(-1)$
$C^{(10)}$	$D9$	

TABLE 3.1: The D-brane content of type IIB string theory

The brane content of the type IIA theory is summarised in Table 3.2. Similarly to the type IIB theory, in type IIA the $D8$ -brane is non-dynamical. Its associated field strength is a ten-form. The “kinetic term” associated to it is proportional to $\int F^{(0)} \times F^{(10)}$, though this is a single derivative term, and thus it is still non-dynamical. This is often skirted by moving to the *massive* type IIA theory where this is allowed to be dynamical, which suggests we should include a $D(-2)$ brane.

²²The p in Dp -brane counts the number of spatial dimensions, not spacetime dimensions, so there is a counting difference of 1 between the differential forms and their associated D-branes

²³By couple magnetically to them it is meant that they couple through the chain of: Dp -brane $\rightarrow p + 1$ -form \rightarrow field strength \rightarrow dual field strength $\rightarrow (d - (p + 2) - 1)$ -form $\rightarrow D(d - p - 4)$ -brane

p -form	Electrically coupled brane	Magnetically coupled brane
$C^{(1)}$	$D0$	$D6$
$C^{(3)}$	$D2$	$D4$
$C^{(5)}$	$D4$	$D2$
$C^{(7)}$	$D6$	$D0$
$C^{(9)}$	$D8$	

TABLE 3.2: The D-brane content of type IIA string theory

So it appears that from the spectrum of the type II strings D-branes appear, but there were hints of their existence as far back as the boundary conditions on the bosonic string. Recall that there were two possible choices for the boundary conditions on open strings, Neumann (N) and Dirichlet (D). For a long time, the Dirichlet condition was considered non-physical and disregarded. However each of the d scalars or, as it might be more useful to picture them, each of the d fluctuations of the string worldsheet can have the choice of N or D boundary conditions. So it is possible to define an open string with $p + 1$ fluctuations that have the N condition, and $d - p - 1$ Dirichlet boundary conditions. The Neumann condition is that at the string endpoints we have $n^a \partial_a x^\mu = 0$, where n^a is a unit normal vector²⁴, and similarly the Dirichlet condition is $x^\nu = c^\nu$, with c^ν being an arbitrary constant vector. Taking $\mu = 0, \dots, p$ and $\nu = p + 1, \dots, d$ defines a $p + 1$ dimensional hypersurface on which the string endpoints are free to propagate, with the caveat that they must attach normal to the surface. This $p + 1$ dimensional surface is the Dirichlet p -brane, or the Dp -brane. In the type II string theories, we can consistently include an open string sector, however they must have even p in the type IIA theory, and odd p in the type IIB theory.

The first excited states of the open string are massless spacetime vectors A^μ . In the presence of a Dp -brane the vector decomposes into a vector field on the worldvolume of the Dp -brane, A^a , with $a = 0, \dots, p$ and a set of $d - p - 1$ scalar fields on the worldvolume of the brane ϕ^i . Perhaps the quickest way to see this, without re-quantising the string in the D-brane background, is to consider a single Dp -brane in 10 dimensional Minkowski space. The presence of the D-brane breaks the symmetry group of the background spacetime into two subgroups, spacetime rotations in the directions the brane fills, and spatial rotations in the direction that the brane is pointlike. The presence of the brane breaks symmetry group of the spacetime from $SO(1, 9)$ to $SO(1, p) \times SO(9 - p)$. Naturally fields living in

²⁴to the $p + 1$ dimensional hyperplane

the spacetime will arrange themselves in representations of the remaining symmetry groups. In this case what previously was a vector field transforming under $SO(1, 9)$ decomposes into a vector field living on the worldvolume, transforming under $SO(1, p)$ and a set of $9 - p$ scalar fields that have an internal $SO(9 - p)$ symmetry that rotates the scalars into one-another. These scalars can be interpreted as describing the position, or fluctuation about the position, of the D-brane in the transverse directions. In the case of N co-incident D-branes, the string endpoints each pick up an index which identifies which brane in the stack the string is attached to. In the low energy limit, when string fluctuations are of vanishing size, these indices, or Chan-Paton factors [52], give rise to a $U(N)$ gauge group under which the vector and scalar fields are charged.

Each of the D-branes has both charge, under their respective Ramond-Ramond p -form, and tension. A nice line of reasoning from Polchinski [28] goes: “One would not expect a perfectly rigid object in a theory with gravity, and indeed the D-brane is dynamical”. To phrase this slightly differently, one could imagine having a hypersurface in a gravitating theory, through which some propagating fluctuation of the metric might pass. Such a gravitational wave would distort the hypersurface, implying that one cannot have rigid hypersurfaces in a gravitating theory, and all such hypersurfaces should be dynamical. As such we can write an action that describes the low energy dynamics of the D-branes. The bosonic part of the action is,

$$S_{Dp} = -\mu_p \int d^{p+1}x e^{-\Phi} \sqrt{-\det[P[G]_{ab} + P[B]_{ab} + (2\pi\alpha')F_{ab}]} \quad (3.68)$$

$$+\mu_p \int \sum_q P[C_{(q+1)}] \wedge e^{P[B] + 2\pi\alpha' F}. \quad (3.69)$$

Taking this term by term, (3.68), is the Dirac-Born-Infeld term. μ_p is a dimensionful factor that encodes the tension of the D-brane, and the integral runs over the co-ordinates that span the worldvolume of the brane. Φ here is the Dilaton, which arises from closed strings in the background solution. Underneath the square root we have: $P[G]$, the pullback of the bulk metric to the brane; $P[B]$ the pullback of the Kalb-Ramond two form to the surface of the brane, and F the field strength induced by the gauge field from open string fluctuations on the brane. This term is the generalisation of the *Nambu-Goto* action from strings to surfaces of higher dimension. Unfortunately, the square root can not be thrown away here, and there is not yet a known analogue of the *sigma model action* for D-branes. This makes them *very* difficult to quantise. The second term, (3.69), encodes the coupling of various RR-forms to the D-brane. $C_{(q+1)}$ are the RR-forms sourced by other

Dq -branes in the system, and is of interest when examining multi-brane systems. A Dp -brane will couple to a $q + 1$ form if $q < p$, and $\frac{1}{2}(p - q) \in \mathbb{Z}$. The second of these conditions is automatically satisfied in the type II theories, which have only odd, or only even p and q respectively. When the first condition is met, then the brane will couple to the $q + 1$ form through powers²⁵ of $(P[B] + F)$. This appears in the action like interactions of the field strength and the q -form, such as the coupling of a four-form to a D7 brane which is proportional to $\int C_{(4)} \wedge F \wedge F$. In the particular case of $p - q = 2$ the coupling looks like a source term for field on the brane worldvolume and this coupling can have a *significant* effect on the dynamics of the brane (as an example see the D3/probe D5 holographic system [53, 54, 55]). It is possible to extend this action to include non-abelian gauge groups²⁶, and coupling of Dp -branes to forms of degree $q > p$, which gives rise to novel interactions between the branes, such as the Myers effect [56]. The low energy open string modes on the D-branes are generically a $(p + 1)$ dimensional gauge theory, this link between branes, their dynamics and gauge theories is reviewed nicely in [57]. An alternate perspective on D-branes, comes from supergravity. In [58] extremal and non-extremal p -brane solutions were presented in type II supergravity, which are generalisations of the familiar black-hole geometries of general relativity to extended objects. The extremal cases were identified with D-branes in [28]. From the perspective of supergravity, D-branes appear as charged extended analogues of black holes. These p -brane solutions are summarised in Table 3.3²⁷. The dual interpretation of the physics of D-branes in terms of how they deform the background spacetime that they inhabit and fields propagating on their worldvolume is central to *holographic dualities*, which is the final topic to cover in this chapter.

$$ds^2 = H(r)^{-\frac{1}{2}} dx_{\parallel}^2 + H(r)^{\frac{1}{2}} dx_{\perp}^2, \quad H(r) = 1 + \frac{\alpha}{r^{(7-p)}}, \quad (p < 7)$$

$$F_{m0\dots p} = \partial_m(H(r)^{-1}), \quad e^{\phi(r)} = H(r)^{\frac{3-p}{4}},$$

$$\alpha = (4\pi)^{\frac{1}{2}(5-p)} \Gamma\left(\frac{1}{2}(7-p)\right) (\alpha')^{\frac{1}{2}(7-p)} g_s N.$$

TABLE 3.3: The $\frac{1}{2}BPS$ supergravity solution, in string frame, corresponding to a stack of N co-incident Dp -branes.

²⁵meaning repeated wedge products

²⁶One has to be careful to say that there is a direct non-abelian analogue of the DBI action. In the case that α' is taken to zero this is true since the result is super Yang-Mills theory. This is sufficient for the purpose of holography, an example case is flavour branes in the Sakai-Sugimoto model; however, it doesn't capture stringy corrections appropriately

²⁷The formulae listed here were taken from chapter 18 in [50]

3.3 Holography and the AdS/CFT Correspondence

This section will be dedicated to reviewing the AdS/CFT correspondence and some of the developments in the years since its inception that are of particular importance to holographic models of quantum chromodynamics. It will begin with the arguments set out in [9], that there are two interpretations of the physics of D3 branes: closed strings absorbed and emitted by the brane, and open string excitations on the brane worldvolume. In the decoupling limit these are conjectured to be equivalent descriptions of the same physics. Consider N parallel D3 branes separated by some distance r , embedded in 10 dimensional Minkowski space. The decoupling limit, involves taking $\alpha' \rightarrow 0$ whilst keeping $U \equiv r/\alpha'$ fixed. From the perspective of the theory on the D3 brane worldvolume, this corresponds to keeping the vacuum expectation value of the scalar field that describes the separation of the branes fixed²⁸. In the low energy theory, the coupling to bulk gravity appears through the effective coupling $g_s \alpha'^2$, so taking $\alpha' \rightarrow 0$ kills off any interaction between the worldvolume theory, and gravity in the bulk. The bosonic part of action for the D3 branes can be written as²⁹

$$S_{D3} = -T_3 \int d^4x \sqrt{-\det(P[G]_{ab} + (2\pi\alpha')F_{ab})}. \quad (3.70)$$

In 10 dimensional flat space, and in static gauge, the pullback of the metric can be written as

$$P[G]_{ab} = \eta_{ab} + \partial_a X^i \partial_b X^i \quad (3.71)$$

where $X^i = (2\pi\alpha')\Phi^i$ represents the fluctuations of the brane in the six transverse directions. Writing in matrix notation, $S = (2\pi\alpha')^2 \eta^{-1} (\partial\Phi\partial\Phi)$ and $A = (2\pi\alpha')\eta^{-1} F$, the action can be then written as

$$S_{D3} = -T_3 \int d^4x \sqrt{-\det(\eta)} \times \sqrt{\det(1 + S + A)}. \quad (3.72)$$

Under matrix transposition $S^T = S$ and $A^T = -A$, so the last part can be written as $(\det M)^{1/2} = (\det(MM^T))^{1/4} = \det((1 + S + A)(1 + S - A))^{1/4}$. Applying the identity $\ln(\det M) = \text{Tr}(\ln M)$, and then replacing natural log by its power series

²⁸equivalently, this is keeping the mass of strings stretched between the branes fixed

²⁹there's an implicit trace of $U(N)$ indices here, that won't be written

for the matrix we arrive at

$$\sqrt{\det(1 + S + A)} = \exp(\text{Tr}(\frac{1}{4}(2S - A^2 + \dots))). \quad (3.73)$$

Only the lowest terms in powers of $2\pi\alpha'$ are written, which in this case is $\mathcal{O}(\alpha'^2)$. Inserting the expression for the D3 brane tension T_3 in terms of the string coupling, the DBI action becomes³⁰

$$S_{D3} = -\frac{1}{2\pi g_s (2\pi\alpha')^2} \int d^4x \frac{(2\pi\alpha')^2}{2} \partial_a \Phi^i \partial^a \Phi^i - \frac{(2\pi\alpha')^2}{4} F_{ab} F^{ab} + \dots, \quad (3.74)$$

$$\lim_{\alpha' \rightarrow 0} S_{D3} = -\frac{1}{2\pi g_s} \int d^4x \frac{1}{2} \partial_a \Phi^i \partial^a \Phi^i - \frac{1}{4} F^2, \quad (3.75)$$

which is the bosonic part of the $\mathcal{N} = 4$ super-Yang-Mills action with coupling $g_{YM}^2 = 2\pi g_s$ on four dimensional flat space³¹. The six scalar fields can be rotated into one another by an $SO(6)$ transformation, which is isomorphic to $SU(4)_R$, the R -symmetry transformation of the supersymmetric theory. So in the decoupling limit there are two sectors of the theory that don't interact, $\mathcal{N} = 4$, $d = 4$ super-Yang-Mills theory with gauge group $SU(N)$ ³², and type IIB supergravity on 10 dimensional Minkowski space. Turning now to the supergravity, the solution to the supergravity equations corresponding to N units of RR 4-form flux³³ is

$$ds^2 = \left(1 + \frac{4\pi\alpha'^2 g_s N}{r^4}\right)^{-\frac{1}{2}} \eta_{ab} dx^a dx^b + \left(1 + \frac{4\pi\alpha'^2 g_s N}{r^4}\right)^{\frac{1}{2}} \delta_{ij} dy^i dy^j. \quad (3.76)$$

The limit, $\alpha' \rightarrow 0$, $U = r/\alpha' \rightarrow \text{fixed}$, requires taking $r \rightarrow 0$ and the 1 in the harmonic functions can be dropped, giving

$$\frac{ds^2}{\alpha'} = \left(\frac{U^2}{\sqrt{4\pi g_s N}} \eta_{ab} dx^a dx^b + \frac{\sqrt{4\pi g_s N}}{U^2} dU^2 + \sqrt{4\pi g_s N} d\Omega_5^2 \right), \quad (3.77)$$

which is the metric of five dimensional Anti-de Sitter space times a five sphere with radius, common to both the AdS space and the sphere, $R^2 = \sqrt{4\pi g_s N}$. The original metric (3.76) features a region that is asymptotically Minkowski, and a warped throat, leading to a near horizon geometry, that is (3.77). Taking the $\alpha' \rightarrow 0$ limit, from the supergravity perspective, splits the theory into two decoupled sectors: type IIB supergravity on $AdS_5 \times S^5$, and type IIB supergravity on $10d$ Minkowski space. The leap of Maldacena was the following: that if these

³⁰again with the ... representing higher order terms in α'

³¹The fermionic part of the D3 brane action similarly reduces to give the fermionic part of the $\mathcal{N} = 4$ action

³²the $U(1)$ photon decouples in this limit also [59].

³³or having N D3 branes

are two different representations of the same physics, then *type IIB supergravity on $AdS_5 \times S^5$ with radius $R^2 = \sqrt{4\pi g_s N}$ is dynamically equivalent to $\mathcal{N} = 4, SU(N)$ supersymmetric Yang-Mills theory on four dimensional Minkowski space*. Further, that given we started in a quantum theory, this is expected to hold for type IIB superstring theory, not just supergravity. At large N on the gauge theory side of the correspondence, one can go to the t'Hooft limit, defining the t'Hooft coupling $\lambda = g_{YM}^2 N$. In the dual string theory, the coupling equates to $\lambda = 2\pi g_s N$. Large t'Hooft coupling in the gauge theory can be satisfied by having a large number of D3 branes $N \gg g_s$, whilst still having $g_s < 1$, and retaining the ability to do perturbative calculations in string theory/supergravity. Thus: *weakly coupled type IIB string theory on $AdS_5 \times S^5$ is dynamically equivalent to $\mathcal{N} = 4, SU(N)$ SYM at large t'Hooft coupling, λ* . This is the statement of the correspondence that will be important to us going forwards. Whilst the most studied form of the correspondence is based upon D3 branes, there is an analogous *field theory limit* that can be defined for most D-branes [60]. This limit links the physics of the gauge theory supported on the brane worldvolume, to the higher dimensional gravitating theory in the near horizon geometry sourced by the branes.

$\mathcal{N} = 4$ super-Yang-Mills is a particularly special theory. It has the maximal amount of supersymmetry allowed in a gauge theory³⁴. It is also a *conformal field theory*. To all orders in perturbation theory, the β -function vanishes, signalling that the coupling is constant all the way along the renormalisation group flow of the theory. This ties into the enhanced *conformal symmetry* that the theory enjoys. It includes, in addition to the usual invariance under Poincaré transformations, an invariance under scale transformations, and *special conformal transformations*. In d dimensions, the conformal group is $SO(2, d)$ (as opposed to the Lorentz group, $SO(1, d - 1)$). This brings us to our second element of the dictionary between gauge theories and gravity³⁵, the matching of the symmetries of field theory, with the isometries of gravity dual. The isometry group of AdS_d is $SO(2, d - 1)$, which stems from the ability to embed AdS_d as a hyperboloid in a higher dimensional space with two time-like directions, similarly the isometry group of a sphere S^d is $SO(d + 1)$, so the isometry group of the spacetime $AdS_5 \times S^5$ is $SO(2, 4) \times SO(6)$. On the other side of the correspondence, $\mathcal{N} = 4$ SYM is invariant under transformations valued in the *Lie superalgebra* $PSU(2, 2|4)$, which has the bosonic subgroup $SO(2, 4)$, and $SU(4)$ ³⁶. Thus the symmetries of the field theory are

³⁴ $\mathcal{N} > 4$ leads to having particles of spin higher than one in the spectrum. This is consistent only in supergravity theories, where the higher spin states appear as the graviton and its superpartners.

³⁵the first was the identification of the couplings on both sides

³⁶which as mentioned previously, is isomorphic to $SO(6)$

reflected in the isometries of the gravity dual. Matter fields, in the field theory, will come packaged in representations of symmetry groups of the dual theory, but how they are represented in the bulk AdS geometry is not obvious at a first glance. The clearest example of how the symmetries of the dual theory are represented in the bulk theory, comes from a scalar field on AdS_5 . Writing now the AdS_5 metric as,

$$ds_{AdS}^2 = \frac{L^2}{z^2}(\eta_{\mu\nu}dx^\mu dx^\nu + dz^2), \quad (3.78)$$

the action for a massive scalar in the geometry is

$$\int d^5x \sqrt{-g} \left(\frac{1}{2} g^{MN} \partial_M \phi \partial_N \phi - \frac{1}{2} M^2 \phi^2 \right). \quad (3.79)$$

The equation of motion for the Klein-Gordon scalar is,

$$\frac{1}{\sqrt{-g}} \partial_M (\sqrt{-g} g^{MN} \partial_N \phi) - M^2 \phi = 0, \quad (3.80)$$

invoking separation of variables we can make an ansatz $\phi(x; z) = e^{-ik \cdot x} \phi(z)$, though we will take the case $k \cdot k = 0$ to focus on the radial profile. The equation of motion becomes

$$z^2 \partial_z^2 \phi - 3z \partial_z \phi - M^2 L^2 \phi = 0. \quad (3.81)$$

From the structure of (3.81), a sensible ansatz for $\phi(z)$ is $\phi \sim z^\Delta$. Which gives a condition on the mass of allowed scalars in the geometry. They have

$$M^2 L^2 = \Delta(\Delta - 4). \quad (3.82)$$

In this writing of the geometry, the asymptotic boundary is at $z \rightarrow 0$. For this to be a sensible solution, it should be normalisable out to the boundary. This constrains us to $\Delta \geq 0$. Under a scale transformation $z \rightarrow \lambda z$, the scalar will transform as $\phi \rightarrow \lambda^\Delta \phi$, and we can identify Δ as the *conformal weight* of the scalar field. Furthermore, the presence $\Delta = 2$ states in the dual theory implies the stability of states in AdS with $M^2 L^2 = -4$. In flat space, this would be worrying, states with negative mass squared are tachyonic and signal instabilities³⁷. However, a small amount of tachyonicity is allowed in negatively curved spaces, like AdS. The requirement that $M^2 \geq -4/L^2$ is known as the Breitenlohner-Friedmann (BF) bound [61]. The violation of this bound introduces instabilities in the dual theory. Critically, BF bound violations can be linked to the breaking of chiral

³⁷or worse, acausal behaviour

symmetry in the dual theory when matter is included [62]. Another aspect of the original correspondence, is the presence of the radial direction, U . In order to understand the mapping between the two theories, one would like to understand the interpretation of this *holographic coordinate* in the dual gauge theory. From the perspective of the field theory, this co-ordinate has dimensions of mass, and a line of analysis based on moving a D3 brane off the stack of N D3 branes in the U direction suggests that it is the energy scale of the dual theory. Moving to large U , towards the conformal boundary of the space is moving to the UV of the dual theory, whereas the interior of the geometry represents the IR.

An early work of importance to the AdS/CFT correspondence was [10]³⁸, where Witten matched the spectrum of chiral primary operators in $\mathcal{N} = 4$ SYM to their counterpart Kaluza-Klein modes in the dual gravity theory. Here it was proposed that the asymptotic behaviour of supergravity fields at the conformal boundary of AdS related to correlators in the dual gauge theory. The asymptotic boundary of $AdS_5 \times S^5$ is conformal to four dimensional flat space, and as such one can think of the dual gauge theory as living on the conformal boundary of the gravity theory, making this an explicit realisation of the *holographic principle* [64], that originated from the study of black holes. That the entropy of various black holes is proportional to the area of their event horizon [65], in Planck units, suggests that there is an upper bound to the amount of information that can be stored in a given volume in a gravitating theory. If one can describe the dual theory as living on the boundary of the space-time, then this principle is realised by the AdS/CFT correspondence, with the bulk theory being completely described by the degrees of freedom living on the boundary.

Unfortunately, whilst the AdS/CFT correspondence provides a novel way to calculate observables in a strongly coupled gauge theory (by doing calculations in weakly coupled gravity), it does not give us the immediate ability to calculate in the theory we want to. QCD has neither the conformal invariance or supersymmetry of the super-Yang-Mills theory. It also has matter, transforming in the fundamental representation of the gauge group, which SYM does not. We must *deform* the correspondence to introduce aspects of more realistic physical theories. There are two major approaches to this, *top down holography*, and *bottom up holography*. In the bottom up approach, one starts with the original correspondence, and notes the following: the argument based on symmetries suggests that the five-sphere is linked to the presence of supersymmetry, so a non supersymmetric theory is expected only to live in the five dimensional space. Further if a gravitating theory AdS_5 represents some four dimensional theory conformal

³⁸A similar work around the same time was [63]

theory, then deforming the interior of the spacetime in some way will represent the breaking of conformal symmetry, and possibly chiral symmetry[66], at some scale in the theory. The new geometry represents the flow of some quantum field theory from a CFT in the UV to some unknown theory in the IR with properties that are nice from a phenomenological point of view, with fields in the new geometry dual to source-operator pairs in the dual theory. This approach has led to successful bottom up holographic models of QCD. However, we will focus on the *top down* approach in this thesis, which starts from some brane setup in string theory, and taking the field theory limit identifies more precisely the dual holographic theory. Deformations of the interior of the bulk theory come from interactions between fields in the type II string theory/supergravity, or are engineered by compactifying a direction wrapped by some of the branes. An advantage to the top down approach, is that we are not limited to examining the physics of D3-branes. This brings us to an important facet of building holographic models, matter.

3.3.1 Probe Branes and Fundamental Matter

In [67] a prescription was set out for including matter fields, transforming in the fundamental representation of $SU(N)$, to the AdS/CFT correspondence by adding probe branes. In the top down picture, one can think of having N_c Dp branes, and N_f Dq branes that are aligned in 10 dimensional Minkowski space, which will be referred to as *colour* branes, and *flavour* branes respectively. For the case that N_c is large, and $N_c \gg N_f$ then it is appropriate to consider the backreaction of the colour branes, but not the flavour branes. In the field theory limit, this is equivalent to having the flavour branes, probing the near horizon geometry sourced by the colour branes. Functionally, this adds an extra sector to the string theory, open strings that have one or both ends on the flavour branes. Strings that stretch from the colour branes to the flavour branes are identified as quarks, with mass proportional to their length. On each end of the string there are indices that identify which brane in the stack the string is attached to. For the case of N_c co-incident colour branes, and N_f co-incident flavour branes, the Chan-Paton factors form an $N_c \times N_f$ matrix, which can be interpreted as having N_f mass degenerate quarks transforming in the fundamental representation of $SU(N_c)$. Similarly, the strings that have both endpoints on the flavour branes are interpreted as mesons, with each string endpoint representing a quark and an anti-quark. Not all allowed intersections of branes give stable theories however, and whether the brane intersection preserves supersymmetry or not plays a large role in this. The decay of

D-branes is mediated by tachyons [68, 69], and in a supersymmetric theory, all the states must have a positive energy³⁹ so there can be no tachyons, and the configuration is stable. Whether a given brane intersection retains supersymmetry can be deduced from the boundary conditions allowed on the open strings. Recall that for a Dp brane, the open string modes obey Neumann, or N, boundary conditions on the $p + 1$ directions spanned by the brane, and a Dirichlet, or D, boundary conditions on the direction the brane is pointlike in. Having multiple branes allows string modes with an N condition at one end, and a D condition at the other (or vice versa). A consideration of the NS sector ground state on the open superstring suggests that the brane intersections break supersymmetry when the number of directions that permit an N and a D condition, hence $\#_{ND}$, is two or six [70]. Loosely, this is the number of directions in a brane intersection with only one brane. Given that the difference in dimension of the branes is always a multiple of two, there are three sets of particular importance: the $Dp/Dp + 4$ intersection, the $Dp/Dp + 2$ intersection, and the Dp/Dp intersection.

In reverse order, the Dp/Dp intersection is not particularly suitable for describing fundamental matter. One could consider the probe p brane as coming from the stack of N_c colour branes, and moving a brane off the stack can be interpreted as breaking the gauge group on the worldvolume of the brane stack from $SU(N_c)$ to $SU(N_c - 1) \times U(1)$, which is a stringy example of *Higgsing* the gauge group. The strings that stretch between the $N_c - N_f$ colour branes, and the N_f “flavour” branes form a massive vector state akin to the W and Z bosons of the standard model. An example of this case is provided in Maldacena’s original paper on the subject, where this is identified as probing the *moduli space* of the Higgs branch of $\mathcal{N} = 4$ SYM.

The $Dp/Dp + 2$ intersection is the next one that shows real promise for describing matter fields. The alignment of these branes that preserves supersymmetry is displayed in the brane scan below. A \bullet indicates a direction that the brane is pointlike in, and $-$ indicates that the brane is extended in that direction,

	0	1	...	p	$p + 1$	$p + 2$	$p + 3$...	9	
Dp	-	-	-	-	•	•	•	•	•	.
$Dp + 2$	-	-	-	•	-	-	-	•	•	

(3.83)

³⁹This is a consequence of the supersymmetry algebra $\{Q_\alpha, \bar{Q}_{\dot{\alpha}}\} = 2\sigma_{\alpha, \dot{\alpha}}^\mu P_\mu$, $\langle \psi | \{Q_\alpha, \bar{Q}_{\dot{\alpha}}\} | \psi \rangle = \langle \psi | Q\bar{Q} + \bar{Q}Q | \psi \rangle = \langle \psi | |Q^\dagger|^2 + |Q|^2 | \psi \rangle$, which is positive semi-definite, hence P_0 is positive semidefinite also.

Note that this intersection has the flavour brane pointlike in one of the directions spanned by the colour brane. This is necessary to preserve supersymmetry, otherwise we would have $\#_{ND} = 2$ which is not allowed, whereas in this configuration we have $\#_{ND} = 4$ which is allowed. The field theory limit, with $\alpha' \rightarrow 0$ is also a limit where the string tension $T = 1/2\pi\alpha'$ diverges. The result is that the open strings are restricted to living on a co-dimension one defect in the dual gauge theory. So this intersection holographically describes a quark supermultiplet in the dual gauge theory, just restricted to a defect. This type of intersection, though with a near extremal stack of colour branes, will be the backbone of the holographic model in Chapters 5 and 6.

Lastly the $Dp/Dp + 4$ intersection, which because $\#_{ND} = 4$ is allowed, can be aligned such that the directions on the Dp brane are covered by the $p + 4$ brane (shown in (3.84)). This implies that the quark supermultiplet described by the open strings between the p and $p + 4$ branes is dynamical on the worldvolume of the p brane. A concrete example of this is the $D3/D7$ intersection, specialisation to $p = 3$, which is holographically dual to the $\mathcal{N} = 2$ Karch-Katz theory ($\mathcal{N} = 4$, $SU(N_c)$ SYM deformed by the presence of N_f , $\mathcal{N} = 2$ quark supermultiplets). In this case the $D7$ brane wraps an asymptotically $AdS_5 \times S^3$ subspace of the full geometry, with embedding field $L^i(\xi^a) = X^{7+i}$ that represents the position of the sevenbrane in the X^8 and X^9 directions (with $i = 1, 2$, and $a = 0, \dots, 7$),

	0	...	p	$p + 1$	$p + 2$	$p + 3$	$p + 4$...	9	
Dp	-	-	-	•	•	•	•	•	•	.
Dp + 4	-	-	-	-	-	-	-	•	•	

(3.84)

Generically the presence of branes breaks the Lorentz symmetry of spacetime, and fluctuations of the branes come packaged in representations of remaining symmetry group. In this case, the brane intersection breaks the symmetry from $SO(1, 9)$ to $SO(1, 3) \times SO(4) \times U(1)$. From the perspective of fluctuations on the $D7$ brane, there is a vector field on the directions covered by the $D3$ brane, which are dual to the vector mesons, scalars with an internal $SO(4)$ rotation, which is doubly covered by $SU(2)$, and indicative of the remaining supersymmetry, and finally two scalars that rotate into one another by a $U(1)$ transformation. This last case is simplest to consider, and can be written in terms of the embedding function L , and fluctuations there about. We can always make a $U(1)$ rotation to choose $X^8 = L$, $X^9 = \phi(x)$. The DBI action for the vacuum state evaluates to,

$$S_{D7} = -T_7 \int d^8x \sqrt{-\det(P[G]_{ab})} = -T_7 \int d^8x \rho^3 \sqrt{1 + (\partial_\rho L)^2}, \quad (3.85)$$

which is solved by $L = \text{const}$. This represents, through the asymptotic value of the field L , the inclusion of quarks with a supersymmetry preserving mass term $L \sim m_q$. The equation of motion that follow from (3.85) is,

$$\frac{\rho^3 \partial_\rho L}{\sqrt{1 + (\partial_\rho L)^2}} = \text{const}, \quad (3.86)$$

which asymptotically is satisfied by

$$L \sim m_q + \frac{c}{\rho^2}, \quad (3.87)$$

where m_q is the current quark mass, and c is the chiral condensate. The supersymmetric theory forbids the formation of condensates, so to realise the breaking of chiral symmetry the theory must be further deformed to break the remaining supersymmetry (see [71]). For $L = 0$, there is a rotational symmetry in the $X^{8,9}$ directions, which is broken by the presence of quark masses. Small fluctuations of the embedding in the $X^{8,9}$ directions, ϕ represents a pseudoscalar meson in the dual theory (the correspond to fluctuations of 7-7 strings in the brane picture). In the $\mathcal{N} = 2$ theory, with $L = \text{const}$, we can calculate the meson spectrum by allowing fluctuations to have spatial dependence on the worldvolume co-ordinates of the D7 brane, ξ^a . Taking the embedding [72]

$$X^8 = L + (2\pi\alpha')\phi(\xi^a), \quad X^9 = 0 + (2\pi\alpha')\psi(\xi^a), \quad (3.88)$$

the pullback of the metric to the D7 brane worldvolume, in static gauge, evaluates to;

$$P[G]_{ab} = g_{ab} + (2\pi\alpha')^2 \frac{R^2}{r^2} (\partial_a \phi \partial_b \phi + \partial_a \psi \partial_b \psi) \quad (3.89)$$

, where g_{ab} is the static-gauge metric on the D7 brane worldvolume co-ordinates. The Lagrangian for the D7 brane fluctuations is then

$$\mathcal{L}_{D7} = -\mu_7 \sqrt{-\det \left[g_{ac} \left(\delta_b^c + (2\pi\alpha')^2 \frac{R^2}{r^2} g^{cd} (\partial_d \phi \partial_b \phi + \partial_d \psi \partial_b \psi) \right) \right]}. \quad (3.90)$$

Expanding this to quadratic order in the fluctuations we have

$$\mathcal{L}_{D7} \sim \sqrt{-\det g} \times \left(1 + \frac{1}{2} (2\pi\alpha')^2 \frac{R^2}{\rho^2 + L^2} g^{cd} (\partial_c \phi \partial_d \phi + \partial_c \psi \partial_d \psi) \right). \quad (3.91)$$

The resulting equations of motion are,

$$\partial_a \left(\frac{\rho^3 g^{ab} \partial_b \phi}{\rho^2 + L^2} \right) = 0. \quad (3.92)$$

The equations of motions for the field ψ , are identical with the replacement $\phi \rightarrow \psi$. Generally, we can take a modified version of a plane-wave ansatz

$$\phi(\xi^a) = e^{-ik \cdot x} f(\rho) \mathcal{Y}^l(S^3), \quad (3.93)$$

which factorises the solution into: plane wave behaviour on $\mathbb{R}^{1,3}$, a radial profile $f(\rho)$, and spherical harmonics $\mathcal{Y}^l(S^3)$ on the three sphere. Neglecting the dynamics on the three sphere, we have

$$\frac{R^4}{(\rho^2 + L^2)^2} \eta^{\mu\nu} \partial_\mu \partial_\nu \phi + \frac{1}{\rho^3} \partial_\rho (\rho^3 \partial_\rho \phi) = 0. \quad (3.94)$$

Inserting the ansatz (3.93), gives

$$f''(\rho) + \frac{3}{\rho} f'(\rho) + \frac{R^4 M^2}{\rho^2 + L^2} f(\rho) = 0, \quad (3.95)$$

which can be solved analytically in terms of the hypergeometric functions,

$$f(\rho) = (\rho^2 + L^2)^{-a} {}_2F_1 \left(-a, 1 - a; 2; -\frac{\rho^2}{L^2} \right), \quad (3.96)$$

where $2a = -1 + \sqrt{1 + (M^2 R^4 / L^2)}$. Ensuring that the solution is normalisable, or demanding that the solution asymptotically falls off with some negative power of ρ , imposes constraints on the allowed values of a . The leading ρ behaviour of this series is $f \sim \text{const} + \rho^{2(1-a)}$. Combined with regularity at the origin, which places integer constraints on the allowed values of a , we must have $1 - a = -n$, $n \in \mathbb{Z}^+$. This *quantisation condition* for a , gives a quantised meson spectrum,

$$M = \frac{2L}{R^2} \sqrt{(n+1)(n+2)}. \quad (3.97)$$

We can identify n with the principle quantum number of the pseudoscalar mesons. For the case of massless quarks, $L = 0$, and the meson spectrum becomes degenerate (up to intrinsic angular momentum l , that has been omitted in this passage). When the quark mass is generated dynamically, these mesons are pseudo-Goldstone bosons of the broken chiral symmetry in the dual gauge theory. This model has some of the requisite features of a holographic dual of QCD. It has

dynamical quarks, which can display dynamical chiral symmetry breaking when the theory is appropriately deformed; calculations can be extended to finite temperature by using the AdS-Schwarzschild geometry (introduced as the finite T dual of $\mathcal{N} = 4$ SYM in [10]); however it is not a confining theory! Holographic Wilson loops were introduced in [73], where the expectation value of the Wilson loop is determined from, the exponential of, the area of string worldsheets which end on the boundary of AdS . For cases where the string is obstructed at some radial scale, the dominant spatial contribution to the worldsheet is proportional to the asymptotic separation of the strings. Giving the overall contribution as proportional to $T \times separation$, which is a holographic incarnation of the area law for Wilson loops. Figure 3.1, is a cartoon that depicts strings with endpoints on the boundary of AdS in a confining theory. The obstruction can arise from strong divergences in the interior of the space, such as in [74, 75] or branes wrapping compact cycles such as in [76, 77]. In pure AdS_5 this does not happen, and thus pure $\mathcal{N} = 4$ SYM is not confining. The expectation value of Wilson loops is instead controlled by conformal symmetry and the value calculated from the supergravity approach reflects this. A holographic dual of QCD is expected to have all of the above features, we will conclude this Chapter by reviewing some existing holographic duals with QCD like phenomenology.

3.3.2 Holographic QCD

This section will review some of the pre-existing approaches to holographic QCD. It will be split into two parts, bottom up approaches, and top down approaches.

3.3.2.1 From the bottom up...

Bottom up approaches to QCD typically feature an Einstein-dilaton gravity living on an asymptotically AdS_5 geometry. The field content of the gravity dual is then informed by the choice of operators that are to be included in the dual gauge theory. These typically subdivide into hard-, and soft-wall models, which refer to how confining behaviour is included in the dual gauge theory. In the hard-wall approach [78] typically some IR cutoff scale is included in the geometry, with boundary conditions for the fields specified on the “IR brane”. This inclusion of a hard-wall in the geometry is inspired by the Klebanov-Strassler model [79], where a similar behaviour is realised from branes probing warped conifolds. In the soft wall approach [80], the Regge behaviour of the meson spectrum is included by

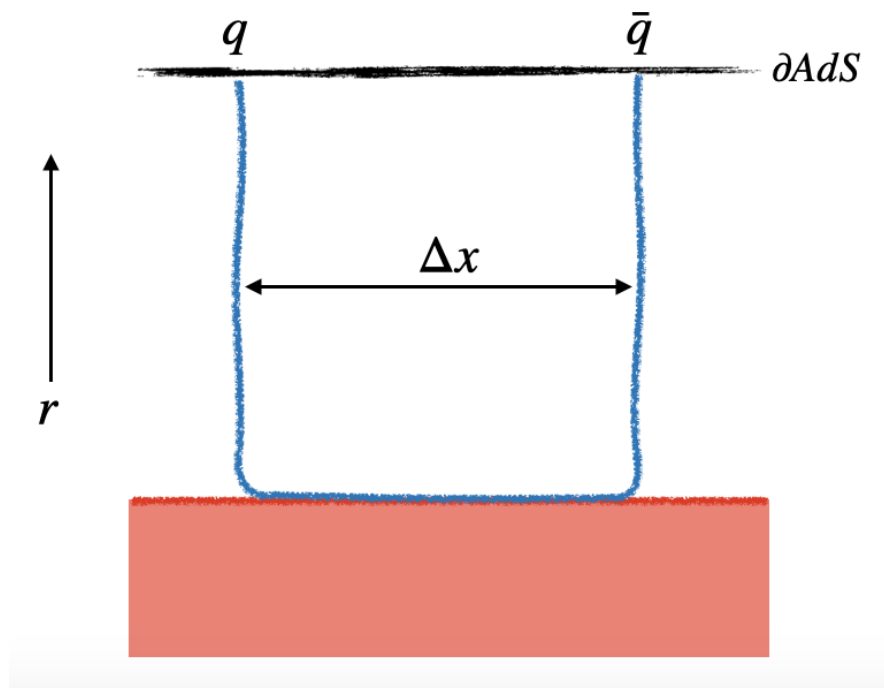


FIGURE 3.1: A cartoon depicting a string (Blue) with endpoints on the boundary of AdS in a confining theory. The string is excluded from the red region, so for sufficiently large Δx the area of the string worldsheet is dominated by the contribution from the part of the string lying across the obstruction.

parameterising the geometry in terms of two factors, which govern the behaviour in the UV and IR respectively. In the IR the *dilaton* grows quadratically, which kills off field fluctuations in the IR of the geometry, whereas in the UV the remaining factor accounts for the restoration of conformal symmetry in the asymptotic region. An approach featuring non-trivial dilaton potentials, which may more accurately mimic QCD is *improved holographic QCD* [81, 82]. There is a class of models that describes large N_c , large N_f QCD in the *Veneziano limit* dubbed *V-QCD* [83], which builds upon improved holographic QCD by including flavour D4 branes, through a tachyonic DBI action (due to Sen [84]). There are a class of models known as *holographic light-front QCD*, which arise from the wavefunction of Baryons in light cone quantised QCD, which obey a Schrödinger equation on an emergent seemingly AdS geometry [85].

3.3.2.2 ...and the top down

Comparably, there are far fewer top down approaches to Holographic QCD. A significant body of work has been done on the D3/D7 intersection, which is a good toy model for understanding how different aspects of QCD arise in top down

models. A sizable amount of this work is reviewed in [86], amongst other things. The understanding of breaking of chiral symmetry is due to [71]; the inclusion of finite baryon density is due to [87], with some exact results therein from [88]; holographic renormalisation of probe branes from [89]. Perhaps the most successful top down holographic model of QCD to date is the *Sakai-Sugimoto model*⁴⁰[77, 90]. This model is based on an intersection of D4 and D8 branes in massive type IIA string theory. A compact direction wrapped by the N_c D4 branes provides a geometry that is *capped*. In the supergravity solution, the S^1 wrapped by the D4 branes collapses to zero size at a finite radial scale, where the geometry “ends”. Crucially probe branes in theory cannot pass the cap, suggesting the presence of a mass gap. At the tip of the geometry the probe D8 branes are forced to turn around, emerging at the antipodal point on the S^1 ⁴¹. This model successfully incorporates the non-abelian $SU(N_f)_L \times SU(N_f)_R$ flavour-chiral symmetry (and its breaking), confinement, and has a meson spectrum comparable to QCD. A baryonic sector can be added to the model by including D4 branes wrapped on spheres [91] (this is analogous to the approach by Witten in AdS_5 in [92]). Ultimately, a potential model of holographic QCD should: have a four dimensional dual theory (at least in the IR), exhibit confining behaviour, and include quark and meson degrees of freedom, with a mechanism to break chiral symmetry dynamically.

3.4 Summary

This chapter has presented some of the necessary background theory pertaining to string theory, supergravity, D-branes, and the AdS/CFT correspondence. We started with a brief early history of strings, dual models, and their connection to hadronic physics, before moving to a discussion of the bosonic string. Upon quantisation we saw that the spectrum of the bosonic string contained gauge fields (for the open strings), and gravity (for the closed strings). It however also contains tachyons, necessitating the move to superstrings. Focussing on closed superstrings we sketched the necessity of the *GSO projection*, which is a consistent truncation of the closed superstring, removing tachyons and yielding spacetime supersymmetry. The Ramond-Ramond sector of the resulting type II superstring theories naturally includes massless p -forms which imply the existence of extended objects that couple to them, generalising Maxwell theory to extended objects. These objects are

⁴⁰sometimes *Witten-Sakai-Sugimoto*.

⁴¹equivalently there are D8 and anti-D8 branes that meet at the tip of the geometry.

D-branes, extended tensionful hypersurfaces that open strings can end on. The D-branes are dynamical non-perturbative objects in the string theory, that generically host gauge theories on their worldvolume. From the perspective of supergravity, these tensionful hypersurfaces are generalisations of charged black holes to higher dimensions. This interplay of perspectives, supergravity and worldvolume theory lies at the heart of the AdS/CFT correspondence. In the decoupling limit it is suggested that the worldvolume theory on D3 branes is dynamically equivalent to type IIB string theory propagating in their *near horizon geometry*. This *duality* between strongly coupled gauge theory and weakly coupled gravity opens up new avenues of approach to non-perturbative QCD. The remainder of this thesis will be concerned with the construction of a candidate holographic dual of QCD, based on the domain wall fermion construction, widely used in the lattice QCD community to represent chiral matter. In Chapter 4 the *Holographic Domain Wall* formalism will be developed, in the D3/D7 holographic model. In Chapter 5, this formalism will be embedded in a higher dimensional, confining background culminating in the Domain Wall AdS/QCD model. This model comes from intersecting D5 and D7 branes, and we will calculate the mesonic observables of the model. Chapter 6 will be devoted to an analysis of this system at finite temperature, examining the thermal meson melting transition when the dual geometry contains a black hole. Finally Chapter 7 will conclude this thesis with an overview of some ongoing work, and a view to the future.

Chapter 4

Domain Wall Fermions

This chapter will focus on the construction of domain walls in the D3/probe D7 brane intersection [1]. It will start by discussing some of the inspiration for this work, taken from the lattice community, going on to detail the holographic domain wall construction. We first construct domain walls by linearising the DBI action for the embedding of a D7 brane in AdS, with an ansatz of sinusoidal X^3 dependence. This allows us to build periodic domain walls at the boundary of AdS via Fourier analysis. The large mass limit will be introduced as the natural next step, allowing us to examine the fluctuations of the brane that live on the domain wall. It is these fluctuations that will be the main characters of the story going forwards. Analysis of the fluctuations reveals that whilst the system displays chiral symmetry breaking, it is not dynamical! Domain walls with worldvolume magnetic fields on the D7 brane, and in deformed AdS geometries are considered. In these cases a Gell-Mann-Oakes-Renner relation is observed for the pseudo-Goldstone bosons of the theory, signalling the dynamical breaking of chiral symmetry.

4.1 Domain Wall Fermions on the lattice, and in the continuum

In [93] domain wall fermions were introduced to address the challenge of simulating chiral fermions on the lattice. Put simply, there is a no-go theorem by Nielsen and Ninomiya [94, 95] which posits that under a very general set of assumptions, namely: locality, hermiticity, and translational invariance; that any attempt to simulate chiral fermion on a lattice will incur fermion doubling. There will always

be the same number of left handed and right handed species of fermion. This presented a clear challenge for any lattice theorist attempting to simulate: the weak interactions, the standard model, or chirally invariant QCD. To quote Kaplan directly “A lattice regulator that achieves this while preserving gauge invariance will have to be devious”. To circumvent the no-go theorem the $2n$ dimensional theories were uplifted to live in $2n + 1$ dimensions, with translational invariance in the $2n + 1$ th direction broken, by a step function like mass profile for the fermions in the $2n + 1$ dimensional theory. Where this step function sharply passes through zero, there lives a theory of $2n$ dimensional massless chiral fermions localised on a co-dimension one defect. This still incurs fermion doubling, however this can be removed by inclusion of a gauge invariant Wilson term in the higher dimensional theory.

In the following passage we will follow the analysis in [93], for the case of reduction from a $3 + 1$ dimensional theory, to a $2 + 1$ dimensional theory. Note however, that there is no notion of chirality in an odd number of spacetime dimensions. More concretely, in an even number of dimensions the $Spin(d - 1, 1)$ group admits two inequivalent complex-linear representations of (complex) dimension $2^{(d/2)-1}$, which are the *chiral* representations. In an odd number of dimensions, then there is a single representation of complex dimension $2^{(d-1)/2}$ [96]. However, we shall explicitly demonstrate that it is possible to split the four component Dirac spinor into two distinct pieces. Whilst these are not Weyl spinors, it serves as a proof of concept. As such, the word “chiral” will be used loosely in this sense throughout this chapter; which deals principally with these $2+1$ dimensional theories, and should be taken with a pinch of salt to refer to this splitting of the spinor components until the next chapter, in which we reduce a $4+1$ dimensional theory to a $3+1$ dimensional theory with genuine chirality.

We begin with the Dirac equation for a free fermion in $3+1$ dimensional Minkowski space, with a fermion mass dependant on position in x^3

$$[-i\gamma^\mu\partial_\mu - i\gamma^3\partial_3 + M(x^3)]\Psi = 0, \quad (4.1)$$

here the Lorentz indices run over $\mu = 0, 1, 2$. Note that in the Dirac basis, the γ matrices are,

$$\begin{aligned} \gamma^0 &= \begin{pmatrix} 1 & 0 & 0 & 0 \\ 0 & 1 & 0 & 0 \\ 0 & 0 & -1 & 0 \\ 0 & 0 & 0 & -1 \end{pmatrix}, \gamma^1 = \begin{pmatrix} 0 & 0 & 0 & 1 \\ 0 & 0 & 1 & 0 \\ 0 & -1 & 0 & 0 \\ -1 & 0 & 0 & 0 \end{pmatrix}, \\ \gamma^2 &= \begin{pmatrix} 0 & 0 & 0 & -i \\ 0 & 0 & i & 0 \\ 0 & i & 0 & 0 \\ -i & 0 & 0 & 0 \end{pmatrix}, \gamma^3 = \begin{pmatrix} 0 & 0 & 1 & 0 \\ 0 & 0 & 0 & -1 \\ -1 & 0 & 0 & 0 \\ 0 & 1 & 0 & 0 \end{pmatrix}. \end{aligned} \quad (4.2)$$

We now wish to define a “projector” such that the four component Dirac spinor is split into a pair of two component spinors in 2+1 dimensions upon dimensional reduction. We define

$$P_{\pm} = \frac{1}{2} (1 \pm i\gamma^3) \quad (4.3)$$

and then write the four component Dirac spinor as (here the $+$, $-$ refers to the static energy eigenvalue)

$$\Psi = \begin{pmatrix} \psi_1^+ \\ \psi_2^+ \\ \psi_1^- \\ \psi_2^- \end{pmatrix}, \quad (4.4)$$

which is acted upon by the projector to give the following four component spinors

$$P_{\pm} \Psi = \begin{pmatrix} \chi_1^{\pm} \\ \chi_2^{\pm} \\ -i\chi_1^{\pm} \\ i\chi_2^{\pm} \end{pmatrix}, \quad \begin{aligned} \chi_1^{\pm} &= (\psi_1^+ \pm i\psi_1^-) \\ \chi_2^{\pm} &= (\psi_2^+ \mp i\psi_2^-) \end{aligned}, \quad (4.5)$$

each of which carries the information content of a two component spinor. Now we consider the mass profile in the x^3 direction, which we write piecewise as,

$$M(x^3) = \begin{cases} +M, & x^3 > 0 \\ 0, & x^3 = 0 \\ -M, & x^3 < 0 \end{cases}, \quad M \in \mathbb{R}^+. \quad (4.6)$$

We can now seek solutions for the massless modes of (4.1), by decomposing the spinor into eigenmodes of the projector (4.3),

$$\Psi(x^M) = [a(x^3)P_+ + b(x^3)P_-] \psi_0(x^\mu). \quad (4.7)$$

Where the index $M = 0, \dots, 3$ runs over the whole space and $a(x^3), b(x^3)$ are simply functions that carry the x^3 dependence of Ψ . It is assumed that the mode ψ_0 is massless on the 2+1 dimensional space spanned by $x^{0\dots 2}$ thus,

$$i\gamma^\mu \partial_\mu \psi_0 = 0. \quad (4.8)$$

This assumption alongside the anticommutation of the γ matrices and the definition of the projector, give the relations $\gamma^\mu P_+ = P_- \gamma^\mu$ and $\gamma^\mu P_- = P_+ \gamma^\mu$, which allows us to drop the first term in (4.1). This leaves just the dynamics of the functions $a(x^3)$ and $b(x^3)$,

$$(-i\gamma^3 \partial_3 + M(x^3)) [a(x^3)P_+ + b(x^3)P_-] \psi_0(x^\mu) = 0. \quad (4.9)$$

Now by noting that γ^3 squares to $-\mathbb{I}_4$, it is straightforward to realise that $i\gamma^3 P_+ = P_+$ and $i\gamma^3 P_- = -P_-$ and, for (4.9) to hold, one must have

$$[M(x^3) - \partial_3] a(x^3) = 0, \quad [M(x^3) + \partial_3] b(x^3) = 0. \quad (4.10)$$

The second of these equations, has a normalisable solution

$$b(x^3) = C_b e^{-|M|x}, \quad (4.11)$$

whereas the first is non-normalisable and as such is an unphysical mode at the discontinuity about $x^3 = 0$. The sign of the change in M is significant here! Including a second discontinuity, at some $x^3 = \text{const} > 0$, with opposite sign will localise the $a(x^3)$ mode on the new discontinuity (here instead $b(x^3)$ will be non-normalisable). So we see that the two, two component spinors localise on individual domain walls separated in the x^3 direction. We will now try to replicate the above construction in a controlled, well understood, holographic setting. The D3/D7 intersection of IIB string theory.

4.2 Domain Walls in the D3/D7 system.

The first system in which we shall construct the domain wall theories, D3/D7 brane intersection, holographically dual to $\mathcal{N} = 4$ super-Yang-Mills with the addition of a matter hypermultiplet in the fundamental representation of $SU(N)$ (quarks), that preserves half the supersymmetries of the original super-Yang-Mills theory [67]. When the D7 branes are considered in the probe limit, this is equivalent to a

quenched approximation in the dual field theory. The quark loops are suppressed but the full effect of the gauge field dynamics on the quarks is considered. In the string picture, the branes are aligned in the half supersymmetry preserving configuration shown in the brane scan,

$$\begin{array}{c|cccccccccc}
 & 0 & 1 & 2 & 3 & 4 & 5 & 6 & 7 & 8 & 9 \\
 \hline
 \text{D3} & - & - & - & - & \bullet & \bullet & \bullet & \bullet & \bullet & \bullet \\
 \text{D7} & - & - & - & - & - & - & - & - & \bullet & \bullet
 \end{array} \tag{4.12}$$

The two sets of D-branes live in a 10 dimensional supersymmetric Minkowski vacuum which, when backreaction of the D3 branes is taken into account, becomes a warped asymptotically Minkowski space. Deep in the “throat” of the geometry, there is a black hole-like horizon and the near horizon region is the familiar $AdS_5 \times S^5$. Still this top down picture is incredibly useful for classifying the fluctuations of the theory, and generally garnering some intuition (there is a beautiful exposition on this in [97]). In the probe limit the D7 branes wrap an asymptotically $AdS_5 \times S^3$ subspace of the full $AdS_5 \times S^5$. Writing the metric in a form that is amenable to the embedding of the probe sevenbranes,

$$ds^2 = \frac{r^2}{R^2} (\eta_{\mu\nu}) + \frac{R^2}{r^2} (d\rho^2 + \rho^2 d\Omega_3^2 + \delta_{ij} dL^{(i)} dL^{(j)}), \tag{4.13}$$

it becomes obvious that branes lying flat in the $L^{(i)}$ (with $i = 1, 2$) directions wrap an asymptotically $AdS_5 \times S^3$ subspace. Here the $d\Omega_3^2$ is a shorthand to denote the line element on the three sphere and the AdS radial direction $r^2 = \rho^2 + (L^{(i)})^2$ the indices μ, ν run over the “field theory” directions, that is to say, the directions shared with the stack of coincident D3 branes generating the near horizon geometry (in this case $\mu, \nu = 0, \dots, 3$). The *embedding functions* that describe the position of the D7 brane in the $X^{(8,9)}$ directions can be written as $L^{(i)}(\xi^a)$. These functions transform as scalar fields on the worldvolume of the probe. The sevenbranes are tensionful, charged objects and as such, will act to minimise their worldvolume. The natural action that governs the dynamics of the embedding scalars is then the Dirac-Born-Infeld (DBI) action [98]. In this case, we take the embedding scalar to be dependant on the x^3 direction (henceforth z), and the radial direction on the probes ρ . The DBI action for the probe branes is

$$S_{D7,DBI} = -T_7 \int d^8 \xi \sqrt{-\det[G_{ab} + B_{ab} + F_{ab}]}, \tag{4.14}$$

and the lowercase latin indicies $(a, b) = 0, \dots, 7$ are worldvolume indices; indicating that bulk quantities like the metric G_{MN} , and the Kalb-Ramond Field B_{MN} , have

been pulled back to the worldvolume of the sevenbrane. Low energy dynamics of strings that start and end on the D7 brane(s) are captured by a $U(1)$ gauge field strength F_{ab} which is native to the sevenbrane, and when considering the lowest energy state of the D7 we can neglect the excited open string modes living on its surface (meaning we set $F_{ab} = 0$). In the $AdS_5 \times S^5$ background, the Kalb-Ramond field is everywhere zero¹, so the DBI action for the scalars $L^{(i)}(z, \rho)$ reads,

$$S_{D7,DBI} = -T_7 \Omega_3 \mathcal{N}_{D7} \int d^4x d\rho \rho^3 \sqrt{1 + (\partial_\rho L^{(i)})^2 + \frac{R^4}{r^4} (\partial_z L^{(i)})^2}. \quad (4.15)$$

This is of course not the full action for the probe branes! The other part describes the coupling to RR forms, the Wess-Zumino terms [99]. The three angular coordinates on the equatorial $S^3 \subset S^5$ have been integrated over, giving the factor Ω_3 , and the factor \mathcal{N}_{D7} denotes the number of probe branes. We shall consider only a single probe in this case.

For D7 probes, the embedding fields $L^{(i)}(\rho)$ describe the mass-chiral condensate source-operator pair, in the asymptotic region, at the conformal boundary. Considering a radially dependent embedding, the action for the D7 probes is simply

$$S_{D7,DBI} \sim \int d\rho \rho^3 \sqrt{1 + (\partial_\rho L)^2}, \quad (4.16)$$

and the resulting equation of motion for the scalar L is ²,

$$\frac{\rho^3 \partial_\rho L}{\sqrt{1 + \partial_\rho L^2}} = c, \quad (4.17)$$

where c is a constant of integration. For probes that asymptotically approach some constant position on the boundary, that is $L \rightarrow const$, $\partial_\rho L \rightarrow 0$, the asymptotic solution is

$$L \sim A + \frac{B}{\rho^2}. \quad (4.18)$$

One can analyse the above on dimensional grounds, and realising that $[L] = [\rho] = 1$ leads to the conclusion that $[A] = 1$, and $[B] = 3$ which is the expected pairing of a dimension one source, and a dimension three operator in a 3+1 dimensional theory. This aides in the identification of the pair A and B as $m, \langle \bar{q}_L q_R \rangle$. Thus the

¹ $AdS_5 \times S^5$ is the near horizon geometry of black threebrane solution corresponding to the D3 branes. The only non-trivial form in the geometry is the four-form which is sourced by the D3 branes

²The scalars have a $U(1)$ symmetry that rotates $L^{(1)}, L^{(2)}$ into one another. Without loss of generality we will set $L^{(1)} = L, L^{(2)} = 0$ for now. Later fluctuations of $L^{(2)}$ about 0 will describe the pseudoscalar mesons of the theory.

DBI scalars describing the D7 embedding give information about the mass and condensate of the $\mathcal{N} = 2$ hypermultiplet. We take our z dependant embedding scalar to asymptotically describe a position dependant source operator pair

$$L(z) \sim m_q(z) + \frac{\langle \bar{q}_L q_R(z) \rangle}{\rho^2}. \quad (4.19)$$

From here the approach will be to write out and then linearise the equations of motion, and apply a z dependant mass perturbation to the massless theory (where the D7 has a flat embedding at $L = 0$). We shall then normalise and sum the perturbations such that the boundary profile for the quark mass is periodic with period K , and describes two sharp walls at z_0 and $K - z_0$ where the sign of the mass changes. The boundary profile for the D7 brane embedding in the z direction can be written as,

$$L(z) = \begin{cases} 1, & 0 \leq z \leq z_0, \text{ and, } K - z_0 \leq z \leq K \\ 0, & z = z_0, \text{ and, } z = K - z_0, \\ -1, & z_0 \leq z \leq K - z_0. \end{cases} \quad (4.20)$$

The equations of motion linearised about $L = 0$ are,

$$\partial_\rho (\rho^3 \partial_\rho L) + \frac{1}{\rho} (\partial_z^2 L) = 0, \quad (4.21)$$

and we seek solutions to these equations of the form,

$$L(\rho, z) = \sum_k f_k(\rho) \cdot a_k \cos kz. \quad (4.22)$$

The linearised equations of motion are independant of value L itself, depending only on the derivatives, and thus the physics is independant of the chosen normalisation for the scalar field. We choose to normalise the solutions such that

$$\lim_{\rho \rightarrow \infty} f_k(\rho) = 1, \quad (4.23)$$

leaving the boundary solution,

$$\lim_{\rho \rightarrow \infty} L(\rho, z) = \sum_k a_k \cos kz. \quad (4.24)$$

What remains is to determine the coefficients a_k through Fourier expansion of (4.20), which decomposes into:

$$f(z) = \frac{a_0}{2} + \sum_{n=1}^{\infty} a_n \cos\left(\frac{2\pi n}{K} z\right),$$

$$a_0 = \frac{8z_0}{K} - 2, \quad (4.25)$$

$$a_n = \frac{2}{\pi n} \left[\sin\left(\frac{2\pi n}{K} z_0\right) - \sin\left(\frac{2\pi n}{K} (K - z_0)\right) \right].$$

The first 10,000 terms of this series are plotted in Figure (4.1). We now must solve

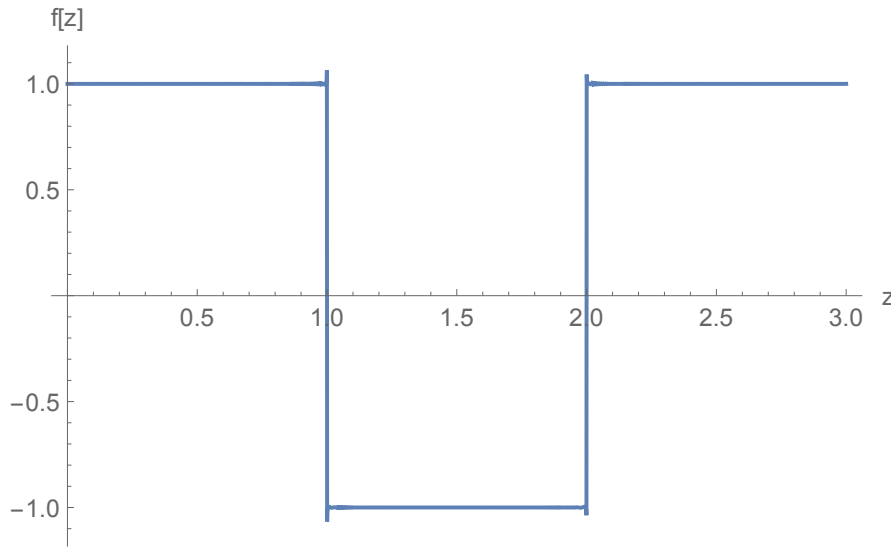


FIGURE 4.1: A plot of the fourier series (4.25) truncated at $n = 10,000$. Here the values $K = 3$, $z_0 = 1$ were used to produce the plot.

for the radial profiles $f_k(\rho)$. With the ansatz (4.22), the linearised equations of motion become,

$$\rho^3 \partial_\rho^2 f_k(\rho) + 3\rho^2 \partial_\rho f_k(\rho) - \frac{k^2}{\rho} f_k(\rho) = 0, \quad (4.26)$$

which can be solved numerically. It should be noted, that since there is no scale in the bulk AdS the solutions will be ill behaved in the IR. To avoid this we include a hardwall regulator at $\rho = 1$, and shoot from $\rho = 1$ with $\partial_\rho L = 0$, however, in doing this we should only trust any structures we see far away from the hardwall, with $\rho \gg 1$. A subset of these solutions are displayed in Figure (4.2), it is shown that the higher k modes are less supported at small radial scales, which is expected.

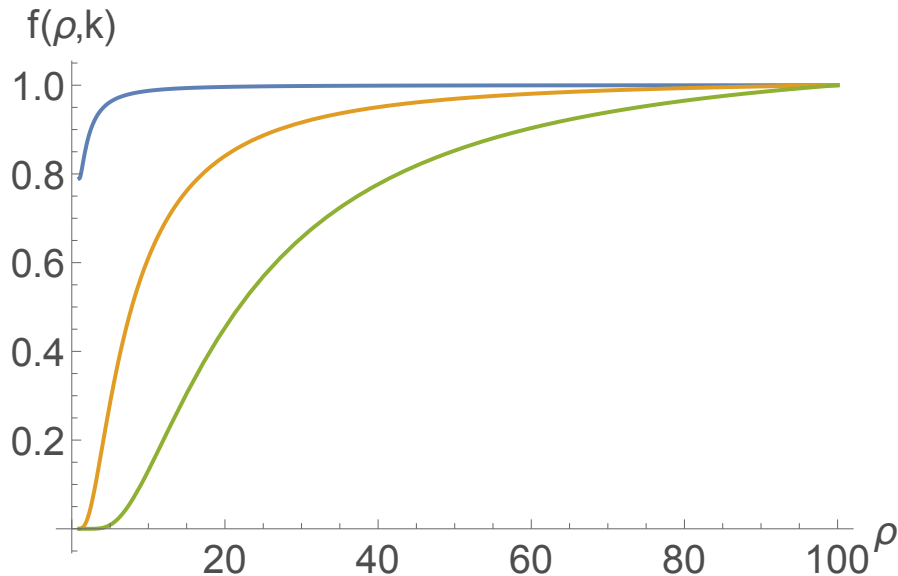


FIGURE 4.2: Some solutions $f_k(\rho)$ in $AdS_5 \times S^5$ with a hardwall at $\rho = 1$ for: $k = \frac{2\pi}{K}$ (blue), $k = \frac{20\pi}{K}$ (orange), and $k = \frac{60\pi}{K}$ (green).

The more highly oscillating (and thus highly energetic) modes are not expected to play a part in the IR physics of the theory. Putting together the radial profiles we can plot out a section of the solution, which is displayed in Figure (4.3). Critically Figure (4.3) shows that the pair of domain walls³, whilst separated in the UV, may join together in the interior of AdS_5 ⁴. This joining behaviour is not so much of a surprise, it is familiar from probe embeddings in systems with branes and anti-branes (such as the Sakai-Sugimoto Model [77, 90], and $D3/D5\overline{D5}$ [102, 53, 103, 54, 89, 55]). Where the walls join in the bulk, we take this to be an indication of the fermions forming a condensate. The operator that condenses is not a local operator. The left-handed, and right-handed fermions are separated in the z direction by some width w at the boundary, so the gauge invariant operator that condenses must be an open Wilson line, with quarks at either end pinned to the domain walls,

$$\mathcal{O} = \bar{q}_1 e^{i \int A^{(1)}} q_2. \quad (4.27)$$

This operator is dual to a long open string [104], which in this case extends between the domain walls. In the IR where the domain walls join there is no separation and thus this operator mixes freely with $\bar{q}_1 q_2$. By fitting to the asymptotic form of the solution (4.18) we plot the local (3+1 dimensional) quark condensate in

³Some work on a similar system with a single defect was done in [100, 101]

⁴One may wonder whether this is a trustworthy behaviour from the comments about the hardwall, strictly we should only trust this behaviour in the region $\rho \gg 1$. However we later devise an analytic way to describe the joining of the walls, or at least the $L=0$ surface, which shows good agreement even around $\rho \sim 5$.

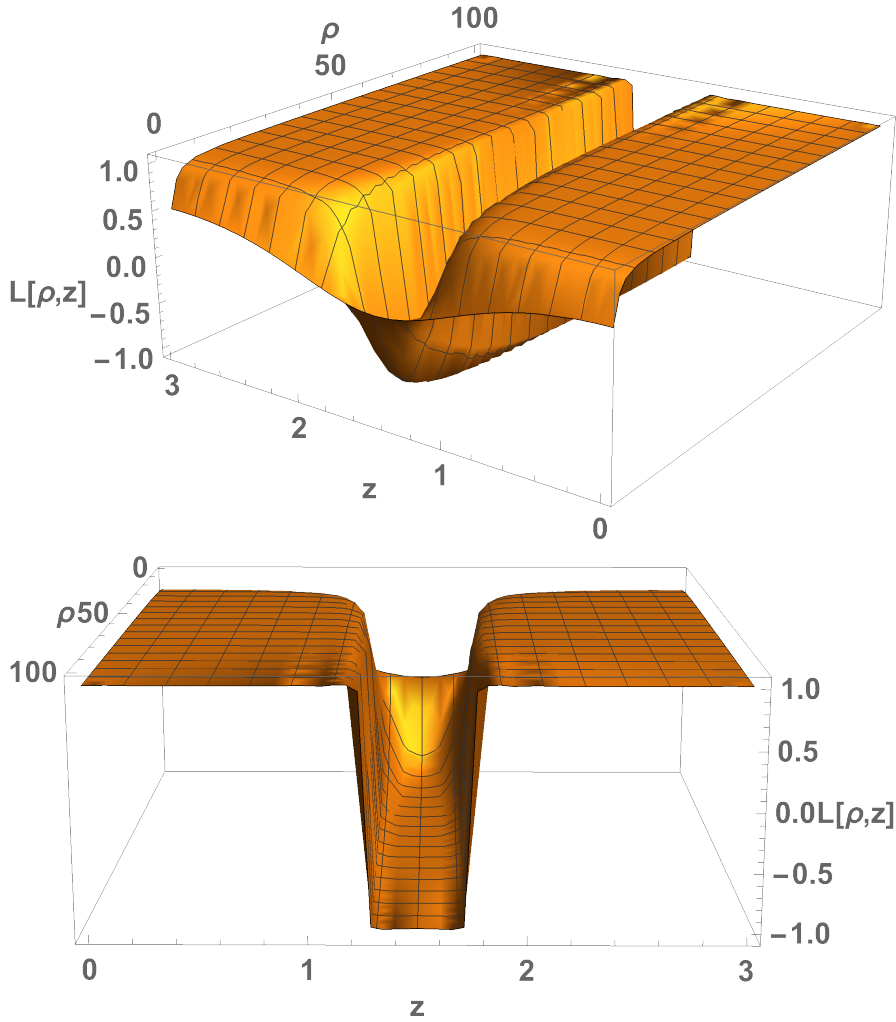


FIGURE 4.3: An example domain wall solution from two perspectives. top: a perspective showing the overall shape, bottom: a perspective “from the boundary” showing the boundary profile of the D7 brane realising (4.20). For these plots $K = 3$, $z_0 = 1.25$, was used and the series was truncated at $n = 350$.

Figure (4.4). This figure shows the numerical value for the condensate localising around the position of the domain walls. The condensate becomes more localised the more terms that are included in the Fourier series, whilst having a zero value at the exact position of the domain wall defects. It is not at this point clear whether the peaks either side of the domain walls, one positive and one negative, will merge in the full theory with the true condensate presumably summing to zero. This however, is difficult to calculate in the linearised theory. To this end, we will aim to dimensionally reduce to the *locus* where the 3+1 dimensional quark mass vanishes. The next section will develop the large mass limit, where we take the magnitude of the 3+1 dimensional quark mass to be infinite⁵, everywhere

⁵technically, of a scale $|M| \gg 1/w$

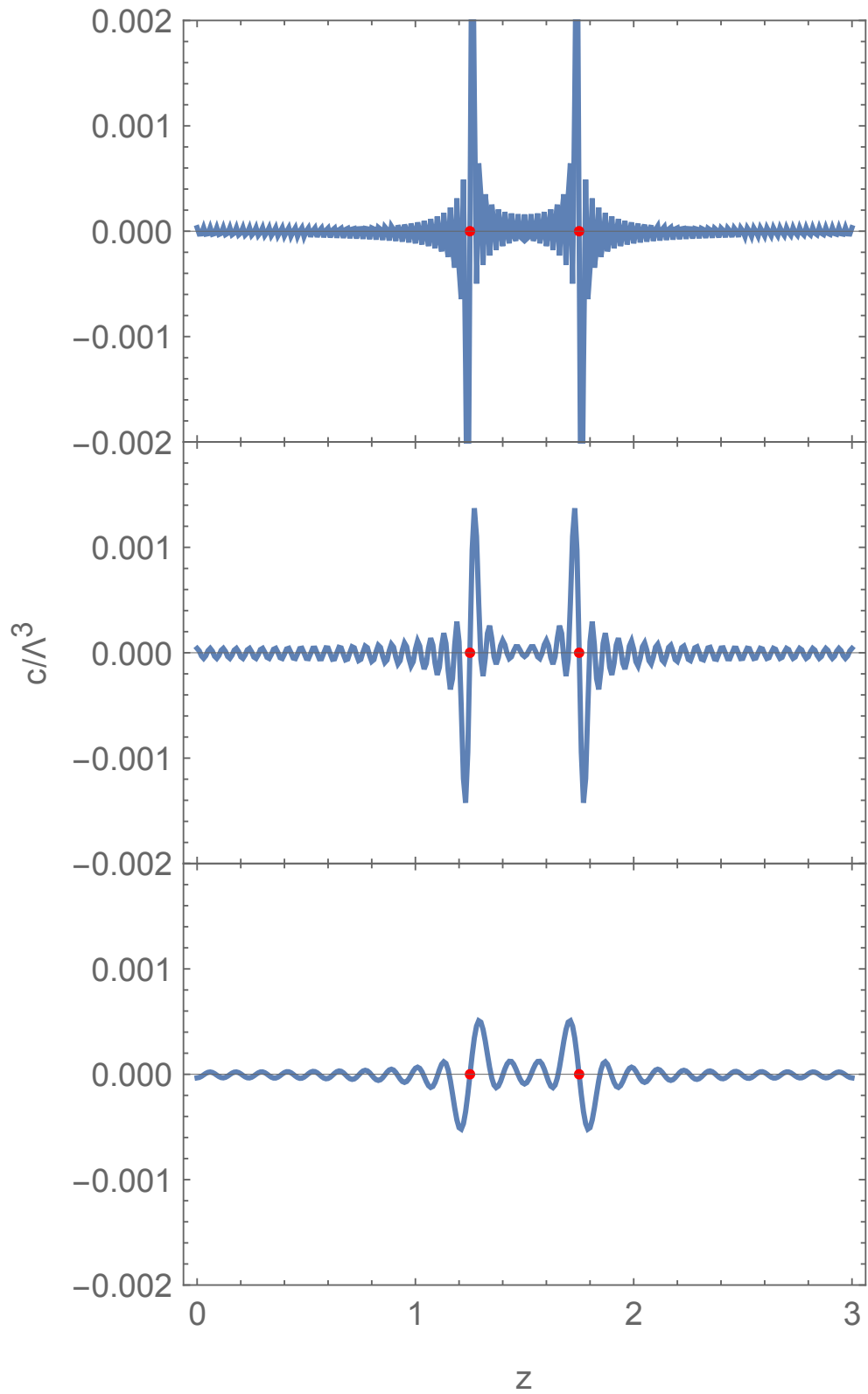


FIGURE 4.4: The 3+1 d quark condensate at the boundary of AdS plotted against z for 150 Fourier modes (top), 100 Fourier modes (middle), and 50 Fourier modes (bottom). The positions of the domain walls are indicated with red dots on the z axes.

except on the *domain wall locus* where it is zero. In this limit the dynamics of the quarks becomes strictly localised on the domain walls, and they then describe a novel holographic theory of quarks on a codimension one defect in the dual theory. We find explicit similarities to another codimension one holographic theories, the $D3/D5\overline{D5}$ intersection. This construction will allow us to explicitly examine the fluctuations living on the domain walls which are in turn dual to operators living on the defect in the gauge theory.

4.3 The Large Mass Limit: a tale of U shaped loci

In this section we develop the large mass limit, and find explicit equations for the *domain wall loci* where the four dimensional quark mass vanishes. This will be done through two methods. The first method, is one in which the embedding fields of the D7 brane are considered to be Heaviside function valued⁶ on some contour $z(\rho)$. The assumption that contour is smooth and monotonic, enables us write down an action for $z(\rho)$ that is analogous to the DBI action for the embedding field of a brane. In this case it is the same action that one would expect to find for the U shaped brane-antibrane configurations of the $D3/D5\overline{D5}$ system. The second approach is more direct and assumes only that the wall is sufficiently steep, such that the brane has a step like profile across the whole of the $z(\rho)$ locus. One can then immediately write down an action functional that extremises the 6+1 dimensional worldvolume of the locus, which is reminiscent of the minimal surface prescriptions seen in discussions of entanglement entropy of holographic CFTs [105]. Ultimately the two approaches are equivalent so far as the cases in this thesis are concerned. They produce the same equations of motion for the various *domain wall loci*, and thus the same physics.

4.3.1 One Large Step for Brane-kind

We will start by making the following ansatz, we are searching for solutions of the DBI action of the form

$$\partial_\rho L \sim J \times \delta(z(\rho) - z) \quad (4.28)$$

⁶more accurately, the radial derivative, $\partial_\rho L \sim \delta(z - z(\rho))$

where J is a Jacobean factor, which is included to adjust the appropriately reduce to the subspace $z(\rho)$. We will identify this factor by considering first a toy example in a three dimensional flat space. The analogous ‘‘DBI’’ action for a ‘‘2-brane’’ in three dimensional Euclidean space is

$$S = \int dx dy \sqrt{1 + (\partial_x L)^2 + (\partial_y L)^2}. \quad (4.29)$$

We see here that by factoring out $\partial_x L$ we arrive at

$$S = \int dx dy \partial_x L \sqrt{1 + \left(\frac{\partial x}{\partial y}\right)^2 + \frac{1}{(\partial_x L)^2}}. \quad (4.30)$$

We claim that the last term under the square root can be neglected on the locus of the domain wall, where $\partial_x L$ is large. Now we want to intuit the form of $\partial_x L$ that gives an action for the curve $y(x)$ on two dimensional euclidean space. This form is naturally

$$\partial_x L \sim \frac{\partial y}{\partial x} \delta(y - y(x)), \quad (4.31)$$

which when inserted into (4.30) gives the action,

$$S = \int dx \sqrt{1 + \left(\frac{\partial y}{\partial x}\right)^2}. \quad (4.32)$$

This is immediately recognisable as the proper length of the line $y(x)$ on a Euclidean two plane. There is still some ambiguity in (4.31) however, metric factors will come into play as we allow non-trivial background geometries. So now we shall examine a case of a ‘‘two brane’’ embedded in a non trivial three dimensional space, with metric

$$ds^2 = g_{xx} dx^2 + g_{yy} dy^2 + g_{LL} dL^2 \quad (4.33)$$

with ‘‘brane’’ embedding $L(x, y)$. The analogous DBI-like action is then,

$$S = \int dx dy (g_{xx} g_{yy})^{1/2} \sqrt{1 + \frac{g_{LL}}{g_{xx}} (\partial_x L)^2 + \frac{g_{LL}}{g_{yy}} (\partial_y L)^2}. \quad (4.34)$$

We can now play a similar game and factor out $\frac{g_{LL}}{g_{xx}} \partial_x L$, whilst modifying (4.31) to include the new metric factors. Now we arrive at

$$S = \int dx dy (g_{LL} g_{yy})^{1/2} (\partial_x L) \sqrt{1 + \frac{g_{xx}}{g_{yy}} \left(\frac{\partial x}{\partial y}\right)^2}. \quad (4.35)$$

Inserting the modified ansatz

$$\partial_x L \sim \tilde{G} \frac{\partial y}{\partial x} \delta(y - y(x)), \quad (4.36)$$

where \tilde{G} is some combination of metric factors to be determined. This gives,

$$S = \int dx (g_{LL})^{1/2} \tilde{G} (g_{xx})^{1/2} \sqrt{1 + \frac{g_{yy}}{g_{xx}} \left(\frac{\partial y}{\partial x} \right)^2}. \quad (4.37)$$

To recover an action that extremises the length of the line $y(x)$, on the two dimensional surface at $L = 0$, we must identify \tilde{G} with $g_{LL}^{-1/2} \Big|_{L=0}$. Given that the dynamics we are interested in will be limited to a three-volume, as in the above example, we have all the tools needed to implement the D3/D7 domain walls. We start from the action (4.14), and factor out $\partial_\rho L$. Then inserting the ansatz

$$\partial_\rho L \sim \frac{1}{\sqrt{g_{LL}}} \Big|_{L=0} \frac{\partial z}{\partial \rho} \delta(z - z(\rho)) = \frac{\rho}{R} \frac{\partial z}{\partial \rho} \delta(z - z(\rho)), \quad (4.38)$$

the resulting action for the *locus* is,

$$\begin{aligned} S_{locus} &= -T_7 \Omega_3 \mathcal{N}_{D7} \int d^4 x d\rho \rho^3 \frac{\rho}{R} \frac{\partial z}{\partial \rho} \delta(z - z(\rho)) \sqrt{1 + \frac{R^4}{r^4} \left(\frac{\partial \rho}{\partial z} \right)^2} \\ &= -T_7 \Omega_3 \mathcal{N}_{D7} R \int d^3 x d\rho \rho^2 \sqrt{1 + \frac{\rho^4}{R^4} \left(\frac{\partial z}{\partial \rho} \right)^2}. \end{aligned} \quad (4.39)$$

It should be noted that performing the integral over the delta function, $\delta(z - z(\rho))$, restricts us to the contour where $L = 0$ by construction. As such, it sets all the metric factors which have dependence on L to $g_{ab}|_{L=0}$. In this case, we must replace any factors of r with factors of ρ .

From here we can now treat $z(\rho)$ as a functional to be varied, and the equation of motion from (4.39) minimises the volume of the domain walls. Since the action carries no explicit dependence on $z(\rho)$, the equations of motion simplify to

$$\frac{\rho^6 \partial_\rho z}{\sqrt{1 + \rho^4 \partial_\rho z^2}} = c_z, \quad (4.40)$$

or

$$\partial_\rho z = \pm \frac{c_z}{\rho^2 \sqrt{\rho^8 - c_z^2}}. \quad (4.41)$$

Here c_z is a constant of integration associated with the independence of the action

on $z(\rho)$, and the co-ordinates have been re-scaled⁷ to pick up stray factors of the AdS radius R . We can now look to (4.41) to identify the constant of integration with a physically useful quantity in the bulk. The derivative $\partial_\rho z$ diverges at some point $c_z^{1/4}$ in the bulk, further into the bulk ($\rho \leq c_z^{1/4}$) the equations of motion become complex, suggesting the solution “ends” at $c_z^{1/4}$. We will thus identify $c_z = \rho_{min}^4$. Conversely, in the asymptotic region it falls off as c_z/ρ^6 . The asymptotic flattening of the solutions, with a sharp divergence in the bulk suggests that we should set boundary conditions at ρ_{min} : $z(\rho_{min}) = 0, z'(\rho_{min}) \rightarrow \pm\infty$. This gives U-shaped solutions for the *locus* $z(\rho)$, with well separated walls joining (and terminating) at ρ_{min} . We should then check that this is in good agreement with the linearised system discussed in the previous section.

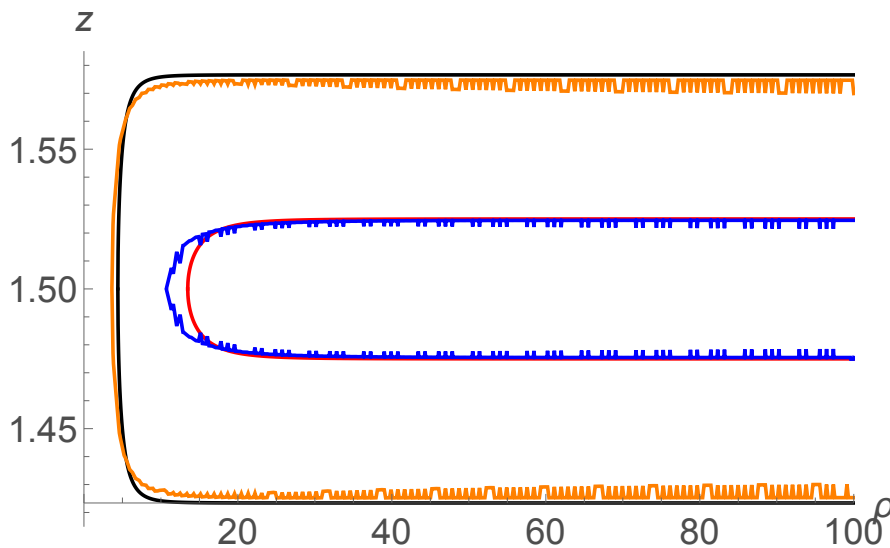


FIGURE 4.5: A plot of the solutions to (4.41) (Black, Red), matched to the $L = 0$ contour of their linearised counterparts (Orange, Blue). The solutions are matched by their separation at the boundary.

Figure (4.5) shows that there is good agreement between the solutions to (4.41), and the $L = 0$ contours of the linearised system. There is some noise present in the plots from the linearised system, which is an artefact of truncating the Fourier series down to a finite number of terms. Presumably, plotting all terms would solve this.

4.3.2 Minimal Surface

Before moving on to discuss the fields that live on the domain wall loci; there is a second, more direct, approach to finding the equations of the loci that should be

⁷This is not a necessary step, it just makes the later formulae look neater.

mentioned. In this approach we start with some prior knowledge of what we want from the solution. We'd like to write down an action that minimises the volume of some fictitious “sixbrane”⁸ that lives in the background, extended along some contour $z(\rho)$, at zero transverse displacement from the stack of D3 branes. The appropriate action to write down is then one that gives the proper volume of the “sixbrane”, which is

$$S \sim \int d^7x \sqrt{-\det \tilde{\mathcal{G}}} \quad (4.42)$$

where $\tilde{\mathcal{G}}$ is the induced metric on the “sixbrane”. Calculating the induced metric, one arrives at

$$S \sim \int d^3x d\rho \rho^2 \sqrt{1 + \rho^4 (\partial_\rho z)^2}, \quad (4.43)$$

which up to factors is the same as (4.39). Ultimately there is no tangible difference between the two methods.

4.3.3 A Non-Supersymmetric D3/D7 Intersection

Late in the writing of this thesis, a third method for calculating the geometry of the domain walls was realised. By taking the large mass limit, the resulting system is a brane configuration that is extended in X^8 , and point-like embedded in z . The remaining flat plateaus have been functionally removed from the system, by taking $|M| \rightarrow \infty$. From the perspective of the dual field theory the quarks living off the locus are non-dynamical and decouple from the theory. Functionally, we have started with a supersymmetric brane intersection and deformed it to study a non-supersymmetric defect system. After the large mass limit the brane system that we are left with is,

	0	1	2	3	4	5	6	7	8	9	
D3	-	-	-	-	•	•	•	•	•	•	.
D7	-	-	-	•	-	-	-	-	-	•	

(4.44)

This intersection has $\#_{ND} = 6$, and therefore preserves none of the supersymmetry of the original theory. By re-writing the metric in a way that manifests the symmetries of the new brane intersection,

$$ds^2 = \frac{r^2}{R^2} (\eta_{\mu\nu} dX^\mu dX^\nu) + \frac{R^2}{r^2} (d\rho^2 + \rho^2 d\Omega_4^2 + (dX^9)^2), \quad (4.45)$$

⁸Non-supersymmetric D-branes of even (odd) spatial dimension in type IIB (IIA) string theory do exist, see [106] for example, but they are unstable. These are not the branes we discuss here. Our “branes” are just a construct to arrive at the right loci intuitively

with $r^2 = \rho^2 + \tilde{L}^2$, we can embed the D7 brane in the geometry with the embedding scalars $X^3 = z(\rho)$, and $X^9 = \tilde{L}(\rho)$. Suddenly we have done away with explicit z dependence in favour of allowing $z(\rho)$ to be determined dynamically⁹. One thing to note here, is that we have redefined the radial co-ordinate ρ . The radial direction in our system is what previously would have been $\rho^2 + L^2$. Clearly on the $L = 0$ contour, these are equivalent. This approach now allows us to solve for the full ρ - X^8 dependence that had previously been neglected. The DBI action for the sevenbrane is,

$$S_{D7} = -T_7 \Omega_4 \int d^4x \frac{\rho^4 R^2}{r^2} \sqrt{1 + (\partial_\rho \tilde{L})^2 + \frac{r^4}{R^4} (\partial_\rho z)^2}. \quad (4.46)$$

The presence of a factor of r in the denominator of the action is worrying. However, by calculating the equation of motion for the field \tilde{L} ,

$$\begin{aligned} & \partial_\rho \left(\frac{\rho^4}{\rho^2 + \tilde{L}^2} \frac{\partial_\rho \tilde{L}}{\sqrt{1 + (\partial_\rho \tilde{L})^2 + \frac{r^4}{R^4} (\partial_\rho z)^2}} \right) \\ & + \frac{\rho^4}{(\rho^2 + \tilde{L}^2)^2} \cdot 2\tilde{L} \cdot \sqrt{1 + (\partial_\rho \tilde{L})^2 + \frac{r^4}{R^4} (\partial_\rho z)^2} \\ & - \frac{\rho^4 (\partial_\rho z)^2}{\sqrt{1 + (\partial_\rho \tilde{L})^2 + \frac{r^4}{R^4} (\partial_\rho z)^2}} \cdot 2\tilde{L} = 0, \end{aligned} \quad (4.47)$$

we realise that $\partial_\rho \tilde{L} = \tilde{L} = 0$ is a solution to the equations of motion. It is possible that this solution is a maximum, and unstable to turning on some non-trivial $\tilde{L}(\rho)$. Setting $\tilde{L} = 0$ the action for the D7 brane becomes,

$$S_{D7} = -T_7 \Omega_4 R^2 \int d^3x d\rho \rho^2 \sqrt{1 + \frac{\rho^4}{R^4} (\partial_\rho z)^2}, \quad (4.48)$$

which up to a multiplicative factor is equivalent to (4.39). With this in mind, we realise that we can solve the resulting equation of motion, (4.41), explicitly for the full spatial dependence of the domain walls,

$$z(\rho, X^8) = \frac{\sqrt{(\rho^2 + (X^8)^2)^4 - c^2} {}_2F_1\left(\frac{3}{8}, 1; \frac{7}{8}; \frac{(\rho^2 + (X^8)^2)^4}{c^2}\right)}{c \sqrt{\rho^2 + (X^8)^2}}, \quad (4.49)$$

⁹which was sort of the point anyways

where c is a constant analogous to c_z that controls the closest approach of the U-shaped brane-antibrane configuration to the origin of the space. Given that we now have three methods of determining the geometry of the loci, and a fourth if one considers the D3/D5 anti-D5 system, which has identically shaped brane embeddings, we can be confident that our large mass limit is reasonably capturing the physics of the domain wall systems. Further, given that the same defect geometry has arisen in several different systems, it seems that the shape of the joined branes/domain walls is controlled by the co-dimension of the defect.

4.4 Fluctuations about the Wall

The next step in the exploration of this system is to understand the fluctuations of the DBI fields restricted to the loci. These fluctuations, restricted to the loci, are then assumed to be holographically describing the quantum field theory that lives on the domain wall defect. The goal is to take the action (4.15) and restrict to the contour $z(\rho)$ that solves (4.41). Schematically, this will look like

$$S_{DW} = \int d^8\xi \Delta(z - z(\rho)) \mathcal{L}_{D7} = \int d^7\xi \mathcal{L}_{DW} \quad (4.50)$$

where Δ is some function that restricts to the contour $z(\rho)$, and dimensionally reduces the action. This function must carry the geometric data of $z(\rho)$, and thus we identify

$$\Delta(z - z(\rho)) = \sqrt{\det \tilde{g}} \delta(z - z(\rho)). \quad (4.51)$$

Here \tilde{g} is the induced metric on the line $z(\rho)$ (in the two plane $z - \rho$). It may at first seem odd that the factor pre-multiplying the δ function is not the same as in (4.38) however, the goal in these two cases is not the same! Here we wish to restrict the D7 action by applying some appropriate function that localises fluctuations of the DBI fields onto the locus, in (4.38) the goal was to find the leading behaviour of the DBI fields that realises the geometry of the domain wall system, and allows us to calculate the *loci*. So it is not surprising that these two delta functions are not the same. For the case at hand we have

$$\begin{aligned} \Delta(z - z(\rho)) &= \sqrt{G_{\rho\rho} + G_{zz}(\partial_\rho z)^2} \Big|_{L=0} \delta(z - z(\rho)), \\ &= \frac{1}{\rho} \sqrt{1 + \rho^4(\partial_\rho z)^2} \delta(z - z(\rho)). \end{aligned} \quad (4.52)$$

The resulting action for the fluctuations is then

$$S_{DW} \simeq \int d^2x d\rho \sqrt{1 + \rho^4(\partial_\rho z)^2} \rho^2 \sqrt{1 + \mathcal{A}(\partial_\rho L)^2 + \frac{(\partial_i L)^2}{(\rho^2 + L^2)^2}}, \quad (4.53)$$

with

$$\mathcal{A} = 1 + \frac{1}{(\rho^2 + L^2)^2 (\partial_\rho z)^2}. \quad (4.54)$$

The indices i run over the $X^{0,1,2}$ directions, and the function \mathcal{A} encodes the z dependence of the solutions. In this case, we do not treat $\partial_\rho z$ as a functional to be varied, but instead as input data to the theory. For the lowest energy state for the scalar L , in which there are no fluctuations in the $X^{0,1,2}$ directions, the equation of motion for L is

$$\partial_\rho \left(\frac{\sqrt{1 + \rho^4(\partial_\rho z)^2} \rho^2 \mathcal{A}(\partial_\rho L)}{\sqrt{1 + \mathcal{A}(\partial_\rho L)^2}} \right) + \frac{1}{2} \rho^2 \sqrt{1 + \rho^4(\partial_\rho z)^2} \frac{\partial \mathcal{A}}{\partial L} \frac{(\partial_\rho L)^2}{\sqrt{1 + \mathcal{A}(\partial_\rho L)^2}} = 0. \quad (4.55)$$

By inspection we can see that this is satisfied by $\partial_\rho L = 0$, $L = \text{constant}$. Now the fluctuations of the field L are dual to the quark mass-chiral condensate source-operator pair for the 2+1 dimensional theory that lives on the domain walls. Its asymptotic behaviour is

$$L \rightarrow m_q + \frac{c}{\rho}, \quad (4.56)$$

therefore we must identify the $L = m_q$ at all points on the RG flow given by (4.55) and thus the system describes a massive quark state in a conformal gauge background. We now can identify the only sensible boundary condition in the IR of the theory, where the domain wall pair join up. Here we must have $L(\rho_{min}) = \rho_{min}$, reflecting the presence of the dimensionful mass scale given by the *loci*, and thus $\rho_{min} = m_{IR} = m_q$. Now that we have described the vacuum of the theory, it is time to look to the mesons. These are described by fluctuations about the vacuum DBI field L . We will consider the system with $X^8 = L(\rho, z)$, $X^9 = \phi(\rho, z, x^i)$, where x^i are the co-ordinates that span the 2+1 dimensional domain wall defect. The linearised action for the fluctuations ϕ about L is

$$S_\phi = \int d^2x d\rho \rho^2 \sqrt{1 + \rho^4(\partial_\rho z)^2} \left(1 + \frac{1}{2} \mathcal{A}(\partial_\rho \phi)^2 + \frac{1}{2} \frac{(\partial_{x^i} \phi)^2}{(\rho^2 + L^2)^2} \right). \quad (4.57)$$

taking the following standard ansatz for ϕ

$$\phi(\rho, X^i) = \tilde{\phi}(\rho)e^{ik \cdot X}, \quad \text{with } k \cdot k = -M_\phi^2. \quad (4.58)$$

We arrive at the equation of motion for the meson ϕ ,

$$\partial_\rho \left(\rho^2 \sqrt{1 + \rho^4 (\partial_\rho z)^2} \mathcal{A} \partial_\rho \tilde{\phi} \right) + M_\phi^2 \frac{\rho^2 \sqrt{1 + \rho^4 (\partial_\rho z)^2}}{(\rho^2 + L^2)^2} \tilde{\phi} = 0. \quad (4.59)$$

By shooting out from ρ_{min} with boundary conditions $\tilde{\phi}(\rho_{min}) = 1$, $\tilde{\phi}'(\rho_{min}) = 0$ numerically it is found that the mass of the mesonic fluctuation ϕ is non-zero¹⁰. Critically, we do not see pseudo-Goldstone boson-like behaviour expected for the field ϕ as we move away from zero quark mass. Really, this tells us that whilst we see “chiral” symmetry breaking by the joining of the domain walls in the IR, *it is not dynamical*.

4.4.1 A system of two levels

In the previous sections we have set up the ingredients for constructing, and working with, with the domain wall theories. Consider this subsection an aside that details more practically how to work with them. Firstly, one takes either of the methods described in Section 4.3, and determines the set of domain wall loci. The loci are, generally, a one parameter family of curves defined by how far they reach into the interior of the geometry. The choice of locus (choice of ρ_{min}) then defines the microscopic theory. One then dimensionally reduces the DBI action for the D7 brane, in such a way that the DBI fields are restricted to live on the locus (as in (4.50) and the following example). The resulting equation of motion for the DBI scalar(s) describes then the (inverse) RG flow, from the IR surface to the UV boundary, of the quark mass-chiral condensate source-operator pair. Fluctuations about the solution describe the pseudoscalar mesons as in the usual D3/D7 intersection. At the UV cutoff, one can then determine the mass of the dimensionally reduced quarks living on the locus (or any other microscopic quantities prescribed by the *holographic dictionary* of the theory). Note here that just because the mass of the quarks in the higher dimensional theory vanishes on the locus, it does not *neccesarily* mean that this is the case in the lower dimensional theory. Indeed, much of the interesting physics in this theory comes from allowing the 2+1 dimensional quark mass to fluctuate away from zero. One is also not limited to working

¹⁰for $\rho_{min} = 1$, we have $M_\phi/m_q \sim 12$, and for $\rho_{min} = 0.1$ we have $M_\phi/m_q \sim 13$.

in “nice” backgrounds, or with just the DBI scalars. Chapter 5 will largely be concerned with embedding this type of domain wall theory in a confining geometry, and with the spectrum of meson fluctuations from gauge fields on the D7 brane. Chapter 6 will be concerned with working in a finite temperature system, and the phase transitions therein. It is important to stress that these systems be taken in two steps, the background geometry (gauge dynamics) dictates the set of *loci*, the *loci* in turn control the dynamics of the fields on their surface.

4.5 Dynamical “Chiral” Symmetry Breaking

So far we have described a 2+1 dimensional theory of massive quarks on the defects, with a quark mass controlled by where the defects join in the interior (or conversely their asymptotic width¹¹). There is breaking of the “chiral” symmetry for quarks on the defects but it is not dynamical! Instead the separation of the walls reflects the presence of a hard quark mass. There are however several known methods to realise dynamical chiral symmetry breaking in D3/D7 systems [71, 107, 108]. In this section we will investigate the methods through which we can dynamically break the “chiral” symmetry in the domain wall theories.

4.5.1 Magnetic Fields on the Probe Brane

The first method, will involve turning on a worldvolume magnetic field on the D7 brane. Starting again from the the DBI action for a D7 brane in $AdS_5 \times S^5$

$$S_{D7} = -T_7 \int d^8\xi \sqrt{-det [G_{ab} + (2\pi\alpha')F_{ab}]}. \quad (4.60)$$

This time, we take

$$F_{12} = -F_{21} = B_z, \quad (4.61)$$

and evaluating the action as before yields

$$S_{D7} = -T_7 \Omega_3 \int d^4x d\rho \sqrt{1 + \frac{B^2 R^4}{(\rho^2 + L^2)^2}} \times \rho^3 \sqrt{1 + (\partial_\rho L)^2 + \frac{R^4}{(\rho^2 + L^2)^2} (\partial_z L)^2}. \quad (4.62)$$

¹¹In the AdS case, these are linked on dimensional grounds and numerically we find $\rho_m = m_q \sim \frac{2}{3w}$

The worldvolume magnetic field acts as an effective dilaton factor, $e^\Phi = \sqrt{1 + \frac{B^2 R^4}{r^4}}$ that makes the interior of the geometry repulsive to the D7 probe. In the D3/D7 system without domain walls, it is found that the D7 brane rises up to some non-zero L at $\rho = 0$. This is true even when the transverse displacement at the boundary vanishes! Given that the embedding scalar is holographically dual to the quark mass-chiral condensate, this “pile-up” behaviour is interpreted as the system dynamically generating a quark mass as it flows into the IR of the theory. This breaks the supersymmetry of the theory and allows non-zero condensates, and thus represents dynamically breaking chiral symmetry on the probe brane. We will now attempt to realise this in the domain wall construction.

As a first attempt we will move back to the linearised regime, applying the spatially dependant mass defect as a perturbation to the massless D3/D7 system. As before we wish to impose (4.20) at the boundary, and take the ansatz (4.22) for the embedding fields L . The linearised equation of motion for the Fourier modes $f_k(\rho)$ in this system is¹²

$$\partial_\rho (e^\Phi \rho^3 \partial_\rho f_k(\rho)) - e^\Phi \frac{k^2}{\rho} f_k(\rho) + \frac{2B^2}{e^\Phi \rho^3} f_k(\rho) = 0. \quad (4.63)$$

This is problematic! The system appears unstable and the low k Fourier modes rise up to very large values on the IR hardwall. This is not the instability we would like to study; and so we abandon the approach of starting by applying the periodic mass defect as a perturbation to the massless system in favour of moving directly to the large mass limit. The linearised system was a useful toy approach to gain some intuition, but it has served its purpose!

So far, we have been careful to emphasise that the interesting physics of the system is governed by the set of *domain wall loci* in the background. We then expect that the pile up behaviour of quarks in the D3/D7 system will be reflected in the geometry of the *loci*. We now show that this is the case for systems that dynamically break “chiral” symmetry in the domain wall theory. Starting from (4.62) we apply the large mass limit, following the steps set out in Section 4.3. This brings us to the locus action for this system,

$$S_{locus} \sim \int d\rho \sqrt{1 + \frac{B^2}{\rho^4} \rho^2 \sqrt{1 + \rho^4 (\partial_\rho z)^2}}. \quad (4.64)$$

This is potentially promising! As in (4.62) the magnetic field makes the interior of the geometry repulsive to the U-shaped loci. The equations of motion however

¹²again with stray factors of R scaled out

tells a different story, defining $h(\rho) = \sqrt{1 + \frac{B^2}{\rho^4}}$, we have

$$\frac{h(\rho)\rho^6\partial_\rho z}{\sqrt{1 + \rho^4(\partial_\rho z)^2}} = c_z,$$

$$\partial_\rho z = \pm \frac{c_z}{\rho^2 \sqrt{h(\rho)^2 \rho^8 - c_z^2}}. \quad (4.65)$$

Now we see that whether the system displays pile-up behaviour or not is controlled by the roots of the polynomial

$$h(\rho)^2 \rho^8 - c_z^2 = 0. \quad (4.66)$$

When this polynomial has only positive powers of ρ , it is possible to tune c_z such that the minimum of the U-shaped configuration (ρ_{\min}) is allowed to smoothly go to zero. This is the case with the worldvolume magnetic field case, and we do not see dynamical chiral symmetry breaking. The repulsion induced by the magnetic field is seemingly not strong enough in this system. However, we can take some inspiration from this system and consider instead an effective dilaton profile

$$h(\rho)^2 = 1 + \frac{b^q}{\rho^q}, \quad (4.67)$$

where b is a positive constant with mass dimension one, which ensures h is dimensionless¹³. In turn this makes the polynomial (4.66)

$$\rho^8 + b^q \rho^{8-q} - c_z^2 = 0. \quad (4.68)$$

Clearly, for $q > 8$ the *loci* display the desired pile up behaviour. As a toy to understand how dynamical chiral symmetry breaking manifests in the domain wall theories, let us take an “effective dilaton flow” with $q = 10$.

4.5.1.1 $q=10$ “effective dilaton flow”

For this toy model, we have a set of *loci* governed by

$$\partial_\rho z = \pm \frac{c_z}{\rho^2 \sqrt{\rho^8 + b^{10} \rho^{-2} - c_z^2}}. \quad (4.69)$$

¹³when performing numerics this will be set to 1.

We can explore this set numerically to identify where the configurations begin to pile up. We can identify the constant c_z^2 with $\rho_{min}^8 + \frac{b^{10}}{\rho_{min}^2}$ with $b, \rho_{min} \in \mathbb{R}^+$, there are no solutions where $c_z = 0$, and thus no flat configurations of domain walls that fall all the way in to $\rho = 0$. Numerically, we find that the loci pile up at $\rho = \bar{\rho} \simeq 0.8706$. The constant b sets the scale in the geometry that the loci pile up at¹⁴

$$\bar{\rho} = \left(\frac{q}{8} - 1\right)^{\frac{1}{q}} b. \quad (4.70)$$

This is clearly visible in Figure (4.6), the loci begin to widen asymptotically the closer to $\bar{\rho}$ they reach into the bulk, diverging sharply as $\rho_{min} \rightarrow \bar{\rho}$.



FIGURE 4.6: The domain wall loci in the toy model showing pile up behaviour. The four loci depicted are $\rho_{min} = 1.5$ (Purple), $\rho_{min} = 1$ (Magenta), $\rho_{min} = 0.89$ (Orange), $\rho_{min} = 0.87056$ (Red), the pile up scale $\bar{\rho}$ is also included (Black, Dashed).

The real test here however will come from examining the fields dual to the quarks living on the domain walls. We expect to see the behaviour of the loci reflected in the fields that live on their surface. The action for the vacuum, $L(\rho)$ is

$$S_{DW} \sim \int d^2x d\rho h(r) \sqrt{1 + \rho^4 (\partial_\rho z)^2} \rho^2 \sqrt{1 + \mathcal{F}(\partial_\rho L)^2} \quad (4.71)$$

with¹⁵

$$\mathcal{F} = 1 + \frac{1}{(\rho^2 + L^2)^2 (\partial_\rho z)^2}. \quad (4.72)$$

¹⁴this is arrived at by minimising the first two terms of (4.68), effectively finding the smallest allowed value of c_z

¹⁵This may seem indistinguishable from (4.54), in large part they are the same, though here we take the geometric data, $\partial_\rho z$ from the new set of loci (4.69)

The effective dilaton flow h now has dependence on r , rather than just ρ . The equation of motion for L is

$$\begin{aligned} & \partial_\rho \left(\frac{h(r)\rho^2 \sqrt{1 + \rho^4(\partial_\rho z)^2} \mathcal{F}}{\sqrt{1 + \mathcal{F}(\partial_\rho L)^2}} \partial_\rho L \right) \\ & - 2L \left(\frac{1}{2} \left(\frac{h(r)\sqrt{1 + \rho^4(\partial_\rho z)^2} \rho^2 (\partial_\rho L)^2}{\sqrt{1 + \mathcal{F}(\partial_\rho L)^2}} \right) \frac{\partial \mathcal{F}}{\partial r^2} \right. \\ & \left. + \frac{\partial h(r)}{\partial r^2} \sqrt{1 + \rho^4(\partial_\rho z)^2} \rho^2 \sqrt{1 + \mathcal{F}(\partial_\rho L)^2} \right) = 0, \end{aligned} \quad (4.73)$$

which we can solve numerically, shooting from ρ_{min} , with boundary conditions $L(\rho_{min}) = \rho_{min}$, $L'(\rho_{min}) = 0$, and examine the behaviour of the field L on *loci* with ρ_{min} approaching $\bar{\rho}$, to understand the dynamics of the quarks as the *loci* pile up. The numerical solutions are plotted in Figure (4.7), the vacuum functions are shown to rise up to nonzero values in the IR of the theory, even from a UV quark mass of zero! This suggests that, in analogy with the worldvolume magnetic field on a D7 probe in $AdS_5 \times S^5$, the “chiral” symmetry in the theory on the domain wall defect is dynamically broken. The final piece of supporting evidence will be a holographic variant of the Gell-Mann-Oakes-Renner relation [109], confirming that fluctuations about L , in the region of small quark mass, act as a pseudo-Goldstone boson of the theory. To do this, we will examine the pseudoscalar meson ϕ , as we did in Section 4.4.

The action for the meson ϕ in the toy model is

$$S_\phi = \int d^2x d\rho g \left(1 + \frac{1}{2} \frac{\mathcal{F}(\partial_\rho \phi)^2}{1 + \mathcal{F}(\partial_\rho L)^2} + \frac{1}{2} \frac{(\partial_{x^i} \phi)^2}{(\rho^2 + L^2)^2 (1 + \mathcal{F}(\partial_\rho L)^2)} \right) \quad (4.74)$$

where \tilde{g} is the collection of geometric factors

$$g(\rho, L, \phi) = h(r) \sqrt{1 + \rho^4(\partial_\rho z)^2} \rho^2 \sqrt{1 + \mathcal{F}(\partial_\rho L)^2} \quad (4.75)$$

evaluated on the solution L , with $r^2 = \rho^2 + L^2 + \phi^2$. Taking the same plane wave ansatz as before, $\phi(x^i, \rho) = \tilde{\phi}(\rho) e^{ik \cdot x}$, the equations of motion for the meson

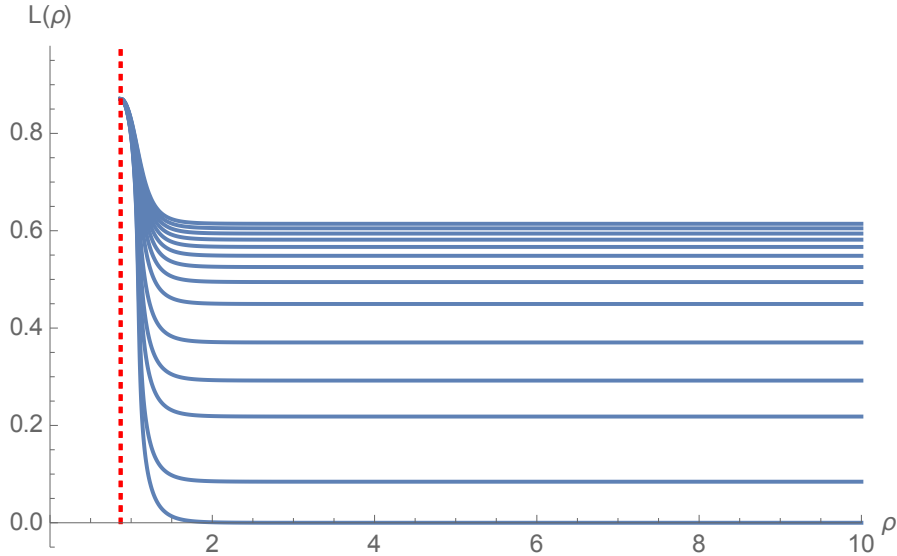


FIGURE 4.7: Numerical solutions to (4.73) (Blue), on loci that join near the pile up scale $\bar{\rho}$ (Red, Dotted) are plotted. The range of ρ_{min} on the loci plotted is $\bar{\rho} < \rho_{min} \leq \bar{\rho} + 0.0003$

become;

$$\partial_{\rho} \left(g \frac{\mathcal{F} \partial_{\rho} \tilde{\phi}}{1 + \mathcal{F}(\partial_{\rho} L)^2} \right) + M_{\phi}^2 \frac{g \tilde{\phi}^2}{(\rho^2 + L^2)^2 (1 + \mathcal{F}(\partial_{\rho} L)^2)} - 2 \left(\frac{\partial g}{\partial r^2} \right) \Big|_{\phi=0} \tilde{\phi} = 0, \quad (4.76)$$

which can be solved numerically subject to the boundary conditions $\tilde{\phi}(\rho_{min}) = 1$, $\tilde{\phi}'(\rho_{min}) = 0$. For each vacuum configuration L , corresponding to a quark mass m_q , we can determine the mass of the meson ϕ by requiring that asymptotically, $\tilde{\phi} \rightarrow 0$. In doing so we can plot M_{ϕ}^2 against m_q , and we expect to find a linear relation between the two when the quark mass is small, and for larger quark masses it will return to the more typical $M_{\phi}^2 \propto m_q^2$. This linear behaviour is known as the Gell-Mann-Oakes-Renner relation and is a characteristic behaviour of pseudo-Nambu-Goldstone boson, such as the pion in QCD [109]. Figure 4.8 is exactly this plot, and shows clearly the holographic Gell-Mann-Oakes-Renner relation. Happy now that the domain wall method can realise a spontaneously broken ‘‘chiral’’ symmetry, we attempt to show this in a backreacted dilaton flow geometry that is a genuine solution to the supergravity equations.

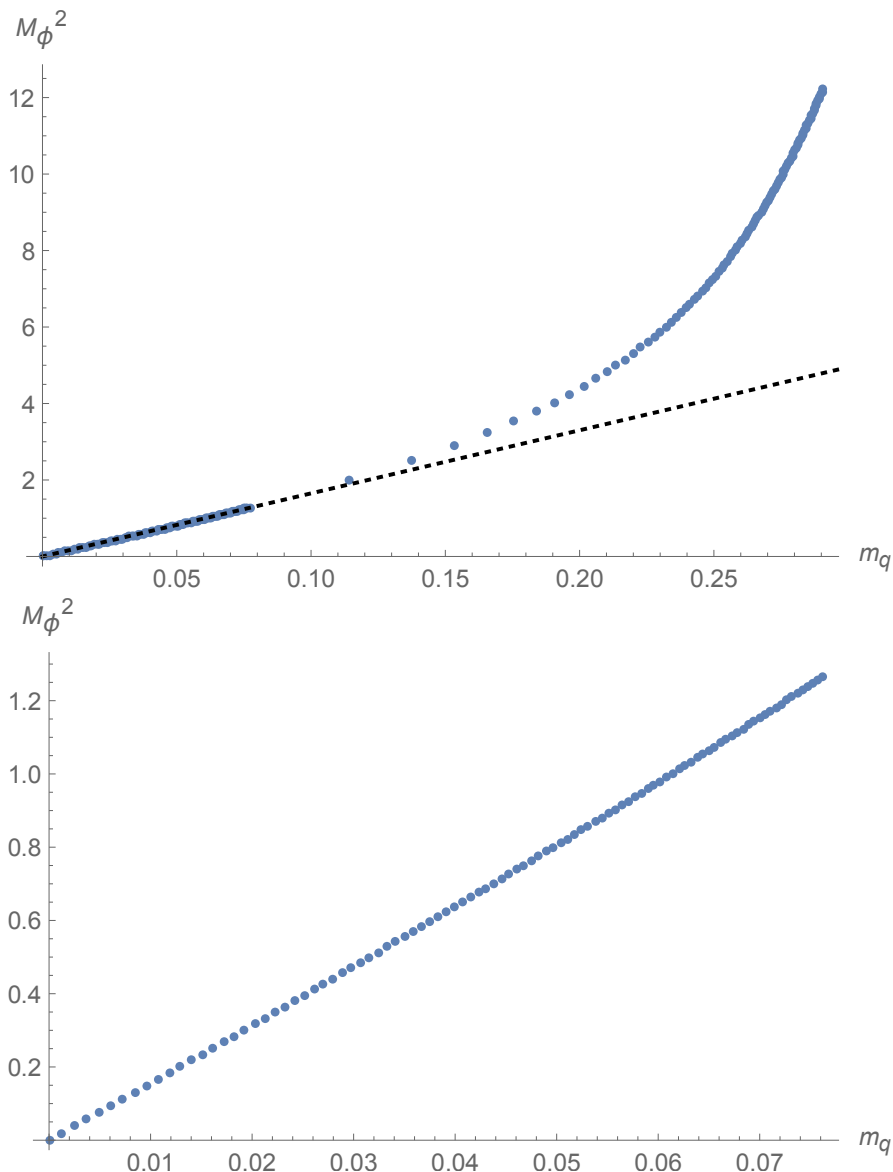


FIGURE 4.8: The meson mass squared against the quark mass, corresponding to the vacuum functions in Figure 4.7. A linear guide function has been added to emphasise the behaviour at small m_q (Top). A magnified view of the small quark mass region clearly showing the linear GMOR behaviour (Bottom).

4.5.2 Constable-Myers Deformation

The dilaton flow background of choice, is the Constable-Myers deformation of $AdS_5 \times S^5$ [74]. This system was first discussed in the context of holographic chiral symmetry breaking in [71]. From the perspective of the dual gauge theory the deformation of the AdS geometry corresponds to turning on a vacuum expectation value for a dimension four operator, such as $Tr F^2$, or $Tr F\tilde{F}$. The metric in

Einstein frame can be written as,

$$ds^2 = G_x(r) dx_4^2 + G_r(r)(d\rho^2 + \rho^2\Omega_3^2 + dL_i^2), \quad (4.77)$$

with metric factors,

$$\begin{aligned} G_x &= H^{-1/2}(r) \left(\frac{r^4 + b^4}{r^4 - b^4} \right)^{\delta/4}, \\ G_r &= H^{1/2}(r) \left(\frac{r^4 + b^4}{r^4 - b^4} \right)^{(2-\delta)/4} \frac{r^4 - b^4}{r^4}, \\ H &= \left(\frac{r^4 + b^4}{r^4 - b^4} \right)^\delta - 1, \end{aligned} \quad (4.78)$$

and dilaton profile,

$$e^{2\Phi} = e^{2\Phi_0} \left(\frac{r^4 + b^4}{r^4 - b^4} \right)^\Delta. \quad (4.79)$$

b is a dimensionful quantity that sets the scale of the deformation. The metric factors and dilaton are singular at $r = b$. It is not known how to resolve this singularity in the context of supergravity, but it is hopeful that in an uplift to the full string theory it may be resolved. This shall not pose an issue to us, as the loci, and fields living on them, will be restricted to lie sufficiently far from the singularities that the supergravity solution is trustworthy. The exponents δ, Δ in (4.78) must sum in quadrature to

$$\delta^2 + \Delta^2 = 10, \quad \text{with } \delta = \frac{R^2}{2}. \quad (4.80)$$

For $\Delta \neq 0$ the geometry allows no killing spinors. As such, this deformation breaks all of the supersymmetries in the dual field theory; permitting condensates and non-trivial renormalisation group flows as discussed in Section (4.5.1). Now we repeat the calculations done in the previous cases in the new geometry. Firstly we set out to reduce the D7 brane action to determine the set of *loci* in this geometry. The DBI action for the D7 probes is

$$S_{D7} = -T_7 \Omega_3 \mathcal{N}_f \int d^4x d\rho e^\Phi G_x^2 G_r^2 \rho^3 \sqrt{1 + (\partial_\rho L_i)^2 + \frac{G_r}{G_x} (\partial_z L_i)^2}. \quad (4.81)$$

Following the example of (4.38) we set

$$\partial_\rho L \sim \frac{1}{\sqrt{g_{LL}}} \Big|_{L=0} \partial_\rho z \delta(z - z(\rho)) = \frac{1}{\sqrt{G_r}} \Big|_{L=0} \partial_\rho z \delta(z - z(\rho)). \quad (4.82)$$

Inserting this into the DBI action gives the locus action,

$$S_{locus} \sim \int d\rho e^\Phi G_x^{3/2} G_r^2 \rho^3 \sqrt{1 + \frac{G_x}{G_r} (\partial_\rho z)^2}. \quad (4.83)$$

This can be extremised to determine the set of *loci*. The resulting equation of motion for the loci simplifies as before due to the presence of a conserved quantity, to the one parameter family of curves,

$$\partial_\rho z = \pm \frac{c_z G_r^{1/2}}{G_x^{1/2} \sqrt{e^{2\Phi} G_x^4 G_r^3 \rho^6 - c_z^2}}. \quad (4.84)$$

This has a non trivial pile up behaviour with, $\bar{\rho}$, the pile up scale determined by solutions to

$$\begin{aligned} & \frac{\left(\frac{3(2-\delta)}{4} + \delta + \Delta\right) (\bar{\rho}^4 - b^4)^3 \left(\frac{4\bar{\rho}^3}{\bar{\rho}^4 - b^4} - \frac{4\bar{\rho}^3(\bar{\rho}^4 + b^4)}{(\bar{\rho}^4 - b^4)^2}\right) \left(\frac{\bar{\rho}^4 + b^4}{\bar{\rho}^4 - b^4}\right)^{\frac{3(2-\delta)}{4} + \delta + \Delta - 1}}{\bar{\rho}^6 \sqrt{\left(\frac{\bar{\rho}^4 + b^4}{\bar{\rho}^4 - b^4}\right)^\delta - 1}} \\ & + \frac{12 (\bar{\rho}^4 - b^4)^2 \left(\frac{\bar{\rho}^4 + b^4}{\bar{\rho}^4 - b^4}\right)^{\frac{3(2-\delta)}{4} + \delta + \Delta}}{\bar{\rho}^3 \sqrt{\left(\frac{\bar{\rho}^4 + b^4}{\bar{\rho}^4 - b^4}\right)^\delta - 1}} \\ & - \frac{6 (\bar{\rho}^4 - b^4)^3 \left(\frac{\bar{\rho}^4 + b^4}{\bar{\rho}^4 - b^4}\right)^{\frac{3(2-\delta)}{4} + \delta + \Delta}}{\bar{\rho}^7 \sqrt{\left(\frac{\bar{\rho}^4 + b^4}{\bar{\rho}^4 - b^4}\right)^\delta - 1}} \\ & - \frac{\delta (\bar{\rho}^4 - b^4)^3 \left(\frac{4\bar{\rho}^3}{\bar{\rho}^4 - b^4} - \frac{4\bar{\rho}^3(\bar{\rho}^4 + b^4)}{(\bar{\rho}^4 - b^4)^2}\right) \left(\frac{\bar{\rho}^4 + b^4}{\bar{\rho}^4 - b^4}\right)^{\frac{3(2-\delta)}{4} + 2\delta + \Delta - 1}}{2\bar{\rho}^6 \left(\left(\frac{\bar{\rho}^4 + b^4}{\bar{\rho}^4 - b^4}\right)^\delta - 1\right)^{3/2}} = 0, \quad (4.85) \end{aligned}$$

which will be determined numerically. For this case we scale the co-ordinates such that $R = 1$, $b = 1$, and the resulting pile up scale is $\bar{\rho} \sim 1.30326$. The pile up scale lies above the singularities at $b = 1$ so the domain wall construction nicely protects us from having to worry too much about the validity of the gravity dual in this case. A sampling of the loci is plotted in Figure 4.9, where pile up behaviour is seen analogous to that in Figure 4.6. Again, we turn to the fluctuations on the

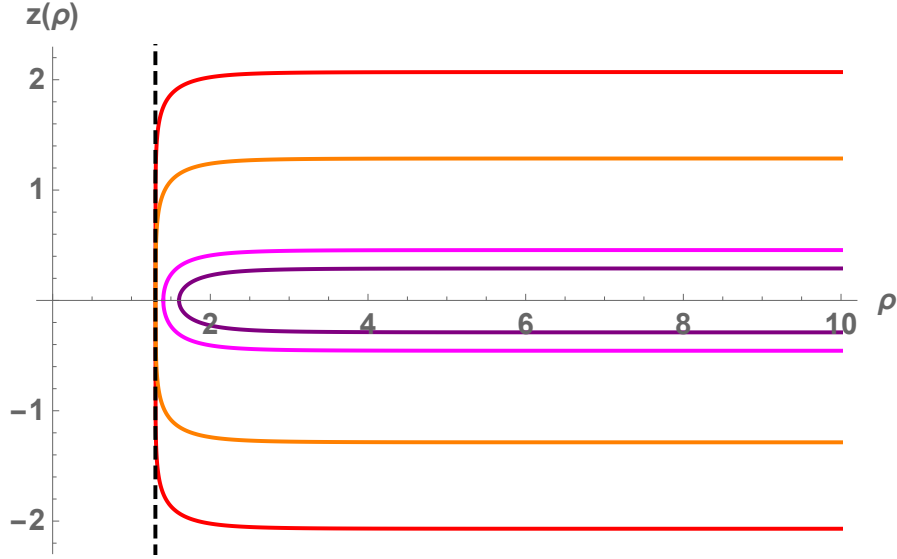


FIGURE 4.9: The domain wall loci in the Constable-Myers deformation of $AdS_5 \times S^5$ displaying pile up behaviour. The configurations plotted are: $\rho_{min} \sim 1.6033$ (Purple), $\rho_{min} \sim 1.4033$ (Magenta), $\rho_{min} \sim 1.3043$ (Orange), $\rho_{min} = \bar{\rho} + 0.00001 \sim 1.30327$ (Red).

loci to confirm that the pile up behaviour corresponds to the dynamical generation of mass (and therefore dynamical breaking of “chiral” symmetry). This time the function we use to dimensionally reduce is¹⁶

$$\begin{aligned} \Delta(z - z(\rho)) &= G_r^{1/2} \sqrt{1 + \frac{G_x}{G_r} (\partial_\rho z)^2} \Big|_{L=0} \delta(z - z(\rho)), \\ &= g_r^{1/2} \sqrt{1 + \frac{g_x}{g_r} (\partial_\rho z)^2} \delta(z - z(\rho)), \end{aligned} \quad (4.86)$$

where we have defined the metric factors on the loci, $g_i = G_i|_{L=0}$, to reduce the notational clutter. When applied by hand to the D7 action, localises the fluctuations on the locus, giving

$$S_{DW} \sim \int d^2 x d\rho g_r^{1/2} \sqrt{1 + \frac{g_x}{g_r} (\partial_\rho z)^2} e^\Phi G_x^2 G_r^2 \rho^3 \sqrt{1 + \mathcal{G} (\partial_\rho L_i)^2} \quad (4.87)$$

with

$$\mathcal{G} = 1 + \frac{G_r}{G_x (\partial_\rho z)^2}. \quad (4.88)$$

¹⁶identically to (4.52)

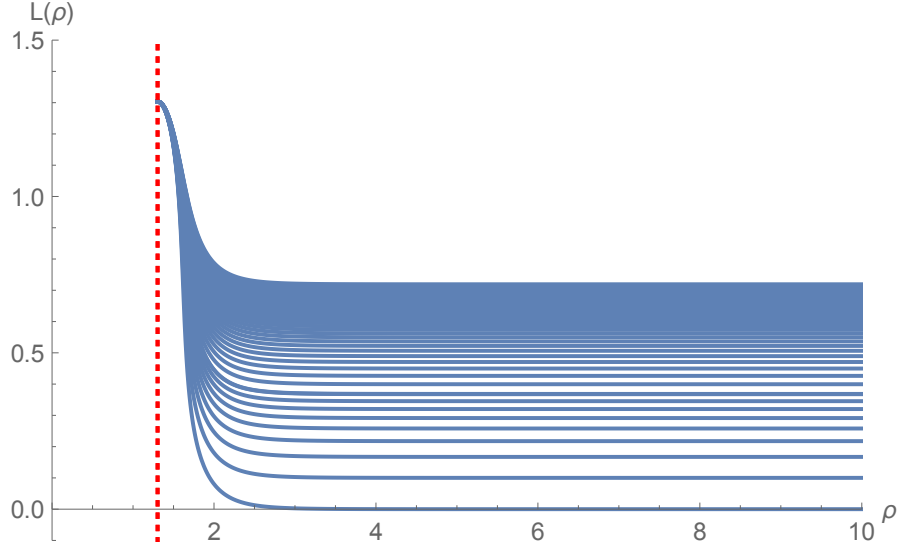


FIGURE 4.10: Plot of the numerical solutions to (4.89) for the vacuum function $L(\rho)$ (Blue) on loci that join near the pile up scale $\bar{\rho}$ (Red,Dotted). The range of ρ_{min} on the loci plotted is $\bar{\rho} < \rho_{min} < \bar{\rho} + 0.00015$.

We can vary the action (4.87) to write down an equation that governs the behaviour of the vacuum $L(\rho)$,

$$\begin{aligned} & \partial_\rho \left(\frac{e^\Phi G_x^2 G_r^2 \rho^3 \sqrt{g_r + g_x (\partial_\rho z)^2} \mathcal{G}}{\sqrt{1 + \mathcal{G}(\partial_\rho L)^2}} \partial_\rho L \right) \\ & - \left(2\rho^3 \sqrt{g_r + g_x (\partial_\rho z)^2} \sqrt{1 + \mathcal{G}(\partial_\rho L)^2} \frac{\partial (e^\Phi G_x^2 G_r^2)}{\partial r^2} L \right) \\ & - \left(\rho^3 \sqrt{g_r + g_x (\partial_\rho z)^2} \frac{e^\Phi G_x^2 G_r^2 (\partial_\rho L)^2}{\sqrt{1 + \mathcal{G}(\partial_\rho L)^2}} \frac{\partial \mathcal{G}}{\partial r^2} L \right) = 0. \end{aligned} \quad (4.89)$$

The numerical solutions for the vacuum function, L , are plotted in Figure 4.10. Moving once again to the mesonic fluctuations will determine whether the pseudo scalar meson has Goldstone boson-like behaviour. Writing the action for the fluctuations, ϕ about the vacuum (to quadratic order),

$$S_\phi \sim \int d^2x d\rho f \left(1 + \frac{1}{2} \frac{\mathcal{G}(\partial_\rho \phi)^2}{1 + \mathcal{G}(\partial_\rho L)^2} + \frac{1}{2} \frac{G_r}{G_x} \frac{(\partial_{x^i} \phi)^2}{1 + \mathcal{G}(\partial_\rho L)^2} \right) \quad (4.90)$$

with

$$f = e^\Phi G_x^2 G_r^2 \rho^3 \sqrt{g_r + g_x (\partial_\rho z)^2} \sqrt{1 + \mathcal{G}(\partial_\rho L)^2}. \quad (4.91)$$

Varying with respect to the mesonic fluctuation gives¹⁷,

$$\partial_\rho \left(f \frac{\mathcal{G} \partial_\rho \tilde{\phi}}{1 + \mathcal{G}(\partial_\rho L)^2} \right) + M_\phi^2 \frac{f G_r \tilde{\phi}^2}{G_x (1 + \mathcal{G}(\partial_\rho L)^2)} - 2 \left(\frac{\partial f}{\partial r^2} \right) \Big|_{\phi=0} \tilde{\phi} = 0, \quad (4.92)$$

which we solve, tuning the meson mass such that ϕ falls off to zero at the asymptotic boundary. Figure 4.11 shows the expected Gell-Mann-Oakes-Renner relation, confirming that ϕ plays the role of a pseudo-Goldstone boson in this theory, and that the ‘‘chiral’’ symmetry on the domain walls is broken spontaneously.

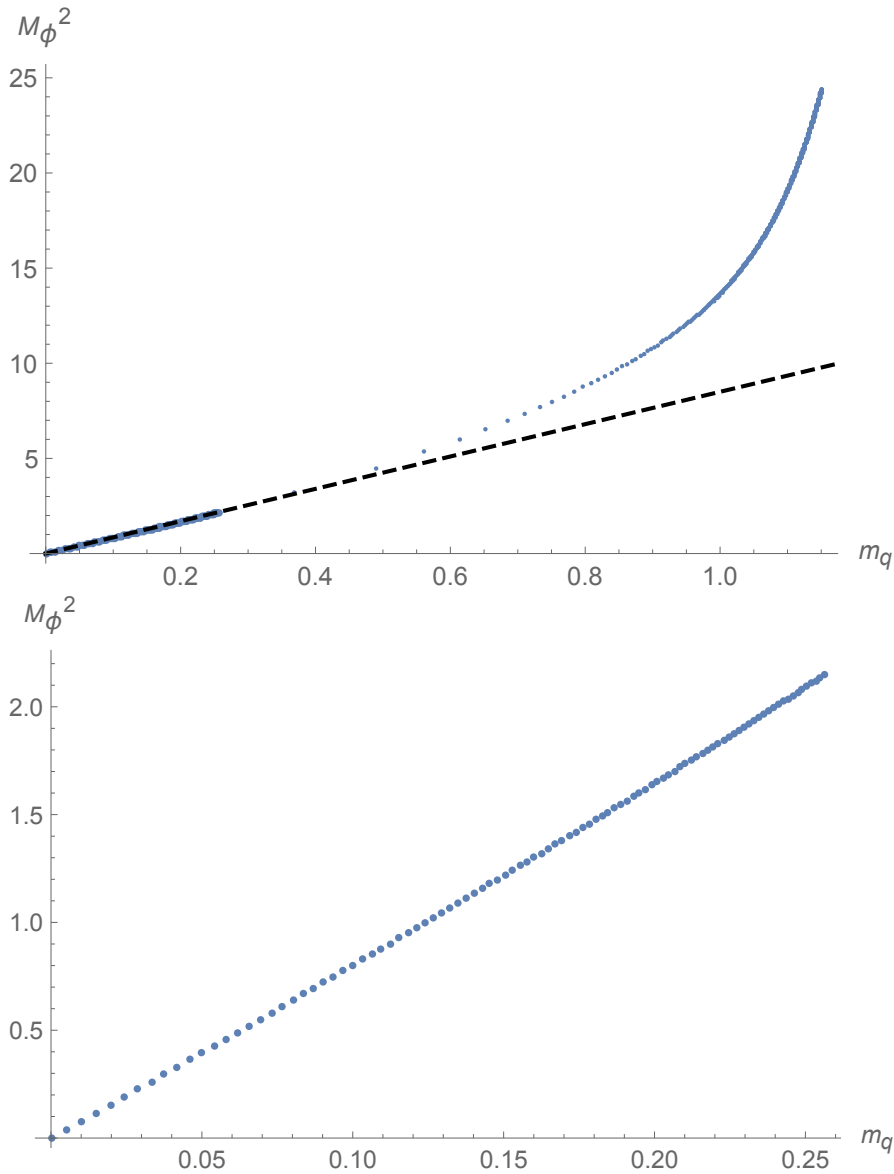


FIGURE 4.11: Meson mass squared M_ϕ^2 plotted against quark mass m_q for domain walls in the Constable-Myers deformation of $AdS_5 \times S^5$, a linear plot has been added to emphasise the GMOR behaviour (Top). A zoomed in section about small quark mass (Bottom)

¹⁷and inserting the familiar separable radial profile \times plane wave ansatz

4.6 Summary

This chapter has been a first exploration of domain wall configurations of D7 branes in $AdS_5 \times S^5$, holographically dual to a $2 + 1$ dimensional “chiral” theory of quarks on the conformal boundary. The dynamics of the domain walls in the interior of the AdS space gives a nice geometric realisation of the breaking of “chiral” symmetry in this theory. We have explored some example cases where the usual methods to break chiral symmetry in D3/D7 systems are not strong enough to overcome the separation of the defects, and two cases where singularities in the bulk are sufficiently strong to break the symmetry. We will move now to a fully top down realisation of chiral symmetry breaking by confinement in a $D5/D7$ domain wall model, that we dub Domain Wall AdS/QCD. Here the theory on the defects is $3 + 1$ dimensional and thus genuinely chiral¹⁸. This theory displays a wealth of QCD-like phenomenology and will take the spotlight for the remainder of this thesis.

¹⁸and we may drop our zealous use of quotation marks.

Chapter 5

Domain Wall AdS/QCD

This chapter will be concerned with the implementation of domain walls on a D7 probe brane, in a background sourced by a large number of coincident D5 branes [2]. In the top down picture, the fivebranes wrap an $\mathbb{R}^{(1,4)} \times S^1$ cycle of the full $\mathbb{R}^{(1,8)} \times S^1$ space. The compact direction wrapped by the brane stack induces a cap in the resulting geometry, which indicates the confinement of the dual gauge theory. The probe D7 branes in this theory are dual to quarks on a 4+1 dimensional defect interacting with quarks in a 5+1 dimensional gauge theory. Applying a spatially dependent quark mass term to create a domain wall defect in the 4+1 dimensional theory reduces us to a theory of massless quarks on a 3+1 dimensional, co-dimension two defect in the 5+1 dimensional confining gauge theory. In the UV of the holographic dual, the quarks are genuinely chiral. As one flows to the IR, the capped geometry forces the domain walls to join, indicating the mixing of left and right handed quarks. Thus the confinement scale breaks chiral symmetry. We show that the domain wall *loci* in this geometry are again generically U-shaped, piling up just before the confinement scale. The UV behaviour of this theory is somewhat peculiar, and we comment on this. The background geometry comes equipped with a dilaton flow that rises linearly into the ultraviolet, suggesting that at some scale we should no longer trust the gravity dual description of this theory. We argue that this is a somewhat necessary quirk of QCD like theories, and that we should only really trust the gravity dual where QCD is strongly coupled. We aim to match observables of the model at an intermediate coupling regime in real world QCD, identifying the UV cutoff scale as $\Lambda_{UV} \sim 3$ GeV. Here we compute the spectrum of the model, fitting the quark and pseudoscalar masses to QCD data, and predicting the masses of the vector and axial vector mesons (and their excited states), as well as the mesonic decay constants f_π , F_A , and F_V . Drawing

further inspiration from the lattice community, we discuss (and implement) the ‘improvement’ of the model and its prediction for observables by considering the effects of higher dimension operators. This somewhat improves the predictions for the radially excited states.

5.1 D5 Background

The field theory limit of the geometry sourced by a stack of coincident D5 branes is known (and is discussed in [60]). The expected low energy modes are a 5+1 dimensional supersymmetric Yang-Mills-type theory in the IR. There is some ambiguity, and discussion of the UV limit of this theory. The D5 brane in type IIB string theory forms an $SL(2, \mathbb{Z})$ multiplet with, and thus S-dualises to, the NS5 brane. The UV limit is expected therefore to be described by the worldvolume theory on an NS5-brane, which is conjectured to be the so called little string theory. Further, NS5-branes are present in both type II superstring theories, in type IIA (and thus in IIB via T-duality) it descends from the M5 brane of 11 dimensional supergravity/M-theory. This system is holographically dual to the 6d (2, 0) super conformal field theory, which famously lacks a Lagrangian description. This is all to say that the UV limit of fivebranes in general is complicated, and bluntly, not of direct interest to us here. We will be sufficiently happy to say that the low energy limit of the type IIB strings on the worldvolume of the D5 branes is a 5+1 dimensional super-Yang-Mills theory. Which when compactified along one of the directions wrapped by the fivebrane, is dual to a 4+1 dimensional confining $U(N)$ gauge theory. We are therefore interested, not in the field theory limit of the D5 geometry, but in the geometry that results from wrapping the stack of D5 branes on a circle. It is known how to achieve this by double-wick-rotation of the near extremal black p -brane geometries of type IIB supergravity [60, 110]. These geometries are dual to the world-volume theories at finite temperature and thus will be referred to as *thermal* geometries. The thermal geometry sourced by the D5 branes is,

$$\frac{ds^2}{\alpha'} = \frac{U}{R} (-h(U)dt^2 + \delta_{ij}dx^i dx^j) + \frac{R}{U} \left(\frac{1}{h(U)}dU^2 + U^2 d\Omega_3^2 \right) \quad (5.1)$$

where the indices span $i, j = 1, \dots, 5$, and

$$\begin{aligned}
 U &= \frac{\tilde{r}}{\alpha'}, & R &= \frac{g_{YM}\sqrt{N}}{(2\pi)^{3/2}}, \\
 e^\Phi &= RU, & g_{YM}^2 &= (2\pi)^3 g_s \alpha' \\
 h(U) &= 1 - \left(\frac{U_0}{U}\right)^2.
 \end{aligned} \tag{5.2}$$

The this geometry comes equipped with two interesting ingredients. First is the presence of a horizon scale U_0 with dimensions of energy. Upon compactification, this scale will become the position of the ‘‘cap’’ in the geometry that signals confinement in the dual field theory. The second is the presence of the dilaton profile, which rises linearly into the infrared. One can think of the presence of the dilaton as the running of the coupling in the dual gauge theory. At some scale in the UV the dilaton, which sets the string coupling, becomes large and we no longer trust the supergravity description. It is here the authors in [60] move to the S-dual NS5-brane solution, which is well behaved. Instead we will impose a UV cut-off, such that we avoid the very stringy region, and match to QCD at the cutoff scale. It is expected that a ‘‘true holographic dual of QCD’’, should one exist, is only valid in the non-perturbative region of QCD, becoming strongly coupled where QCD becomes weakly coupled. Whilst the linear behaviour of this theory does not seemingly capture the full running coupling of QCD, it is an interesting example where the gravity dual reflects the ‘‘finiteness’’ of the non-perturbative regime. With this *thermal* geometry in mind, we can double wick rotate to exchange a temporal, and a spatial direction. In this case we take

$$\begin{aligned}
 t &\rightarrow i\tilde{x}^5, \\
 x^5 &\rightarrow i\tilde{t},
 \end{aligned} \tag{5.3}$$

which in turn changes the metric to

$$\frac{ds^2}{\alpha'} = \frac{U}{R} \left(-d\tilde{t}^2 + \delta_{ij} dx^i dx^j + h(U)(d\tilde{x}^5)^2 \right) + \frac{R}{U} \left(\frac{1}{h(U)} dU^2 + U^2 d\Omega_3^2 \right). \tag{5.4}$$

Now the indices i, j span $1, \dots, 4$, and the 5-direction is written explicitly¹. The effect here, is to put the ‘‘horizon’’ onto one of the spatial directions, which then becomes a conical deficit. The easiest way to see this, is by expanding the metric around the ‘‘horizon’’ U_0 in the $x^5 - U$ plane. Taking $U = U_0 + \delta U$, for the relevant

¹We will now drop the tilde on the t , and x^5 directions. It was just there to make it obvious which two co-ordinates had been exchanged.

part of the metric, we find to leading order in δU ,

$$ds^2 \sim \frac{2\delta U}{R}(dx^5)^2 + \frac{R}{2\delta U}d\delta U^2. \quad (5.5)$$

Performing the co-ordinate transformation

$$\alpha = \frac{x^5}{R}, \quad \delta U = \frac{\sigma^2}{2R}, \quad (5.6)$$

which sends (5.5) to

$$ds^2 \sim d\sigma^2 + \sigma^2 d\alpha^2 \quad (5.7)$$

which is clearly a two plane in polar co-ordinates! To *avoid* a conical deficit, then we *must* have $0 \leq \alpha \leq 2\pi$. Which in turn means that we must periodically identify the x^5 direction, with period

$$0 \leq x^5 \leq 2\pi R. \quad (5.8)$$

This geometry, with x^5 periodically identified, is one of the so called ‘‘capped’’ geometries². As one approaches $U = U_0$, the radius of the compactified direction shrinks to zero, and the geometry closes off. As a result, no branes (or strings) probing the geometry may reach $U \leq U_0$. This is therefore a representation of confinement in holography. If one considers a long open string with endpoints on the boundary of the space (or in this case the UV cut-off) and evaluates the exponential of worldsheet action for the static string, with finite separation at the boundary one finds that the presence of a cap in the geometry forces the leading contribution to the action to be proportional to $\Delta t \cdot l$, where l is the asymptotic separation. This is the holographic area law for Wilson loops in the dual theory [73], and thus the dual theory is confined. We are not quite done with our manipulations of the background geometry. Before embedding D7 probes in the background geometry, we must perform one last co-ordinate transformation to make manifest the flat plane, transverse to the D5 brane (some example cases are discussed in [71]). In particular, we would like to write

$$ds^2 \supset \frac{R}{U} \left(\frac{1}{h(U)} dU^2 + U^2 d\Omega_3^2 \right) = f(r) (dr^2 + r^2 d\Omega_3^2). \quad (5.9)$$

The co-ordinate change that realises this must have

$$\frac{dr^2}{r^2} = \frac{dU^2}{U^2 h(U)}, \quad (5.10)$$

²or ‘‘cigar’’ geometries.

which is satisfied by ,

$$r^2 = \frac{1 + \frac{U}{\sqrt{U^2 - U_0^2}}}{\frac{U}{\sqrt{U^2 - U_0^2}} - 1}. \quad (5.11)$$

More usefully, this can be written as,

$$\frac{U}{U_0} = \frac{1 + r^2}{2r}. \quad (5.12)$$

The interesting point here is that the left hand side of (5.12) is dimensionless, so r is also dimensionless. It represents measuring the energy scales in the dual theory by the confinement scale U_0 and runs from 1 at $U = U_0$ to r_Λ at the UV cutoff, where r_Λ is given by the positive real root of the polynomial,

$$r_\Lambda^2 - 2\frac{\Lambda}{U_0}r_\Lambda + 1 = 0. \quad (5.13)$$

Crucially, when calculating any observables in this model we will have to translate them back into physical units (either by setting scales with other quantities, or into U co-ordinates³). The metric now reads,

$$ds^2 = G_x(r) (-dt^2 + \delta_{ij}dx^i dx^j + h(r)(dx^5)^2) + G_r(r) (dr^2 + r^2 d\Omega_3^2). \quad (5.14)$$

The corresponding metric factors, when expressed in the r co-ordinates, are

$$G_x(r) = \frac{U_0}{R} \frac{1 + r^2}{2r}, \quad G_r(r) = U_0 R \cdot \frac{1 + r^2}{2r^3},$$

$$h(r) = 1 - \left(\frac{2r}{1 + r^2} \right)^2, \quad e^{-\Phi} = \frac{1}{U_0 R} \frac{2r}{1 + r^2}. \quad (5.15)$$

We will now go on to embed D7 branes in this geometry.

5.2 D7 Probes

We consider the D-brane intersection described by the brane scan,

	0	1	2	3	4	(5)	6	7	8	9	
D5	-	-	-	-	-	-	•	•	•	•	
D7	-	-	-	-		•	-	-	-	•	

(5.16)

where the brackets around the 5 direction indicate that it is compact. The

³We will do the former in this chapter, and necessarily the latter in the next chapter when discussing the thermal phase transitions.

|| symbol in the 4 direction is designed to indicate that the D7 brane fills this direction, but we will place the pair of domain wall defects in this direction. We will choose the embedding $x^5 = \text{constant}$, $x^9 = L(\rho, z)$. We will label the x^4 direction z . This might be slightly counter intuitive, but for the sake of consistency, the direction that we put the domain walls in will be denoted z from here on out. This choice of embedding breaks the isometry group of the space tangent to the D5 branes from $SO(4)$ to $SO(3) (\times U(1))$ for the massless case, and this is reflected by splitting the co-ordinate r into $r^2 = \rho^2 + L^2$, and writing the metric as,

$$ds^2 = G_x(r) (-dt^2 + \delta_{ij} dx^i dx^j + h(r) (dx^5)^2) + G_r(r) (d\rho^2 + \rho^2 d\Omega_2^2 + dL^2). \quad (5.17)$$

The DBI action for the D7 probes in this geometry is,

$$S_{D7} = -T_7 \Omega_2 \int d^5 x d\rho e^{-\Phi} G_x^{5/2} G_r^{3/2} \times \rho^2 \sqrt{1 + (\partial_\rho L)^2 + \frac{G_r}{G_x} (\partial_z L)^2}, \quad (5.18)$$

and we can then begin to determine the set of *domain wall loci* that live in this geometry. We take the large mass limit as in Section 4.3, taking the functional form for L

$$\partial_\rho L \sim \frac{1}{\sqrt{g_{LL}}} \Big|_{L=0} \frac{\partial z}{\partial \rho} \delta(z - z(\rho)) = \frac{1}{\sqrt{G_r(\rho)}} \partial_\rho z \delta(z - z(\rho)) \quad (5.19)$$

which when inserted into the action (5.18) gives the action functional for the loci

$$S_{locus} = -T_7 \Omega_2 \int d^4 x d\rho e^{-\Phi(\rho)} g_x^2 g_r^{3/2} \times \rho^2 \sqrt{1 + \frac{g_x}{g_r} (\partial_\rho z)^2}, \quad (5.20)$$

where as in the previous examples, the lower case metric factors⁴ are those evaluated on $L = 0$. The loci of this geometry obey the equation of motion

$$\partial_\rho z = \frac{g_r^{1/2} c_z}{g_x^{1/2} \sqrt{e^{-2\Phi(\rho)} g_x^5 g_r^2 \rho^4 - c_z^2}} \quad (5.21)$$

with the constant of motion

$$c_z^2 = \left(\frac{U_0}{R} \frac{1 + \rho_{min}^2}{2\rho_{min}} \right)^5. \quad (5.22)$$

⁴ ϕ however is reserved for the pseudoscalar meson fluctuation, and therefore the cases with a dilaton evaluated on $L = 0$ will have to be $\Phi(\rho)$.

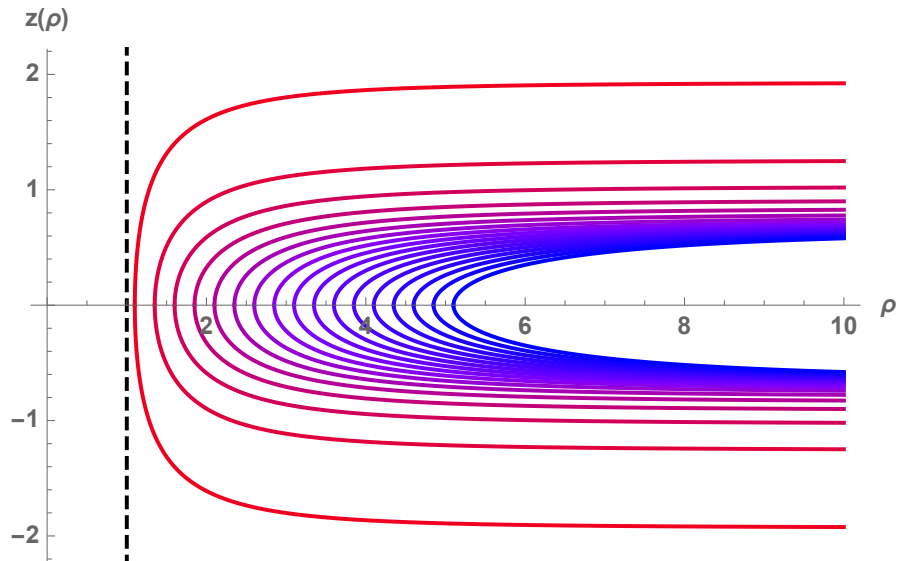


FIGURE 5.1: The domain wall loci (Blue/Red, Solid) in the capped AdS/QCD geometry. The loci display pile up behaviour, widening as they approach the cap in the geometry (Black, Dashed).

The loci in this geometry are plotted in Figure 5.1, where they clearly display the pile-up behaviour associated with chiral symmetry breaking. This time the breaking of chiral symmetry is directly induced by the confinement of the dual gauge theory, which serves to exclude the loci from a region of the space, reflecting the presence of a mass gap. With the set of loci determined, we can examine the behaviour of quarks in the model. By restricting the sevenbrane action to the loci and solving the resulting equations of motion, we can verify that the fields on the sevenbrane are displaying spontaneously broken chiral symmetry.

5.2.1 Fluctuations on the Walls

We now restrict (5.18) to the loci described by (5.21) by including the factor,

$$\begin{aligned} \Delta(z - z(\rho)) &= \sqrt{G_{\rho\rho} + G_{zz}(\partial_\rho z)^2} \Big|_{L=0} \delta(z - z(\rho)), \\ &= \sqrt{g_r + g_x(\partial_\rho z)^2} \times \delta(z - z(\rho)), \end{aligned} \quad (5.23)$$

by hand. This gives us the action for the fluctuations L ,

$$S_{DW} \sim \int d^4x d\rho e^{-\Phi} G_x^{5/2} G_r^{3/2} \sqrt{g_r + g_x(\partial_\rho z)^2} \times \rho^2 \sqrt{1 + \mathcal{F}(\partial_\rho L)^2}, \quad (5.24)$$

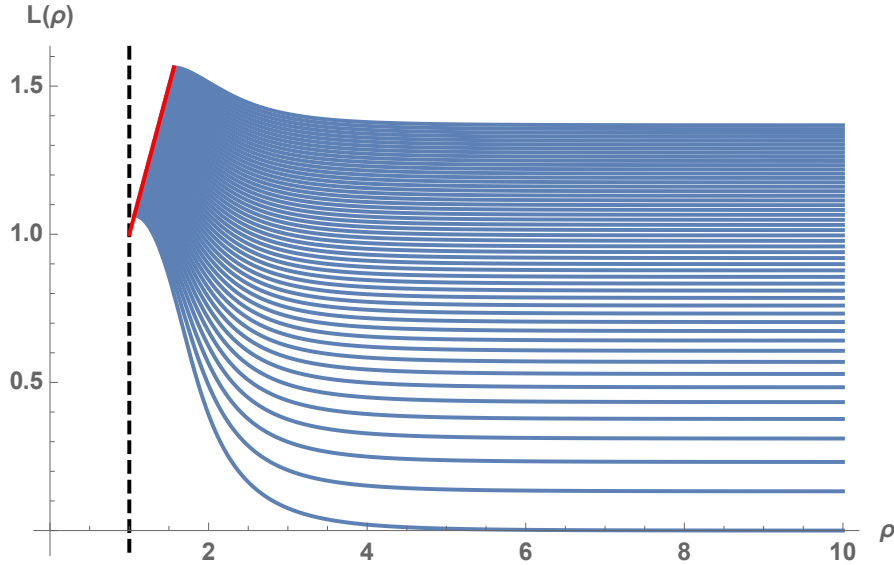


FIGURE 5.2: Solutions to (5.26) for the vacuum functions L (Blue). The cap at $\rho = 1$ is also plotted (Black, Dashed), alongside the line $L(\rho_{min}) = \rho_{min}$ (Red) representing the boundary condition on the vacuum functions in the IR.

with the factor

$$\mathcal{F} = 1 + \frac{G_r}{G_x(\partial_\rho z)^2}. \quad (5.25)$$

This action describes 3+1 dimensional chiral quarks, living on the pair domain wall defects. The field L describes the dynamics of the quark mass and chiral condensate source-operator pair. Its equation of motion is,

$$\partial_\rho \left(\frac{e^{-\Phi} G_x^{5/2} G_r^{3/2} \sqrt{g_r + g_x(\partial_\rho z)^2} \rho^2 \mathcal{F} \partial_\rho L}{\sqrt{1 + \mathcal{F}(\partial_\rho L)^2}} \right) - 2\rho^2 \sqrt{g_r + g_x(\partial_\rho z)^2} \frac{\partial}{\partial r^2} \left(e^{-\Phi} G_x^{5/2} G_r^{3/2} \sqrt{1 + \mathcal{F}(\partial_\rho L)^2} \right) \cdot L = 0. \quad (5.26)$$

The solutions for the vacuum functions L are displayed in Figure 5.2 and display similar pile up behaviour to those in Figures 4.7 and 4.10. Whilst it looks like the chiral symmetry is broken dynamically as in the previous examples, we will now explicitly check this by examining the behaviour of pseudoscalar meson fluctuations $\phi(x^i, \rho, z)$.

5.2.2 Mesons in Domain Wall AdS/QCD

Having set out, and subsequently solved, the equations for the vacuum functions; it is time to solve for the mesonic fluctuations. However, the brane scan (5.16)

suggests that there are two DBI scalars, associated with fluctuations of the D7 brane embedding in the X^5 , and X^9 directions. The fluctuations in the X^5 direction will not be considered here, and the fluctuations in the X^9 direction play the role of the vacuum function L . So what fluctuation is dual to pseudoscalar mesons in this theory? We argue that there is another fluctuation, akin to perturbing the embedding in an “ X^{10} ” direction. The $X^9 + iX^{10}$ complex number can then be written as $L(\rho)e^{i\varphi}$ and acted upon by a $U(1)_A$ transformation that sets $\varphi = 0$. This effectively “hides” the extra fluctuation. The degrees of freedom still remain and we can write down an action that describes them. To quadratic order we have,

$$S_\phi = \int d^4x d\rho f \left(1 + \frac{1}{2} \frac{\mathcal{F}(\partial_\rho \phi)^2}{1 + \mathcal{F}(\partial_\rho L)^2} + \frac{1}{2} \frac{G_r \partial_i \phi \partial^i \phi}{G_x (1 + \mathcal{F}(\partial_\rho L)^2)} \right) + \mathcal{O}(\phi^3) \quad (5.27)$$

where the index i spans the field theory directions $i = 0, \dots, 3$, and

$$f(\rho, L, \phi) = e^{-\Phi} G_x^{5/2} G_r^{3/2} \sqrt{g_r + g_x (\partial_\rho z)^2} \rho^2 \sqrt{1 + \mathcal{F}(\partial_\rho L)^2} \Big|_{r^2 = \rho^2 + L^2 + \phi^2}. \quad (5.28)$$

We can now vary ϕ keeping terms to quadratic order, and implement the plane wave ansatz $\phi(\rho, x^i) = \tilde{\phi}(\rho)e^{ik \cdot x}$, to arrive at the following equation of motion,

$$\begin{aligned} & \partial_\rho \left(\frac{e^{-\Phi} G_x^{5/2} G_r^{3/2} \sqrt{g_r + g_x (\partial_\rho z)^2} \rho^2 \mathcal{F}}{\sqrt{1 + \mathcal{F}(\partial_\rho L)^2}} \Big|_{\phi=0} \cdot \partial_\rho \tilde{\phi} \right) \\ & - 2\rho^2 \sqrt{g_r + g_x (\partial_\rho z)^2} \frac{\partial}{\partial r^2} \left(e^{-\Phi} G_x^{5/2} G_r^{3/2} \sqrt{1 + \mathcal{F}(\partial_\rho L)^2} \right) \Big|_{\phi=0} \cdot \tilde{\phi} \\ & + M_\phi^2 \frac{e^{-\Phi} G_x^{3/2} G_r^{5/2} \rho^2 \sqrt{g_r + g_x (\partial_\rho z)^2}}{\sqrt{1 + \mathcal{F}(\partial_\rho L)^2}} \Big|_{\phi=0} \cdot \tilde{\phi} = 0. \end{aligned} \quad (5.29)$$

Plots of the meson mass squared against the quark mass are plotted in Figure 5.3, showing the linear Gell-Mann-Oakes-Renner behaviour at small quark mass, suggesting that the chiral symmetry in this theory is spontaneously broken in the IR. In this figure, both the meson mass, and the quark mass are in units of U_0 , but since they are both in these units, we can trust the linear behaviour without having to move back to physical units⁵. This model now displays confinement, by virtue of the cap in the geometry, and spontaneously broken chiral symmetry in a four dimensional quark theory. This means two things! Firstly we may take

⁵which requires fitting a few extra parameters anyways!

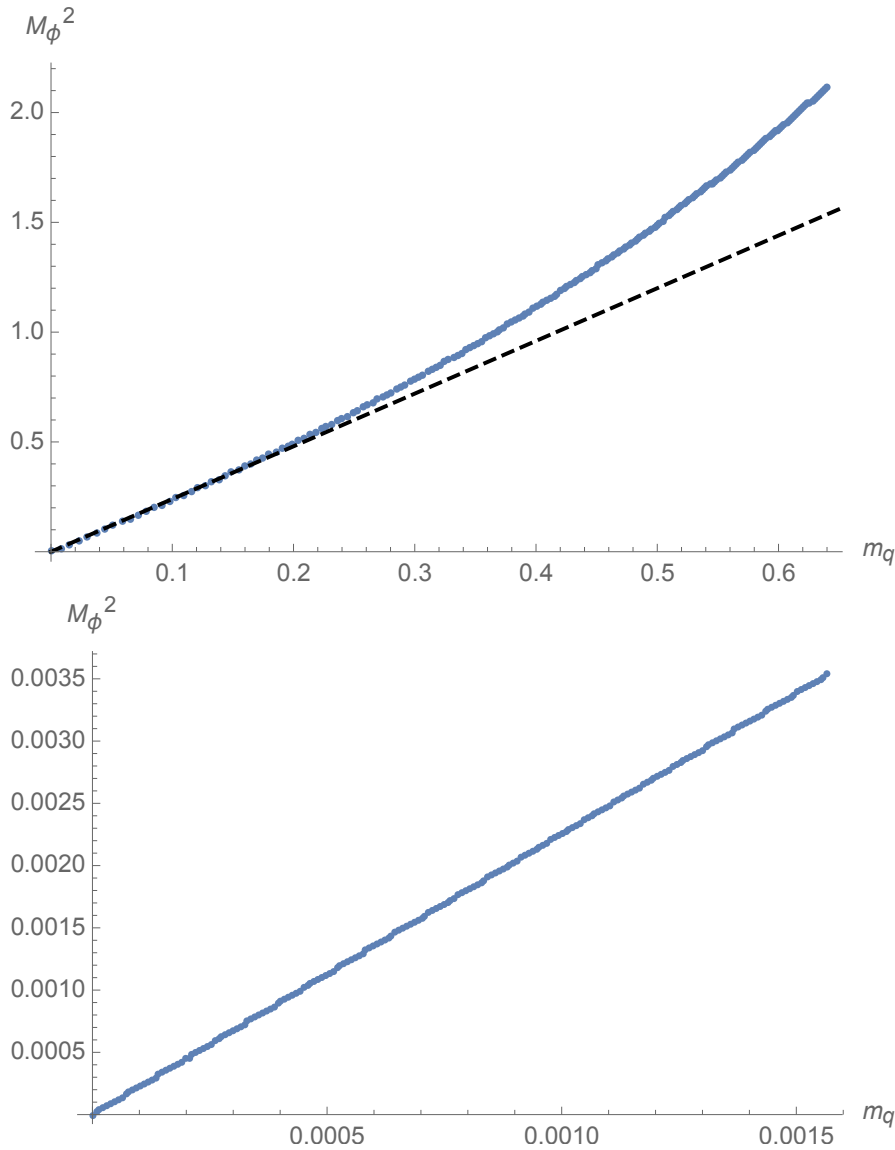


FIGURE 5.3: The meson mass squared against the quark mass, corresponding to the vacuum functions in Figure 5.2. A linear guide function has been added to emphasise the behaviour at small m_q (Top). A magnified view of the small quark mass region clearly showing the linear GMOR behaviour (Bottom).

the pseudoscalar mesons ϕ and now dub it the pion of our model. It acts as the pseudo-Goldstone boson of the broken chiral symmetry, as the pion does in QCD. Secondly, this is now a good candidate for a holographic model of QCD! It is a holographic dual with confinement and chiral symmetry breaking, and we should compute the remainder of its meson spectrum. The rest of this chapter will be devoted to doing exactly this.

5.3 Worldvolume Gauge Fields, Vector Mesons, and Matching to QCD

This section will set about writing down the Lagrangian for the fluctuations of the (axial-)vector mesons; determining their source normalisation, by requiring that they have a canonically normalised kinetic term at the UV cut-off; and calculating their masses and decay constants, by matching to QCD at an intermediate scale of around 3 GeV in physical units.

5.3.1 Worldvolume Gauge Fields

We include gauge fields propagating on domain wall loci⁶ in the following way,

$$S_{DW} \sim \int d^4x d\rho dz \Delta(z - z(\rho)) \times e^{-\phi} \sqrt{-\det[G_{ab} + (2\pi\alpha')F_{ab}]} \quad (5.30)$$

which when expanded to quadratic order in the fluctuations F_{ab} , about the background vacuum solutions $L(\rho)$ calculated in the previous section, gives

$$S_F \sim \int d^4x d\rho f \left(1 + \frac{1}{2} \frac{g^{ab}g^{cd}F_{ac}F_{bd}}{1 + \mathcal{F}(\partial_\rho L)^2} + \mathcal{O}(F^3) \right) \quad (5.31)$$

with f defined in (5.28)⁷. Since this prefactor has no dependence on any of the worldvolume gauge fields, we may drop the 1 inside the brackets, because it will not show up in the equations of motion for the gauge fields. We are interested here in the components corresponding to the spatial fluctuations $A_x \sim a_x(\rho) e^{ik \cdot x}$. Their equation of motion is

$$\begin{aligned} \partial_\rho \left(\frac{e^{-\Phi} G_x^{3/2} G_r^{1/2} \rho^2 \sqrt{g_r + g_x(\partial_\rho z)^2} \mathcal{F} \partial_\rho A_x}{\sqrt{1 + \mathcal{F}(\partial_\rho L)^2}} \right) \\ + M_x^2 \frac{e^{-\Phi} G_x^{1/2} G_r^{3/2} \rho^2 \sqrt{g_r + g_x(\partial_\rho z)^2} A_x}{\sqrt{1 + \mathcal{F}(\partial_\rho L)^2}} = 0. \end{aligned} \quad (5.32)$$

The spatial components of the gauge fields encode the behaviour of both the vector, and axial-vector states of the model, which will be referred to as the ρ -meson, and

⁶on the D7 brane

⁷I'd like to take a moment to apologise for using three different script f's in one equation. Sorry about that! To ward off any confusion I vote we call them: little f , curly \mathcal{F} , and F .

the a -meson respectively. The difference between them comes down to boundary conditions. Both states obey a Dirichlet boundary condition at the UV boundary, $A_{V,A}(\Lambda_{UV}) = 0$. However, on the IR surface at $\rho = \rho_{min}$, the vector state obeys a Neumann boundary condition, $\partial_\rho A_V(\rho_{min}) = 0$ with $A_V \neq 0$, and the axial vector state obeys a Dirichlet boundary condition, $A_A(\rho_{min}) = 0$ with $\partial_\rho A_A \neq 0$. In practice one sets these boundary conditions in the IR then varies the mass squared, $M_{V,A}^2$, to satisfy the Dirichlet condition in the UV. The wavefunction for the vector, and axial-vector mesons must then be normalised. By hand we enforce that the kinetic term must be canonically normalised, requiring that

$$\int_{\rho_{min}}^{\Lambda} d\rho \frac{e^{-\Phi} G_x^{3/2} G_r^{1/2} \rho^2 \sqrt{g_r + g_x (\partial_\rho z)^2} A_x^2}{\sqrt{1 + \mathcal{F} \partial_\rho L^2}} = 1. \quad (5.33)$$

We may also compute the decay constants F_V , F_A , and f_π . By definition, F_V^2 is the Feynman rule for the vector meson to turn directly into its source at $q^2 = 0$. We solve (5.32) with $M^2 = 0$ to represent the source, $A_{V,S}$ and then F_V follows as, (after removing the UV surface term),

$$F_V^2 = \int d\rho \partial_\rho \left[\frac{e^{-\Phi} G_x^{3/2} G_r^{1/2} \rho^2 \sqrt{g_r + g_x (\partial_\rho z)^2} \mathcal{F} \partial_\rho A_V}{\sqrt{1 + \mathcal{F} (\partial_\rho L)^2}} \right] A_{V,S}(\rho). \quad (5.34)$$

The normalisation of the sources here is tricky. Usually in AdS/QCD models, the UV of the theory is conformal, and this symmetry enforces an asymptotic $\sim \log(Q^2/\rho^2)$ form for the sources, which can be used to fix their normalisation. We are not so lucky here, the UV of the domain wall AdS/QCD theory is not conformal, and so we must set the normalisation of the sources such that F_V lies on its QCD value of ~ 345 MeV. We are then free to use this source normalisation to predict F_A and f_π . The decay constant for the axial-vector mesons is a repeat of the above calculation (5.34), but using the axial-vector solutions,

$$F_A^2 = \int d\rho \partial_\rho \left[\frac{e^{-\Phi} G_x^{3/2} G_r^{1/2} \rho^2 \sqrt{g_r + g_x (\partial_\rho z)^2} \mathcal{F} \partial_\rho A_A}{\sqrt{1 + \mathcal{F} (\partial_\rho L)^2}} \right] A_{A,S}(\rho). \quad (5.35)$$

Similarly, the pion decay constant can be computed from the axial-axial correlator

$$f_\pi^2 = \int d\rho \frac{e^{-\Phi} G_x^{3/2} G_r^{1/2} \rho^2 \sqrt{g_r + g_x (\partial_\rho z)^2} \mathcal{F}}{\sqrt{1 + \mathcal{F} (\partial_\rho L)^2}} (\partial_\rho A_{A,S})^2. \quad (5.36)$$

The final step in our matching to QCD is determining which of the vacuum functions $L(\rho)$ is an appropriate “physical” vacuum. The vacuum functions are described by one parameter, ρ_{min} , so this choice is the same as picking out which of the loci best describes QCD. There are several ways to do this, though three stand out as “morally superior”. The first is that we can set some ρ_{min} , then compute the pion, and vector meson masses, calculate their ratio, and then iteratively tune ρ_{min} until we hit the desired ratio of $\frac{M_\rho}{m_\pi} = \frac{775}{139}$, which is observed in nature. We may then predict the axial mass, and the two decay constants. This is the standard approach and, in this case, the best fit to QCD⁸. There are two other approaches that I would like to mention here as well. Equally one could fit the axial-vector meson mass instead of the vector meson mass, predicting M_V, F_A and f_π . Finally, one could attempt a “best average” vacuum; where one asserts that the mass is 139 MeV and is the scale by which your system will be measured, then one could tune the parameter that controls the vacuum to minimise the RMS deviation

$$\text{RMS}(M_\rho, M_A) = \frac{1}{\sqrt{2}} \sqrt{\left(\frac{139 M_\rho}{m_\pi} - 775\right)^2 + \left(\frac{139 M_A}{m_\pi} - 1230\right)^2}, \quad (5.37)$$

from the QCD values. The numerical results for these three vacua are displayed in Figure 5.4. Whilst fitting the vector meson mass gives the most reasonable predictions for the decay constants, it consistently over-predicts axial sector of the model. Fitting the axial-vector meson, and the RMS vacuum, likewise predicts a comparably light vector meson, but massively overshoots the decay constants. However these two vacua are much better at predicting the masses of the excited states for both the vector and axial-vector mesons. Whilst it is clear that this model is not perfect, it can be good at predicting the decay constants or the excited state masses. But frustratingly, not both at the same time! We may now however take further inspiration from our colleagues in lattice field theory, and consider “improving” the action [111, 112]. We will do this by considering the effect of higher dimension, multi-trace operators at the UV cutoff through the Witten prescription.

⁸by a slightly naïve metric

	QCD	Fitting M_ρ $\rho_{min} = 1.05065$	Fitting M_A $\rho_{min} = 1.0607$	RMS Vacuum $\rho_{min} = 1.06298$
m_π	139 MeV	139*	139*	139*
M_ρ	775 MeV	775*	353 (-53%)	376 (-51%)**
M_a	1230 MeV	2910 (+136%)	1230*	1327 (+10%)**
F_V	345 MeV	345*	345*	345*
F_A	433 MeV	583(+35%)	1219 (+182%)	1153 (+166%)
f_π	93 MeV	95 (+2%)	451 (+385%)	398 (+328%)
$M_{v,n=1}$	1465 MeV	3258 (+122%)	1390 (-5%)	1496 (+2%)
$M_{A,n=1}$	1655 MeV	4724 (+185%)	2037 (+23%)	2190 (+32%)
mean deviation		96%	129%	98%

FIGURE 5.4: Mesonic observables in the Domain Wall AdS/QCD model. QCD data is displayed in the lefthand column, with the three chosen vacua displayed alongside. The starred numbers indicate quantities that were used to set scales and are not predictions. The two doubly starred values in the rightmost column are found from minimising (5.37). The percentages in brackets indicate the deviation from the QCD value.

5.3.2 Higher Dimension Operators via Witten Prescription

In [113], a prescription was set out for including the effects of multi-trace, higher dimension operators in gauge gravity duals, which is extended to conderations of NJL-type interactions [114] in [115]. Here the logic is to fix by hand the masses of the mesons, relaxing the Dirichlet boundary condition at the UV cutoff. Considering generically an operator of the form

$$G\mathcal{O}^\dagger\mathcal{O} \subset \mathcal{L}, \quad (5.38)$$

we attribute the boundary value of the holographic fields to the condensing of an operator \mathcal{O} . This leaves an effective source $G\langle\mathcal{O}\rangle$. For the present case, we consider an NJL type four quark interaction, schematically

$$\mathcal{J} \sim \frac{g^2}{\Lambda^2}\mathcal{O}, \quad (5.39)$$

as discussed in [116]; with an operator $\frac{g_V^2}{\Lambda_{UV}^2}|\bar{q}\gamma^\mu q|$, and $\frac{g_A^2}{\Lambda_{UV}^2}|\bar{q}\gamma^\mu\gamma^5 q|$ in the vector and axial sectors respectively. We may then compute the couplings from the values of the leading and subleading components, source and operator parts, of

the holographic fields $A_{V/A}$ ⁹. The masses of the radial excited states can then be read off, as the next massive states that have the same coupling $\frac{g}{\Lambda_{UV}}$ for the vector, and axial-vector states. This gives the following improvement to the spectrum. In

	QCD	DW AdS/QCD $\rho_{min} = 1.05065$	“Improved Model” $\rho_{min} = 1.05065$
m_π	139 MeV	139*	139*
M_ρ	775 MeV	775*	775*
M_a	1230 MeV	2910 (+136%)	1230*
F_V	345 MeV	345*	
F_A	433 MeV	583(+35%)	$g_V/\Lambda_{UV} \sim 2.3 \text{ GeV}^{-1}$
f_π	93 MeV	95 (+2%)	$g_A/\Lambda_{UV} \sim 2.1 \text{ GeV}^{-1}$
$M_{v,n=1}$	1465 MeV	3258 (+122%)	1228 (-16%)
$M_{A,n=1}$	1655 MeV	4724 (+185%)	3019 (+82%)

FIGURE 5.5: Mesonic observables in the base Model, and the numerical results of the improvement to the model to more accurately describe the excited states. The starred numbers are fixed to set scales and normalisations. The percentages in brackets are the deviations from the QCD values

principle one could repeat the above for all three of the vacua considered in Figure 5.4, however the goal here is just to estimate the rough order of magnitude of the effect of including higher dimension operators on the spectrum¹⁰. Still the axial sector remains heavier than is observed in experiment, though now the radially excited vector meson is in much better agreement with QCD.

5.4 Summary

This chapter has covered the realisation of a fully top down, holographic theory of 4+1 dimensional gluons, interacting with quarks on a 3+1 dimensional defect. The theory on the defect displays both confinement and dynamical chiral symmetry breaking; and has neither conformal symmetry, nor supersymmetry, making it a good candidate for a holographic model of QCD. The spectrum of mesonic observables has been presented, showing a comparable accuracy to other holographic models for either the radially excited states, or the decay constants¹¹.

⁹This is more of an aside here, and will be discussed more concretely in the next chapter when examining the thermal transitions in a domain wall model with an NJL interaction generating the quark mass.

¹⁰which in this case seems to be a reduction in the deviation from the QCD value of $\sim 100\%$

¹¹Though sadly not both

Consistently, the model predicts a heavier axial sector than is observed in nature, though it does accurately represent the hierarchy of masses seen in QCD bound states at colliders. The excited states rise rapidly in mass, suggesting they scale $M_n \sim n$, rather than $M_n \sim \sqrt{n}$ which is more common in AdS/QCD models [117]. An improvement of the model, from inclusion of higher dimension operators, to cure the problems with the abnormally heavy radially excited states was considered; though it comes with the caveat of sacrificing predictive power, setting another meson mass by hand. The next chapter will explore this model in the presence of a black hole, dual to the field theory at finite temperature. We will go on to explore phase transitions with respect to temperature in this model, with a thorough discussion on the interpretation of the fields that live on the surface of the D7 brane.

Chapter 6

Thermal Transitions in Domain Wall AdS/QCD

Having set out the Domain Wall AdS/QCD model in the previous chapter, based on the intersection of D5 and D7 branes, this chapter will go on to discuss the model at finite temperature [3]. It is expected that at high temperatures, there will be a transition from a confined phase of QCD to a deconfined plasma phase. In this plasma phase, hadrons are no longer “good” degrees of freedom¹. These bound states will decay into their constituent quarks and gluons in a meson melting phase transition, dissipating into the background plasma, much like ice cubes in a glass of water at room temperature. The quark-gluon plasma has been observed at heavy ion collider experiments². Any good description of QCD, holographic or not, should be able to accommodate a deconfined plasma phase. This chapter will cover exactly this, for the Domain Wall AdS/QCD model. Starting from a geometry attributed to a near extremal stack of D5 branes, our *thermal* geometry, we perform the appropriate co-ordinate transformations to nicely embed D7 branes in the background. From this point we begin the construction of the domain wall defects by the large mass limit described in Chapter 4. The loci in this geometry are explored and a new possibility is uncovered. Alongside the usual U-shaped loci, one can have a pair of flat disconnected solutions. Here the bottom of the U-shape has been swallowed by the black hole horizon lurking in the geometry. It is also shown that the asymptotic separation of the loci, or width, in this system is no longer monotonically increasing as one decreases ρ_{min} to small values. The width of the loci decreases close to the horizon, creating a situation where one can have

¹Meaning appropriate descriptors of the physics.

²such as the Relativistic Heavy Ion Collider (RHIC) at Brookhaven national laboratory [118]

potentially three different configurations of the same width at the boundary; with two U-shaped loci and one pair of disconnected loci. Immediately this suggests that there may be a first order transition in this system, but this is by no means the full story. A careful examination of the DBI fields, restricted to the loci, reveals that whilst they all have the same asymptotic width; *they are different theories*. More precisely, they are theories with different values for the UV quark mass. Reorganising the theory, insisting that we must look for loci equipped with DBI fields asymptoting to the same quark mass³, reorders the solutions; revealing the true nature of the phase transition, which is *second order*.

6.1 Black Branes and Finite Temperature

The thermal geometry that will be used to represent the finite temperature gauge background has already been mentioned in Chapter 5. It is the same geometry that was doubly Wick rotated to find the confining background of the Domain Wall AdS/QCD model at zero temperature. We restate the solution here, the metric is:

$$\frac{ds^2}{\alpha'} = \frac{U}{R} (-h(U)dt^2 + \delta_{ij}dx^i dx^j) + \frac{R}{U} \left(\frac{1}{h(U)}dU^2 + U^2 d\Omega_3^2 \right) \quad (6.1)$$

where the indices span $i, j = 1, \dots, 5$, and

$$\begin{aligned} U &= \frac{\tilde{r}}{\alpha'}, & R &= \frac{g_{YM}\sqrt{N}}{(2\pi)^{3/2}}, \\ e^\Phi &= RU, & g_{YM}^2 &= (2\pi)^3 g_s \alpha', \\ h(U) &= 1 - \left(\frac{U_0}{U} \right)^2. \end{aligned} \quad (6.2)$$

It is expected that at some temperature T_c , there will be a phase transition between the thermal and confining geometries. These two geometries, when Wick rotated back to Euclidean signature, have the same boundary at the UV cutoff. The usual approach when discussing these types of transition in a gravitational setting is to consider some appropriate boundary condition, in this case metrics with the same boundary structure. Then one evaluates the gravitational path integral to determine the rest of the metric. In practice one can evaluate this path integral within a saddle-point approximation, where solutions to the supergravity equations

³Measured in units of Λ_{UV}

of motion, make up the dominant saddles. At some temperature scale the black hole geometry becomes the dominant contributor to the path integral, and thus emerges victorious from the battle of the metrics, signalling the transition to the deconfined plasma phase. This however is an aside, justifying the use of the thermal geometry. It is not the transition we are going to study in this section. Instead we are interested in the behaviour of quarks living on domain wall defects in this background. Before we can begin to look at domain walls in this background, we must identify quite what is meant by temperature in this fivebrane system. We will do this generally by examining the near extremal black p-brane solutions in the field theory limit

6.1.1 Temperature of near extremal p-branes

Taking the result from [60] for the field theory limit of the near extremal black p-brane geometry, we have⁴

$$\frac{ds^2}{\alpha'} = \left\{ \frac{U^{\frac{1}{2}(7-p)}}{R_p^{\frac{1}{2}(7-p)}} \left[- \left(1 - \left(\frac{U_0}{U} \right)^{7-p} \right) dt^2 + dy_{||}^2 \right] + \frac{R_p^{\frac{1}{2}(7-p)}}{U^{\frac{1}{2}(7-p)}} \left[\frac{dU^2}{\left(1 - \left(\frac{U_0}{U} \right)^{7-p} \right)} + U^2 d\Omega_{8-p}^2 \right] \right\}, \quad (6.3)$$

with

$$R_p^{\frac{1}{2}(7-p)} \equiv g_{YM} \sqrt{N} \times \sqrt{2^{7-2p} \pi^{\frac{9-3p}{2}} \Gamma\left(\frac{7-p}{2}\right)}. \quad (6.4)$$

Our next steps are to Wick rotate the time direction to Euclidean signature, taking $t \rightarrow i\tau$, and to expand about the horizon $U = U_0 + \delta U$, demanding that the geometry is free of any conical singularities (this is identical to the steps taken in (5.5), only this time in a general geometry). This yields,

$$ds^2 \supset (7-p) \frac{U_0^{\frac{5-p}{2}}}{R_p^{\frac{7-p}{2}}} \delta U d\tau^2 + \frac{1}{(7-p)} \frac{R_p^{\frac{7-p}{2}}}{U_0^{\frac{5-p}{2}}} \frac{d\delta U^2}{\delta U}. \quad (6.5)$$

Defining

$$K = \frac{7-p}{2} \sqrt{\frac{U_0^{5-p}}{R_p^{7-p}}}, \quad (6.6)$$

⁴I am certain that this is not novel. I am merely presenting a calculation, with no doubt that it is already published somewhere!

we have

$$ds^2 \supset 2K\delta U d\tau^2 + \frac{1}{2K\delta U} d\delta U^2, \quad (6.7)$$

which when augmented with the co-ordinate transformation

$$\alpha = K\tau, \quad \sigma = \sqrt{\frac{2\delta U}{K}}, \quad (6.8)$$

reveals that (6.7) is in fact a flat two plane in the (α, σ) co-ordinates,

$$ds^2 \supset d\sigma^2 + \sigma^2 d\alpha^2. \quad (6.9)$$

Therefore to have a complete plane, without an angular deficit, we must have

$$\begin{aligned} 0 &\leq \alpha \leq 2\pi, \\ \therefore 0 &\leq \tau \leq \frac{2\pi}{K}. \end{aligned} \quad (6.10)$$

Periodically identifying the Euclidean time direction, with period β , is in field theory language equivalent to calculating at a temperature $T = 1/\beta$ in the dual Yang-Mills theory. Thus the temperature associated with the black p-brane is

$$T = \frac{7-p}{4\pi} \left(\frac{U_0^{5-p}}{R_p^{7-p}} \right)^{1/2}. \quad (6.11)$$

This presents us with a problem. We are working in a fivebrane system, and thus the temperature is independent of the horizon position (therefore the size of the black hole). However hope is not lost. Still the position of the horizon is a dimension 1 scale in the theory, which alongside the introduction of the UV cutoff act as “ends” of the geometry. Still, branes can fall into the black hole in the geometry, supporting the quasi-normal modes associated with meson melting in the dual theory as in [119]. In fact we will see in the coming sections that to the fields living on the domain walls, the position of the horizon acts exactly like a temperature. This is all to say that, in the remainder of this chapter, we will refer to U_0 as a temperature. We shall label the axes of the figures $U_0(T)/\Lambda_{UV}$, indicating that whilst we do not completely understand the interpretation of U_0 ; from the view of the fields living on the loci it is temperature-like.

6.1.2 Thermal geometry

In order to progress we must perform the co-ordinate change,

$$\frac{U}{U_0} = \frac{1+r^2}{2r}, \quad (6.12)$$

as in (5.11, 5.12). This leaves the metric in the form we will use going forwards,

$$ds^2 = G_x(r) (-h(r)dt^2 + \delta_{ij}dx^i dx^j) + G_r(r) (dr^2 + r^2 d\Omega_3^2), \quad (6.13)$$

with the i, j indices spanning $i, j = 1, \dots, 5$. The corresponding metric factors,

$$G_x(r) = \frac{U_0}{R} \frac{1+r^2}{2r}, \quad G_r(r) = U_0 R \cdot \frac{1+r^2}{2r^3},$$

$$h(r) = 1 - \left(\frac{2r}{1+r^2} \right)^2, \quad e^{-\Phi} = \frac{1}{U_0 R} \frac{2r}{1+r^2}, \quad (6.14)$$

are identical to those in (5.15). As discussed previously, in this co-ordinate system the factors U_0 and R are dimensionful. As a consequence, the radial direction r , becomes dimensionless, and runs from $r = 1$ at $U = U_0$ to $r = r_\Lambda$ at the UV cutoff $U = \Lambda$. This also means that the DBI fields carry no mass dimension, and when asymptotics are considered, must be converted into units in terms of Λ . This will be discussed in more detail when examining the fluctuations on the domain walls. It should be noted here that (6.12) implies that scaling the temperature $U_0 \rightarrow AU_0$, is equivalent to scaling the cutoff $\Lambda \rightarrow \Lambda/A$ from the perspective of the r co-ordinates. As such, varying the temperature will amount to variation of the UV cutoff in the r co-ordinate system, r_Λ . In the dimensionful U co-ordinates, Λ will remain fixed. Now this is a geometry that it is simple to embed probe D7 branes within, and we shall do so in the following configuration:

	0	1	2	3	4	5	6	7	8	9	
D5	-	-	-	-	-	-	•	•	•	•	.
D7	-	-	-	-		•	-	-	-	•	

(6.15)

Again the $||$ symbol in the x^4 direction indicates that the D7 brane wraps this direction, but we will place the domain wall pair here effectively eliminating it from the dynamics of fluctuations in the theory. Again we will refer to x^4 as the z direction, to keep consistent with the previous chapter(s). The major differences from the previous chapter are: that now the x^5 direction is not compact, the D7

brane is pointlike in this direction and we will consider sevenbrane embeddings that have $x^5 = \text{const}$; and that the probe brane now wraps a direction that comes equipped with the emblackening factor $h(r)$. The DBI action for the probe branes, with embedding $x^9 = L(\rho, z)$, in this background is

$$S_{D7} = -T_7 \Omega_2 \int d^5x d\rho e^{-\Phi} h(r) G_x^{5/2} G_r^{3/2} \rho^2 \sqrt{1 + (\partial_\rho L)^2 + \frac{G_r}{G_x} (\partial_z L)^2}. \quad (6.16)$$

The next step will be to determine the set of loci in the thermal geometry, and restrict the DBI fields to small fluctuations living on the surface of the domain walls.

6.2 Domain Walls and Loci at Finite Temperature

As set out in Section 4.3, we take the following functional form for the embedding field $L(\rho, z)$,

$$\partial_\rho L \sim \frac{1}{\sqrt{g_{LL}}} \Big|_{L=0} \frac{\partial z}{\partial \rho} \delta(z - z(\rho)) = \frac{\partial_\rho z}{\sqrt{g_r}} \delta(z - z(\rho)), \quad (6.17)$$

to determine the action functional for the loci, S_{locus} . We continue the convention here, that metric factors which are lowercase are evaluated on $L = 0$. Implementing (6.17) on the D7 action, we are lead to the action,

$$S_{locus} \sim \int d^7x e^{-\Phi(\rho)} h(\rho) g_x^2 g_r^{3/2} \rho^2 \sqrt{1 + \frac{g_x}{g_r} (\partial_\rho z)^2}. \quad (6.18)$$

Varying (6.18) with respect to $z(\rho)$ gives the equations of motion that describes the set of loci in the thermal geometry

$$\partial_\rho z = \frac{g_r^{1/2} c_z}{g_x^{1/2} \sqrt{e^{-2\Phi(\rho)} h(\rho)^2 g_x^5 g_r^2 \rho^4 - c_z^2}}, \quad (6.19)$$

with a constant of motion c_z that parameterises the loci. This parameter is identified as

$$c_z^2 = \left(1 - \left(\frac{2\rho_{min}}{1 + \rho_{min}^2} \right)^2 \right)^2 \left(\frac{U_0}{R} \frac{1 + \rho_{min}^2}{2\rho_{min}} \right)^5. \quad (6.20)$$

We see now that even with $1 \leq \rho_{min} < r_\Lambda$ it is possible to have $c_z = 0$, which was not possible in the confining geometry. This gives rise to flat loci, which come in

disconnected pairs. The approach now will be to analyse the system of domain walls with some appropriate organising principle. We will elucidate what is meant by this, with an example of a poor organising principle.

6.3 The Width Transition - A Naïve Approach

Our goal going forward will be to organise the theory by a good UV parameter. One potential candidate is given by the asymptotic separation, or width, of the domain wall pair. In holography at finite temperature, we associate the free energy of a given configuration⁵, in the grand canonical ensemble, with the Legendre transform of the probe brane action with respect to the chemical potential [87, 120]. In this system we argue that the dominant contribution to the action will be proportional to the action S_{locus} , with the contribution of the fluctuations being a subleading part of the action that need not be considered in the free energy calculations⁶. The loci are not explicitly dependant on any thermodynamic variables, other than temperature which changes the background geometry. The free energy F is therefore,

$$F = -T S_{locus} [\rho_{min}, T] + (\text{counter term}), \quad (6.21)$$

evaluated on the solutions $z(\rho)$. A numerical analysis of the loci reveals that at any given temperature, there are two U-shaped loci at a given width. This is displayed in Figure 6.1. Trivially there is also a pair of flat disconnected solutions at any width, and so this is evocative of a Maxwell construction for a first order phase transition in a thermodynamical system. An example set of solutions is displayed in Figure 6.2. With this in mind we should calculate the free energies of these solutions to determine whether there is a first order phase transition in this system when the width is kept fixed. Problematically, the action S_{locus} is UV divergent, and thus the free energy is dominated by the contribution from the UV cutoff. We must endeavour to regularise it. There are two possibilities here, either one can carefully examine the asymptotics of S_{locus} and construct a UV counterterm that removes the dependence on the cutoff (and do the same for the flat solutions), or one can note that the action for the flat configurations has the same UV divergence as the connected solutions, and set this as the “zero point”

⁵specifically, βF

⁶formally there should be a factor of the 5-dimensional quark mass difference, M , between them. So it is sufficient to consider just the locus action.

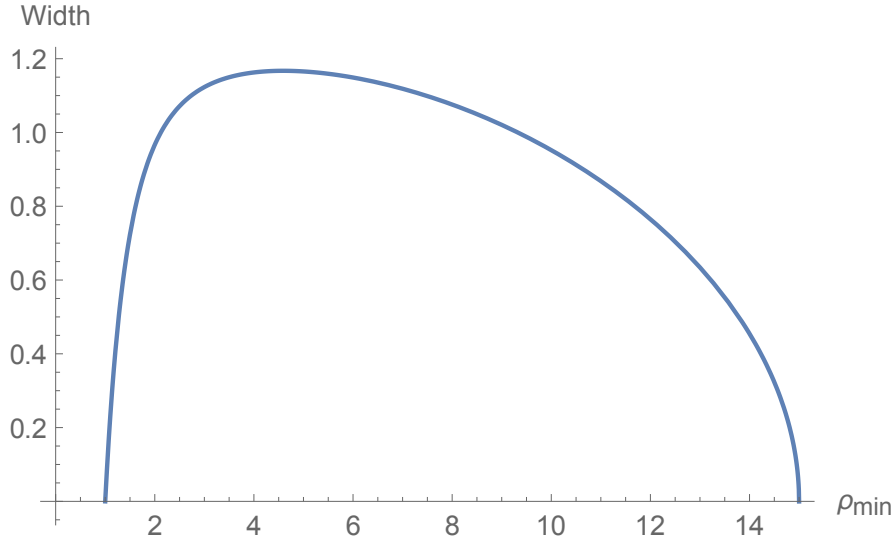


FIGURE 6.1: The asymptotic separation of a domain wall pair, against ρ_{min} for system at a temperature of $U_0(T) \sim 0.066\Lambda_{UV}$

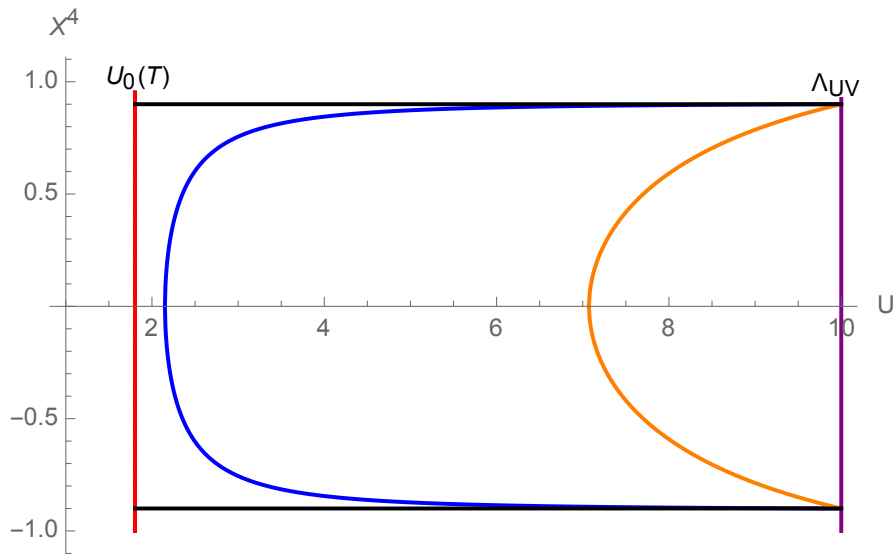


FIGURE 6.2: A cartoon depicting the set of three loci for a chosen width and temperature, in the dimensionful “U” co-ordinate system.

of the free energy, defining the regularised free energy

$$F_{reg} = -T (S_{locus}[\rho_{min}, T] - S_{locus}[0, T]). \quad (6.22)$$

We will choose to do the latter⁷. Equipped with a properly regulated free energy we can go on to numerically calculate and plot this for the three configurations in Figure 6.3. Here we clearly see the swallowtail form associated with a first

⁷We will take $T \sim \frac{U_0}{\Lambda}$ whilst doing numerics here. Formally the free energies should be multiplied through by the energy scale Λ , but this is common to all the configurations.

order phase transition, with a critical temperature of $U_0(T_c)/\Lambda \simeq 0.33$. With the

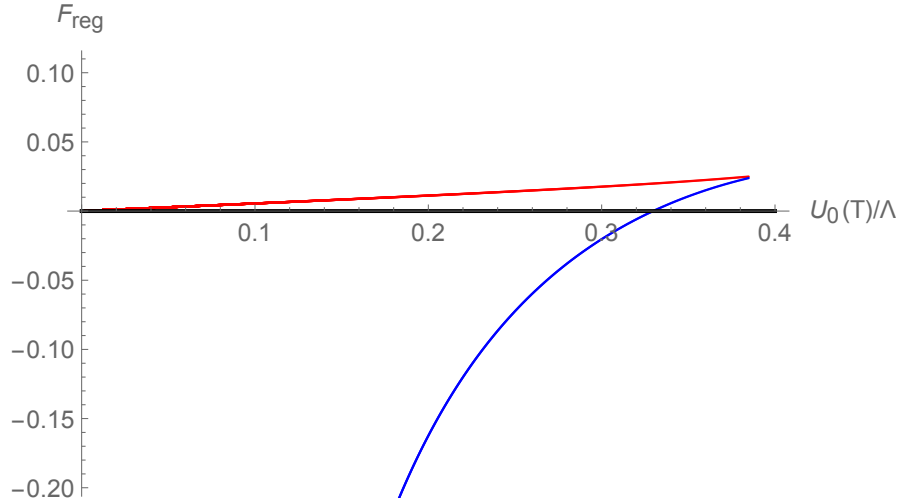


FIGURE 6.3: A plot of the regulated free energy against temperature U_0/Λ , for an asymptotic width of $W \sim 0.964$. The two U shaped loci are depicted (Blue, Red), alongside the zero line representing the flat disconnected loci (Black).

presentation of Figure 6.3, it would be easy to assume that the meson melting transition here is first order. However we have more powerful tools at our disposal than just an examination of the domain wall loci. We can deal directly with the fluctuations on the loci, dual to the quark mass/chiral condensate source/operator pair.

6.4 The Domain Wall Theory at Finite Temperature.

We now restrict the DBI fields to live on the domain walls as set out in Section 4.4. The action for fluctuations in the domain wall theory is

$$S_{DW} = -T_7 \Omega_2 \int d^5 x d\rho e^{-\Phi} h(r) G_x^{5/2} G_r^{3/2} \times \sqrt{g_r + g_x (\partial_\rho z)^2} \rho^2 \sqrt{1 + \mathcal{F}(\partial_\rho L)^2}. \quad (6.23)$$

Yet again the function \mathcal{F} encodes the z dependence of the solutions, and is given by

$$\mathcal{F} = 1 + \frac{G_r}{G_x (\partial_\rho z)^2}. \quad (6.24)$$

We can go on to extremise this action to write down the equations of motion associated with the field $L(\rho)$,

$$\partial_\rho \left(\frac{e^{-\Phi} h(r) G_x^{5/2} G_r^{3/2} \sqrt{g_r + g_x (\partial_\rho z)^2} \rho^2 \mathcal{F} \partial_\rho L}{\sqrt{1 + \mathcal{F}(\partial_\rho L)^2}} \right) - 2\rho^2 \sqrt{g_r + g_x (\partial_\rho z)^2} \frac{\partial}{\partial r^2} \left(e^{-\Phi} h(r) G_x^{5/2} G_r^{3/2} \sqrt{1 + \mathcal{F}(\partial_\rho L)^2} \right) \cdot L = 0, \quad (6.25)$$

solving them numerically⁸ to determine the UV quark mass from the boundary values of the field. It has been stated previously that this field is dimensionless in these co-ordinates. Whilst this was not an issue before, now we must convert the values that we compute numerically into physical units. Noting that the co-ordinate transformation (6.12) maps between dimensionful U co-ordinates and dimensionless r co-ordinates, we apply this directly to the field L . The asymptotic form for L given by the equations of motion is⁹

$$L \rightarrow \tilde{m} + \frac{\tilde{c}}{\rho^{11/2}}, \quad (6.26)$$

where the tilde-variables are dimensionless, by (6.12) we have¹⁰:

$$\frac{m}{U_0} = \frac{1 + \tilde{m}^2}{2\tilde{m}}, \quad (6.27)$$

which allows us to express the quark mass in terms of the temperature. Given that we will be varying temperature in the examination of this system this is not so useful. For direct comparison between theories at different temperatures we should express the quark mass instead in terms of the ultraviolet cutoff scale Λ , which is constant. A second application of (6.12) will aid us here! Clearly,

$$\frac{m}{\Lambda} = \frac{m}{U_0} \frac{U_0}{\Lambda} = \frac{1 + \tilde{m}^2}{\tilde{m}} \frac{\rho_\Lambda}{1 + \rho_\Lambda^2}. \quad (6.28)$$

We would like to write down a similar expression for the condensate, however this is more challenging. Both L and ρ are dimensionless, so we will have to make an assumption (though a well motivated one). We will assume that the dimensionless

⁸Again, we take the IR BCs $L(\rho_{min}) = \rho_{min}$ such that the IR mass gap is consistent, and then shoot out to the UV.

⁹This might seem slightly odd, but often the nice asymptotia in AdS/CFT come from the underlying conformal symmetry of the dual theory. This theory has no such symmetry.

¹⁰For $\tilde{m} > 1$, which we always have on the connected loci.

value \tilde{c} , is the physical condensate measured in units of temperature¹¹, $\tilde{c} \sim c/U_0^3$, thus we can write physical condensate in terms of the cutoff as

$$\frac{c}{\Lambda^3} = \tilde{c} \left(\frac{U_0}{\Lambda} \right)^3 \simeq \frac{8\tilde{c}}{\rho_\Lambda^3}. \quad (6.29)$$

With these relations in mind, we can go on to numerically explore the configurations with fixed quark mass, m/Λ .

6.4.1 Fixed Quark Mass

Demanding that the UV quark mass is kept fixed we realise that, at a given temperature, there are no longer three configurations to choose from. This is the first obvious departure from keeping the asymptotic width fixed. In fact we find only one configuration at each temperature that gives the chosen quark mass. In this system, there cannot be a first order phase transition when the quark mass is kept fixed. Instead we find that as the temperature rises the U-shaped loci begin to narrow until they shrink to zero width, at which point they become a co-incident pair of disconnected flat loci. In this respect, the U shaped loci smoothly map onto the disconnected ones as temperature is increased at fixed quark mass. This is illustrated in Figure 6.4. Note that there is variation in ρ_{min} , however it is small in the U co-ordinates displayed in Figure 6.4. In Figure 6.5 we display the numerical results for the asymptotic width of example configurations with fixed quark mass, $m/\Lambda \sim 0.2$. We confirm that a phase transition occurs when the loci dip into the horizon by calculating the condensate on each configuration displayed in Figure 6.5. The numerical results are displayed in Figure 6.6. From this, we conclude that the transition must be a meson-melting transition, that restores chiral symmetry in the theory on the domain walls. We go on to explore the variation in the critical temperature with respect to quark mass, and plot these results in Figure 6.7; indicating that for temperatures above the $U_0(T_c)$ we have a phase of melted mesons, with chiral symmetry restored, and below the critical temperature we have stable mesons and a chirally broken phase. We conclude that the phase transition in this case is at least second order.

¹¹This is the simplest dimensionless ratio of the condensate and scales that we can write down.

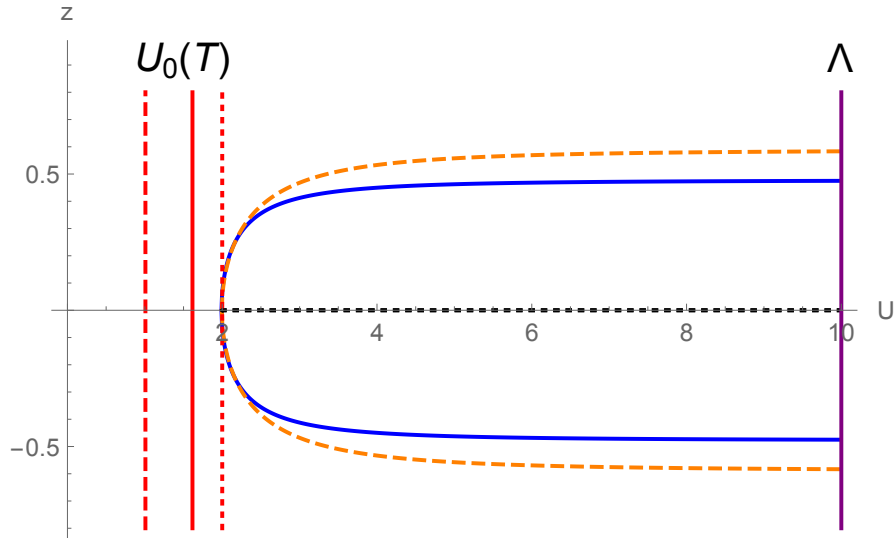


FIGURE 6.4: A cartoon showing the evolution of a domain wall system, with fixed quark mass m/Λ , as the temperature is increased from $U_0(T_1)$ (Dashed configuration), to $U_0(T_2) > U_0(T_1)$ (solid configuration), finally to $U_0(T_c)$ where the tip of the U-shape has fallen into the horizon, becoming two disconnected flat pieces (dotted configuration). The position of the horizon is drawn in red (dashed, solid, and dotted respectively).

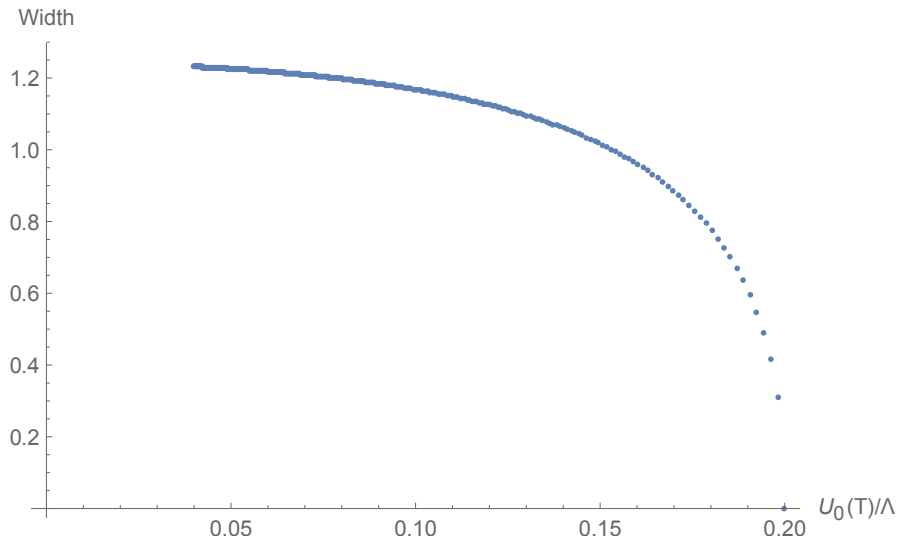


FIGURE 6.5: Numerical results tracking the asymptotic width of configurations with fixed quark mass $m/\Lambda \sim 0.2$ as the temperature is varied. At a critical temperature of $U_0(T_c)/\Lambda \sim 0.2$ the loci dip into the horizon and disconnect.

6.4.2 NJL Coupling

There is a second potential interpretation for the solutions living on the loci. We could also consider the quark mass to be dynamically generated by the presence of an NJL interaction. The NJL interaction term, as a higher dimension operator, is introduced through the Witten prescription for multi-trace operators. This was

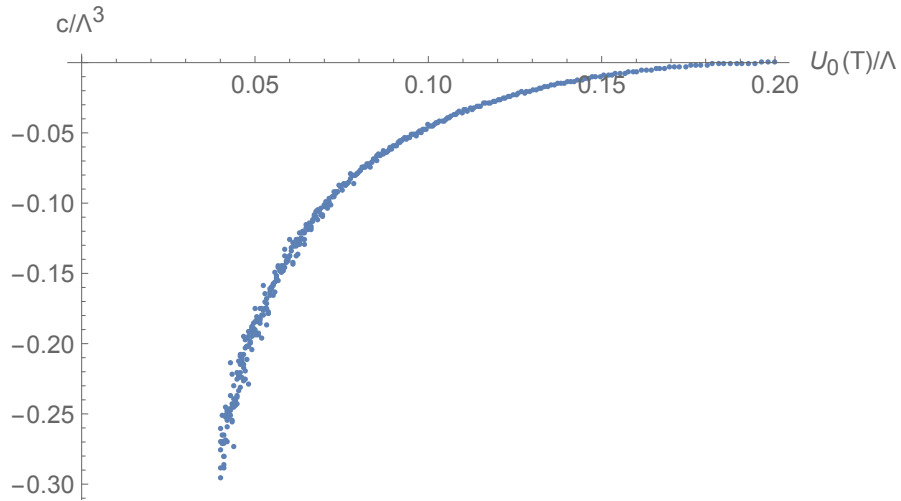


FIGURE 6.6: The chiral condensate (in units of Λ) plotted for the configurations in Figure 6.5. We see explicitly that at the critical temperature $U_0(T_c) \sim 0.2$, the condensate drops to zero, indicating the transition to a chirally restored phase.

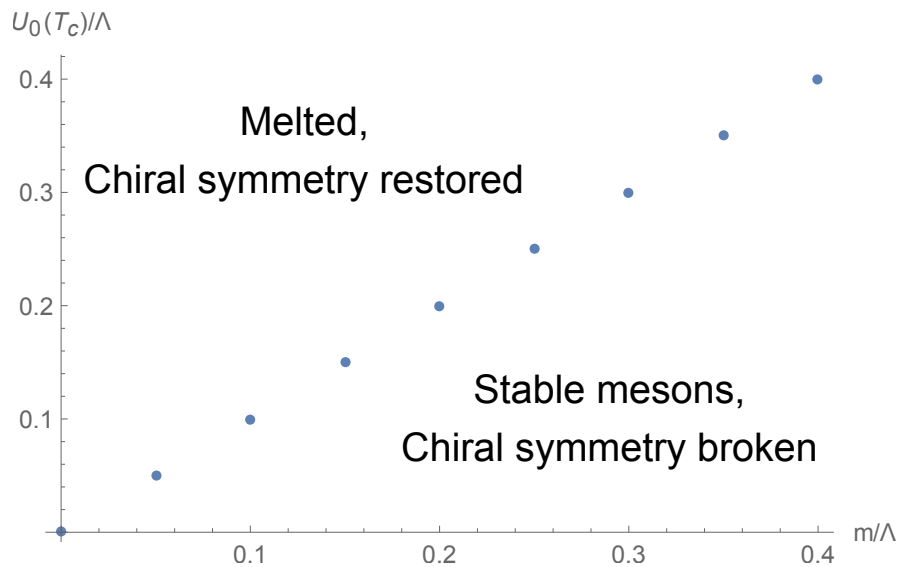


FIGURE 6.7: A plot of the numerical results of the critical temperature $U_0(T_c)$ varying with quark mass m/Λ .

mentioned in Chapter 5. Here we enforce by hand at the classical level;

$$\frac{g^2}{\Lambda^2} \langle \bar{\psi}_L \psi_R \rangle = m \quad (6.30)$$

or rearranging for the NJL coupling g^2 , and expressing in terms of the dimensionless outputs of the holographic model,

$$g^2 = \frac{m}{c} \Lambda^2 = \frac{m}{U_0} \frac{U_0^3}{c} \frac{\Lambda^2}{U_0} = \frac{1 + \tilde{m}^2}{2\tilde{m}\tilde{c}} \left(\frac{1 + v_\Lambda^2}{2v_\Lambda} \right)^2. \quad (6.31)$$

In this case, we would consider any configurations with the same value for g^2 as being the same theory, and can investigate the model holding the NJL coupling fixed, and varying the temperature. The picture we see here is strikingly different! Infact, at each temperature, we see again two U-shaped configurations with the same NJL coupling. A third configuration with the same NJL coupling is given by the flat disconnected loci, suggesting that the phase transition in this case is first order. This is an interesting feature of the domain wall theories! There are seemingly multiple interpretations for the field theory living on the domain wall loci. Another way to say this is the following; in these models there are a set of loci, that come equipped with DBI fields living on their surface. Reinterpreting the boundary data provided by the solutions moves you between types of theory. In this case, we go from a theory with a quark mass term in the Lagrangian, to one with a quark mass generated by the condensation of an NJL interaction term. Both of these theories share the same set of domain wall loci, they just re-order them. We plot the free energies for a theory with NJL coupling $g^2 \sim 0.57$ in Figure 6.8, which shows the swallowtail form expected in the case of a first order phase

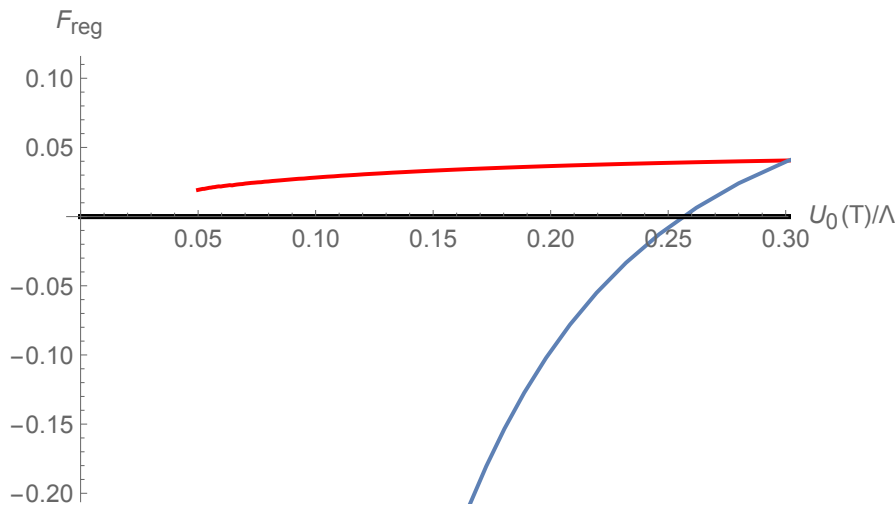


FIGURE 6.8: The free energy of the three configurations with fixed $g^2 \sim 0.57$, at varying temperature. The two U-shaped solutions are displayed (Red, Blue), the disconnected solutions are also drawn on (Black)

transition. There is a gap in the solutions between $0 < U_0(T)/\Lambda < 0.05$, due to the difficulty of numerical analysis at very low temperatures in this system. In Figure 6.9 we plot the variation in critical temperature with respect to g^2 , in analogy with Figure 6.7, showing clearly a phase with melted mesons that is chirally restored, and a phase with stable mesons that is chirally broken.

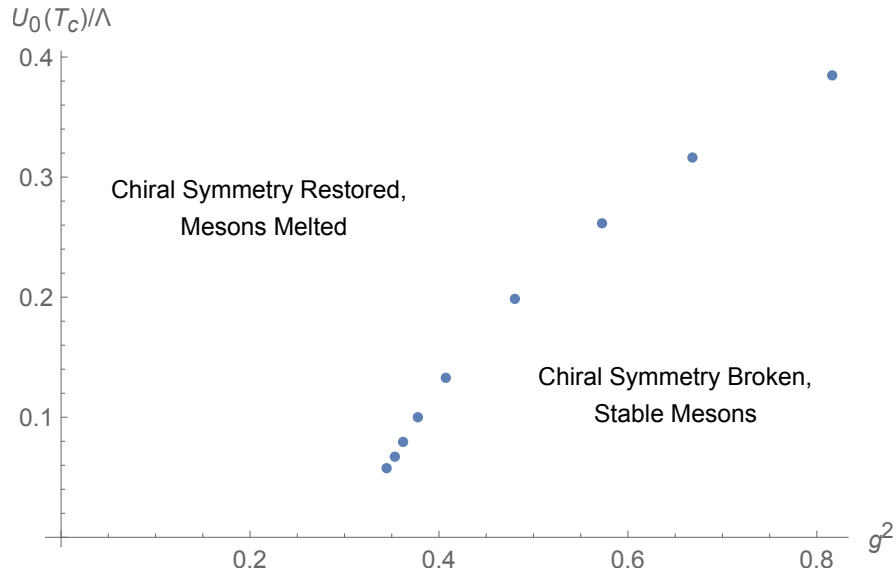


FIGURE 6.9: A plot of the numerical results of the critical temperature $U_0(T_c)$ varying with the NJL coupling g^2 . Again there are numerical difficulties at very low temperatures.

6.5 Summary

This chapter has covered the extension of the Domain Wall AdS/QCD model to finite temperature. Whilst on dimensional grounds one may expect the asymptotic width of the domain wall configurations to be inversely proportional to the quark mass, and indeed this is the case in the D3/D7 model, our analysis in this chapter has disabused us of this notion. Not only does organising the loci by fixed width not characterise the quark mass well, it shows a discrepancy in the order of the phase transition compared to dealing with the fields that live on the loci. Solving the equations of motion for the DBI fields restricted to the domain walls, allows us to label the loci by the mass of quarks living on their surface, which is a genuine UV parameter of the theory. Keeping the quark mass fixed, the loci rearrange themselves, revealing that the meson melting transition is in fact second order. To the authors knowledge, this is unique in holography. We have also shown that the same set of loci can describe a different, though related theory. Using the Witten prescription for multi-trace operators we can also describe a theory of massless quarks, with an NJL four-fermion interaction that provides an effective quark mass. Interestingly this theory does have a first order phase transition with respect to temperature! It is wholly possible that the width of the loci is an indirect measure of the coupling strength in an NJL type model rather than a direct measure of the quark mass.

Chapter 7

Conclusion and Outlook

This thesis has detailed the development of holographic domain wall fermions, inspired by implementations of chiral matter in lattice QCD. We start with a well controlled holographic system: the D3/probe D7 intersection dual to $\mathcal{N} = 4$ super-Yang-Mills theory, with a dynamical $\mathcal{N} = 2$ quark supermultiplet. Searching for D7 brane embeddings that have sinusoidal, spatial dependence on one of the directions spanned by the D3 branes, allows us to build a step-like mass function for the quark multiplet on the boundary of AdS. Where this mass function passes sharply through zero, massless quarks are localised on a pair of $2 + 1$ dimensional *domain wall* defects in the $3 + 1$ dimensional gauge theory. Solving the radial profile for the D7 brane embedding reveals that the domain walls will join together in the interior of AdS, mixing the quark degrees of freedom on each domain wall. This is analogous to breaking the “chiral” symmetry on the defect quark theory. Taking the *large mass limit*, where the quarks off the domain walls are taken to be very heavy, and thus no-dynamical, leaves only a $2 + 1$ dimensional domain wall *locus* on which the dynamical quarks are restricted to live. Restricting the DBI action for the probe branes, to the surface of the locus, provides us with tools to analyse the behaviour of quarks in the dual theory. Specifically it provides us with a handle on the quark mass/chiral condensate source/operator pair. Here we see that the joining of the domain walls represents a hard mass term in the Lagrangian, with a mass equal to the radial scale at which the domain walls join together. Unfortunately, this is not a quark mass generated by the non-perturbative dynamics of the theory, and it can be removed by taking the asymptotic separation of the domain walls to infinity, where the locus then is free to fall all the way to $r = 0$, destroying the IR mass gap. By deforming the background AdS geometry, the quark mass can be dynamically generated. This is represented by the domain wall

loci being excluded from an interior region of the geometry, *piling up* before the obstruction. The quark field on the loci also reflect this, having zero asymptotic quark mass, while being gapped in the IR. In these cases the fluctuations about the quark vacuum function, dual to a pseudoscalar meson, reveals that the symmetry breaking is dynamical by way of a holographic *Gell-Mann-Oakes-Renner relation*.

Understanding how to construct the holographic domain walls, by use of the *large mass limit*, we turn to the intersection of D5 and D7 branes. Taking the fivebrane to wrap a compact cycle induces a cap in the geometry, which signals that the dual theory is confining. By implementing the holographic domain walls, we restrict the quarks to living on a co-dimension two defect in the dual theory. This defect, being $3 + 1$ dimensional, hosts quarks which are genuinely chiral. This model has the requisite properties to be a holographic model of QCD, and we calculate the spectrum of mesonic observables. The D5 background, comes equipped with a linear dilaton profile which includes the running coupling of the dual theory, though it does not match the running calculated from QCD perturbation theory. It also forces us to cut the gravity dual off at some energy scale, beyond which we can no-longer trust the supergravity description of the branes. We argue that this naturally includes the region where a QCD-like theory becomes weakly coupled. For the mesonic observables, we match at a scale of $\sim 3 \text{ GeV}$, which would correspond to an intermediate coupling regime of QCD. The spectrum can be reasonably improved by including the effects of higher dimension operators in the dual theory. Arguably this begins to capture some of the stringy corrections to the model.

Lastly we examine the behaviour of the model in a black hole geometry, which is dual to the gauge theory at finite temperature. This presence of the black hole in the interior of the geometry enlarges the set of allowed domain wall loci, to include flat pairs of domain walls that fall into the black hole. We then examine the thermal phase transitions in the theory, from several perspectives. The first is to treat the asymptotic separation of the domain walls as a genuine parameterisation of the dual gauge theory, and keep it fixed as the temperature is varied. Doing so suggests that the theory should have a first order phase transition with respect to temperature. However, the fluctuations on the domain wall loci reveal that this moves us *between* theories with different quark mass. Exploiting the fluctuations on the loci to keep the quark mass fixed reveals that the phase transition is *second order*. This realisation of a second order meson melting phase transition is seemingly novel. By changing the asymptotic boundary conditions for the fields on the domain walls, we can use the pre-existing loci to describe *different theories*. By implementing a variant of the Witten multi-trace prescription, we can use the

loci to describe a theory with a quark mass generated by the condensation of an NJL four fermion interaction. Similarly, we can examine the phase transition with respect to temperature while keeping the NJL coupling, and therefore effective quark mass, fixed. Somewhat surprisingly, this theory displays a first order phase transition.

At time of writing, we are working to extend the model to finite density. By turning on the temporal component of a U(1) gauge field on the loci, we can examine the phase transitions with respect to quark chemical potential, μ (as in [87]). This project seems promising, and draws particular attention to the boundary conditions obeyed by the fields on the domain wall loci. The extra field on the locus can functionally be replaced by its equation of motion, yielding a modified equation of motion for the quark field, and an enlarged set of permissible boundary conditions. This greatly increases the number of configurations capable of supporting quarks of a given mass, and the effort to catalogue and characterise the phase transitions in the $\mu - T$ plane is ongoing. It is possible that a re-examination of the domain walls, as a non-supersymmetric brane anti-brane system might provide us with the ability to make progress here. Being able to describe the loci without use of the large mass limit may allow the gauge fields to deform the loci, increasing the set of allowed configurations, resulting in a richer phase diagram. This approach would also make the inclusion of a baryonic phase simpler. Ultimately, we would like to include finite density, and baryons in the model before attempting to determine the QCD *equations of state*. From there, it is planned to use the equations of state to solve the *Tolman-Oppenheimer-Volkoff equation* [121], and see whether the model is capable of producing astrophysical neutron stars. Ideally, it would be capable of modelling a fully holographic neutron star, following the example of [122].

References

- [1] J. Cruz Rojas, N. Evans, and J. Mitchell, “Domain wall fermions on the brane,” *Phys. Rev. D*, vol. 104, no. 5, p. 054029, 2021.
- [2] N. Evans and J. Mitchell, “Domain wall AdS/QCD,” *Phys. Rev. D*, vol. 104, no. 9, p. 094018, 2021.
- [3] N. Evans and J. Mitchell, “Thermal transitions in domain wall AdS/QCD,” *Phys. Rev. D*, vol. 106, no. 8, p. 086018, 2022.
- [4] D. J. Gross and F. Wilczek, “Ultraviolet Behavior of Nonabelian Gauge Theories,” *Phys. Rev. Lett.*, vol. 30, pp. 1343–1346, 1973.
- [5] K. G. Wilson, “Confinement of quarks,” *Phys. Rev. D*, vol. 10, pp. 2445–2459, Oct 1974.
- [6] N. Seiberg and E. Witten, “Electric - magnetic duality, monopole condensation, and confinement in N=2 supersymmetric Yang-Mills theory,” *Nucl. Phys. B*, vol. 426, pp. 19–52, 1994. [Erratum: *Nucl.Phys.B* 430, 485–486 (1994)].
- [7] A. Einstein, “The foundation of the general theory of relativity.,” *Annalen Phys.*, vol. 49, no. 7, pp. 769–822, 1916.
- [8] M. H. Goroff and A. Sagnotti, “The Ultraviolet Behavior of Einstein Gravity,” *Nucl. Phys. B*, vol. 266, pp. 709–736, 1986.
- [9] J. M. Maldacena, “The Large N limit of superconformal field theories and supergravity,” *Adv. Theor. Math. Phys.*, vol. 2, pp. 231–252, 1998.
- [10] E. Witten, “Anti-de Sitter space and holography,” *Adv. Theor. Math. Phys.*, vol. 2, pp. 253–291, 1998.
- [11] W.-j. Fu, “QCD at finite temperature and density within the fRG approach: an overview,” *Commun. Theor. Phys.*, vol. 74, no. 9, p. 097304, 2022.

- [12] N. Seiberg and E. Witten, “Monopoles, duality and chiral symmetry breaking in $N=2$ supersymmetric QCD,” *Nucl. Phys. B*, vol. 431, pp. 484–550, 1994.
- [13] E. D. Bloom, D. H. Coward, H. DeStaebler, J. Drees, G. Miller, L. W. Mo, R. E. Taylor, M. Breidenbach, J. I. Friedman, G. C. Hartmann, and H. W. Kendall, “High-energy inelastic $e - p$ scattering at 6° and 10° ,” *Phys. Rev. Lett.*, vol. 23, pp. 930–934, Oct 1969.
- [14] M. Breidenbach, J. I. Friedman, H. W. Kendall, E. D. Bloom, D. H. Coward, H. DeStaebler, J. Drees, L. W. Mo, and R. E. Taylor, “Observed behavior of highly inelastic electron-proton scattering,” *Phys. Rev. Lett.*, vol. 23, pp. 935–939, Oct 1969.
- [15] L. D. Faddeev and V. N. Popov, “Feynman Diagrams for the Yang-Mills Field,” *Phys. Lett. B*, vol. 25, pp. 29–30, 1967.
- [16] M. Gell-Mann, “Symmetries of baryons and mesons,” *Phys. Rev.*, vol. 125, pp. 1067–1084, 1962.
- [17] Y. Ne’eman, “Derivation of strong interactions from a gauge invariance,” *Nucl. Phys.*, vol. 26, pp. 222–229, 1961.
- [18] M. Gell-Mann, “The Eightfold Way: A Theory of strong interaction symmetry,” 3 1961.
- [19] S. Scherer, “Introduction to chiral perturbation theory,” *Adv. Nucl. Phys.*, vol. 27, p. 277, 2003.
- [20] H. Georgi, *Weak Interactions and Modern Particle Theory*. 1984.
- [21] I. Zahed and G. Brown, “The skyrme model,” *Physics Reports*, vol. 142, no. 1, pp. 1–102, 1986.
- [22] G. ’t Hooft, “A Planar Diagram Theory for Strong Interactions,” *Nucl. Phys. B*, vol. 72, p. 461, 1974.
- [23] E. Kiritsis, “Dissecting the string theory dual of QCD,” *Fortsch. Phys.*, vol. 57, pp. 396–417, 2009.
- [24] G. ’t Hooft, “On the Phase Transition Towards Permanent Quark Confinement,” *Nucl. Phys. B*, vol. 138, pp. 1–25, 1978.

- [25] J. Bardeen, L. N. Cooper, and J. R. Schrieffer, “Microscopic theory of superconductivity,” *Phys. Rev.*, vol. 106, pp. 162–164, Apr 1957.
- [26] R. L. Workman and Others, “Review of Particle Physics,” *PTEP*, vol. 2022, p. 083C01, 2022.
- [27] Y. Makeenko, “A Brief Introduction to Wilson Loops and Large N,” *Phys. Atom. Nucl.*, vol. 73, pp. 878–894, 2010.
- [28] J. Polchinski, “Dirichlet Branes and Ramond-Ramond charges,” *Phys. Rev. Lett.*, vol. 75, pp. 4724–4727, 1995.
- [29] G. Veneziano, “Construction of a crossing - symmetric, Regge behaved amplitude for linearly rising trajectories,” *Nuovo Cim. A*, vol. 57, pp. 190–197, 1968.
- [30] K. Nishijima, *Broken symmetry: Selected papers of Y. Nambu*. 1995.
- [31] L. Susskind, “Harmonic-oscillator analogy for the veneziano model,” *Phys. Rev. Lett.*, vol. 23, pp. 545–547, Sep 1969.
- [32] D. B. Fairlie and H. B. Nielsen, “An analog model for ksv theory,” *Nucl. Phys. B*, vol. 20, pp. 637–651, 1970.
- [33] M. A. Virasoro, “Alternative constructions of crossing-symmetric amplitudes with regge behavior,” *Phys. Rev.*, vol. 177, pp. 2309–2311, 1969.
- [34] C. Lovelace, “Pomeron form-factors and dual Regge cuts,” *Phys. Lett. B*, vol. 34, pp. 500–506, 1971.
- [35] J. Scherk and J. H. Schwarz, “Dual Models for Nonhadrons,” *Nucl. Phys. B*, vol. 81, pp. 118–144, 1974.
- [36] M. B. Green and J. H. Schwarz, “Anomaly Cancellation in Supersymmetric D=10 Gauge Theory and Superstring Theory,” *Phys. Lett. B*, vol. 149, pp. 117–122, 1984.
- [37] J. Dai, R. G. Leigh, and J. Polchinski, “New Connections Between String Theories,” *Mod. Phys. Lett. A*, vol. 4, pp. 2073–2083, 1989.
- [38] P. Horava, “Background Duality of Open String Models,” *Phys. Lett. B*, vol. 231, pp. 251–257, 1989.
- [39] E. Witten, “String theory dynamics in various dimensions,” *Nucl. Phys. B*, vol. 443, pp. 85–126, 1995.

- [40] K. Becker, M. Becker, and J. H. Schwarz, *String theory and M-theory: A modern introduction*. Cambridge University Press, 12 2006.
- [41] M. A. Virasoro, “Subsidiary conditions and ghosts in dual-resonance models,” *Phys. Rev. D*, vol. 1, pp. 2933–2936, May 1970.
- [42] P. Goddard and C. B. Thorn, “Compatibility of the Dual Pomeron with Unitarity and the Absence of Ghosts in the Dual Resonance Model,” *Phys. Lett. B*, vol. 40, pp. 235–238, 1972.
- [43] P. Ramond, “Dual Theory for Free Fermions,” *Phys. Rev. D*, vol. 3, pp. 2415–2418, 1971.
- [44] A. Neveu and J. H. Schwarz, “Factorizable dual model of pions,” *Nucl. Phys. B*, vol. 31, pp. 86–112, 1971.
- [45] A. Neveu and J. H. Schwarz, “Quark Model of Dual Pions,” *Phys. Rev. D*, vol. 4, pp. 1109–1111, 1971.
- [46] S. Mandelstam, “Interacting String Picture of the Neveu-Schwarz-Ramond Model,” *Nucl. Phys. B*, vol. 69, pp. 77–106, 1974.
- [47] F. Gliozzi, J. Scherk, and D. I. Olive, “Supersymmetry, Supergravity Theories and the Dual Spinor Model,” *Nucl. Phys. B*, vol. 122, pp. 253–290, 1977.
- [48] M. B. Green and J. H. Schwarz, “Supersymmetrical Dual String Theory,” *Nucl. Phys. B*, vol. 181, pp. 502–530, 1981.
- [49] M. B. Green and J. H. Schwarz, “Supersymmetrical String Theories,” *Phys. Lett. B*, vol. 109, pp. 444–448, 1982.
- [50] R. Blumenhagen, D. Lüst, and S. Theisen, *Basic concepts of string theory*. Theoretical and Mathematical Physics, Heidelberg, Germany: Springer, 2013.
- [51] N. Seiberg and E. Witten, “Spin Structures in String Theory,” *Nucl. Phys. B*, vol. 276, p. 272, 1986.
- [52] J. E. Paton and H.-M. Chan, “Generalized veneziano model with isospin,” *Nucl. Phys. B*, vol. 10, pp. 516–520, 1969.
- [53] O. DeWolfe, D. Z. Freedman, and H. Ooguri, “Holography and defect conformal field theories,” *Phys. Rev. D*, vol. 66, p. 025009, 2002.

- [54] K. Skenderis and M. Taylor, “Branes in AdS and p p wave space-times,” *JHEP*, vol. 06, p. 025, 2002.
- [55] J. L. Davis and N. Kim, “Flavor-symmetry Breaking with Charged Probes,” *JHEP*, vol. 06, p. 064, 2012.
- [56] R. C. Myers, “Dielectric branes,” *JHEP*, vol. 12, p. 022, 1999.
- [57] A. Giveon and D. Kutasov, “Brane Dynamics and Gauge Theory,” *Rev. Mod. Phys.*, vol. 71, pp. 983–1084, 1999.
- [58] G. T. Horowitz and A. Strominger, “Black strings and P-branes,” *Nucl. Phys. B*, vol. 360, pp. 197–209, 1991.
- [59] O. Aharony, S. S. Gubser, J. M. Maldacena, H. Ooguri, and Y. Oz, “Large N field theories, string theory and gravity,” *Phys. Rept.*, vol. 323, pp. 183–386, 2000.
- [60] N. Itzhaki, J. M. Maldacena, J. Sonnenschein, and S. Yankielowicz, “Supergravity and the large N limit of theories with sixteen supercharges,” *Phys. Rev. D*, vol. 58, p. 046004, 1998.
- [61] P. Breitenlohner and D. Z. Freedman, “Stability in Gauged Extended Supergravity,” *Annals Phys.*, vol. 144, p. 249, 1982.
- [62] R. Alvares, N. Evans, and K.-Y. Kim, “Holography of the Conformal Window,” *Phys. Rev. D*, vol. 86, p. 026008, 2012.
- [63] S. S. Gubser, I. R. Klebanov, and A. M. Polyakov, “Gauge theory correlators from noncritical string theory,” *Phys. Lett. B*, vol. 428, pp. 105–114, 1998.
- [64] L. Susskind, “The World as a hologram,” *J. Math. Phys.*, vol. 36, pp. 6377–6396, 1995.
- [65] S. W. Hawking, “Particle Creation by Black Holes,” *Commun. Math. Phys.*, vol. 43, pp. 199–220, 1975. [Erratum: *Commun. Math. Phys.* 46, 206 (1976)].
- [66] L. Da Rold and A. Pomarol, “Chiral symmetry breaking from five dimensional spaces,” *Nucl. Phys. B*, vol. 721, pp. 79–97, 2005.
- [67] A. Karch and E. Katz, “Adding flavor to AdS / CFT,” *JHEP*, vol. 06, p. 043, 2002.
- [68] A. Sen, “Rolling tachyon,” *JHEP*, vol. 04, p. 048, 2002.

- [69] A. Sen, “Tachyon matter,” *JHEP*, vol. 07, p. 065, 2002.
- [70] J. Polchinski, *String theory. Vol. 2: Superstring theory and beyond*. Cambridge Monographs on Mathematical Physics, Cambridge University Press, 12 2007.
- [71] J. Babington, J. Erdmenger, N. J. Evans, Z. Guralnik, and I. Kirsch, “Chiral symmetry breaking and pions in nonsupersymmetric gauge / gravity duals,” *Phys. Rev. D*, vol. 69, p. 066007, 2004.
- [72] M. Kruczenski, D. Mateos, R. C. Myers, and D. J. Winters, “Meson spectroscopy in AdS / CFT with flavor,” *JHEP*, vol. 07, p. 049, 2003.
- [73] J. M. Maldacena, “Wilson loops in large N field theories,” *Phys. Rev. Lett.*, vol. 80, pp. 4859–4862, 1998.
- [74] N. R. Constable and R. C. Myers, “Exotic scalar states in the AdS / CFT correspondence,” *JHEP*, vol. 11, p. 020, 1999.
- [75] A. Kehagias and K. Sfetsos, “On asymptotic freedom and confinement from type IIB supergravity,” *Phys. Lett. B*, vol. 456, pp. 22–27, 1999.
- [76] E. Witten, “Anti-de Sitter space, thermal phase transition, and confinement in gauge theories,” *Adv. Theor. Math. Phys.*, vol. 2, pp. 505–532, 1998.
- [77] T. Sakai and S. Sugimoto, “Low energy hadron physics in holographic QCD,” *Prog. Theor. Phys.*, vol. 113, pp. 843–882, 2005.
- [78] J. Erlich, E. Katz, D. T. Son, and M. A. Stephanov, “QCD and a holographic model of hadrons,” *Phys. Rev. Lett.*, vol. 95, p. 261602, 2005.
- [79] I. R. Klebanov and M. J. Strassler, “Supergravity and a confining gauge theory: Duality cascades and chi SB resolution of naked singularities,” *JHEP*, vol. 08, p. 052, 2000.
- [80] A. Karch, E. Katz, D. T. Son, and M. A. Stephanov, “Linear confinement and AdS/QCD,” *Phys. Rev. D*, vol. 74, p. 015005, 2006.
- [81] U. Gursoy and E. Kiritsis, “Exploring improved holographic theories for QCD: Part I,” *JHEP*, vol. 02, p. 032, 2008.
- [82] U. Gursoy, E. Kiritsis, and F. Nitti, “Exploring improved holographic theories for QCD: Part II,” *JHEP*, vol. 02, p. 019, 2008.

- [83] M. Jarvinen and E. Kiritsis, “Holographic Models for QCD in the Veneziano Limit,” *JHEP*, vol. 03, p. 002, 2012.
- [84] A. Sen, “Tachyon dynamics in open string theory,” *Int. J. Mod. Phys. A*, vol. 20, pp. 5513–5656, 2005.
- [85] S. J. Brodsky and G. F. de Téramond, “Light-front hadron dynamics and AdS/CFT correspondence,” *Phys. Lett. B*, vol. 582, pp. 211–221, 2004.
- [86] J. Erdmenger, N. Evans, I. Kirsch, and E. Threlfall, “Mesons in Gauge/-Gravity Duals - A Review,” *Eur. Phys. J. A*, vol. 35, pp. 81–133, 2008.
- [87] D. Mateos, R. C. Myers, and R. M. Thomson, “Holographic phase transitions with fundamental matter,” *Phys. Rev. Lett.*, vol. 97, p. 091601, 2006.
- [88] A. Karch and A. O’Bannon, “Holographic thermodynamics at finite baryon density: Some exact results,” *JHEP*, vol. 11, p. 074, 2007.
- [89] A. Karch, A. O’Bannon, and K. Skenderis, “Holographic renormalization of probe D-branes in AdS/CFT,” *JHEP*, vol. 04, p. 015, 2006.
- [90] T. Sakai and S. Sugimoto, “More on a holographic dual of QCD,” *Prog. Theor. Phys.*, vol. 114, pp. 1083–1118, 2005.
- [91] H. Hata, T. Sakai, S. Sugimoto, and S. Yamato, “Baryons from instantons in holographic QCD,” *Prog. Theor. Phys.*, vol. 117, p. 1157, 2007.
- [92] E. Witten, “Baryons and branes in anti-de Sitter space,” *JHEP*, vol. 07, p. 006, 1998.
- [93] D. B. Kaplan, “A Method for simulating chiral fermions on the lattice,” *Phys. Lett. B*, vol. 288, pp. 342–347, 1992.
- [94] H. B. Nielsen and M. Ninomiya, “Absence of Neutrinos on a Lattice. 1. Proof by Homotopy Theory,” *Nucl. Phys. B*, vol. 185, p. 20, 1981. [Erratum: *Nucl.Phys.B* 195, 541 (1982)].
- [95] H. B. Nielsen and M. Ninomiya, “Absence of Neutrinos on a Lattice. 2. Intuitive Topological Proof,” *Nucl. Phys. B*, vol. 193, pp. 173–194, 1981.
- [96] R. Brauer and H. Weyl, “Spinors in n dimensions,” *American Journal of Mathematics*, vol. 57, no. 2, pp. 425–449, 1935.
- [97] R. C. Myers and R. M. Thomson, “Holographic mesons in various dimensions,” *JHEP*, vol. 09, p. 066, 2006.

- [98] R. G. Leigh, “Dirac-Born-Infeld Action from Dirichlet Sigma Model,” *Mod. Phys. Lett. A*, vol. 4, p. 2767, 1989.
- [99] M. R. Douglas, “Branes within branes,” *NATO Sci. Ser. C*, vol. 520, pp. 267–275, 1999.
- [100] C. Hoyos-Badajoz, K. Jensen, and A. Karch, “A Holographic Fractional Topological Insulator,” *Phys. Rev. D*, vol. 82, p. 086001, 2010.
- [101] A. Karch, J. Maciejko, and T. Takayanagi, “Holographic fractional topological insulators in 2+1 and 1+1 dimensions,” *Phys. Rev. D*, vol. 82, p. 126003, 2010.
- [102] A. Karch and L. Randall, “Open and closed string interpretation of SUSY CFT’s on branes with boundaries,” *JHEP*, vol. 06, p. 063, 2001.
- [103] J. Erdmenger, Z. Guralnik, and I. Kirsch, “Four-dimensional superconformal theories with interacting boundaries or defects,” *Phys. Rev. D*, vol. 66, p. 025020, 2002.
- [104] O. Aharony and D. Kutasov, “Holographic Duals of Long Open Strings,” *Phys. Rev. D*, vol. 78, p. 026005, 2008.
- [105] S. Ryu and T. Takayanagi, “Holographic derivation of entanglement entropy from AdS/CFT,” *Phys. Rev. Lett.*, vol. 96, p. 181602, 2006.
- [106] E. Witten, “Anomalies and Nonsupersymmetric D-Branes,” 5 2023.
- [107] K. Ghoroku and M. Yahiro, “Chiral symmetry breaking driven by dilaton,” *Phys. Lett. B*, vol. 604, pp. 235–241, 2004.
- [108] V. G. Filev, C. V. Johnson, R. C. Rashkov, and K. S. Viswanathan, “Flavoured large N gauge theory in an external magnetic field,” *JHEP*, vol. 10, p. 019, 2007.
- [109] M. Gell-Mann, R. J. Oakes, and B. Renner, “Behavior of current divergences under $SU(3) \times SU(3)$,” *Phys. Rev.*, vol. 175, pp. 2195–2199, 1968.
- [110] G. T. Horowitz and R. C. Myers, “The AdS / CFT correspondence and a new positive energy conjecture for general relativity,” *Phys. Rev. D*, vol. 59, p. 026005, 1998.
- [111] N. Evans, J. P. Shock, and T. Waterson, “Towards a perfect QCD gravity dual,” *Phys. Lett. B*, vol. 622, pp. 165–171, 2005.

-
- [112] N. Evans and A. Tedder, “Perfecting the Ultra-violet of Holographic Descriptions of QCD,” *Phys. Lett. B*, vol. 642, pp. 546–550, 2006.
- [113] E. Witten, “Multitrace operators, boundary conditions, and AdS / CFT correspondence,” 12 2001.
- [114] Y. Nambu and G. Jona-Lasinio, “Dynamical Model of Elementary Particles Based on an Analogy with Superconductivity. 1.,” *Phys. Rev.*, vol. 122, pp. 345–358, 1961.
- [115] N. Evans and K.-Y. Kim, “Holographic Nambu–Jona-Lasinio interactions,” *Phys. Rev. D*, vol. 93, no. 6, p. 066002, 2016.
- [116] W. Clemens and N. Evans, “A Holographic Study of the Gauged NJL Model,” *Phys. Lett. B*, vol. 771, pp. 1–4, 2017.
- [117] M. Shifman, “Highly excited hadrons in QCD and beyond,” in *1st Workshop on Quark-Hadron Duality and the Transition to pQCD*, pp. 171–191, 7 2005.
- [118] J. Adams *et al.*, “Experimental and theoretical challenges in the search for the quark gluon plasma: The STAR Collaboration’s critical assessment of the evidence from RHIC collisions,” *Nucl. Phys. A*, vol. 757, pp. 102–183, 2005.
- [119] C. Hoyos-Badajoz, K. Landsteiner, and S. Montero, “Holographic meson melting,” *JHEP*, vol. 04, p. 031, 2007.
- [120] S. Kobayashi, D. Mateos, S. Matsuura, R. C. Myers, and R. M. Thomson, “Holographic phase transitions at finite baryon density,” *JHEP*, vol. 02, p. 016, 2007.
- [121] J. R. Oppenheimer and G. M. Volkoff, “On massive neutron cores,” *Phys. Rev.*, vol. 55, pp. 374–381, 1939.
- [122] N. Kovensky, A. Poole, and A. Schmitt, “Building a realistic neutron star from holography,” *Phys. Rev. D*, vol. 105, no. 3, p. 034022, 2022.